

Volume 26 Number 1 June 1995

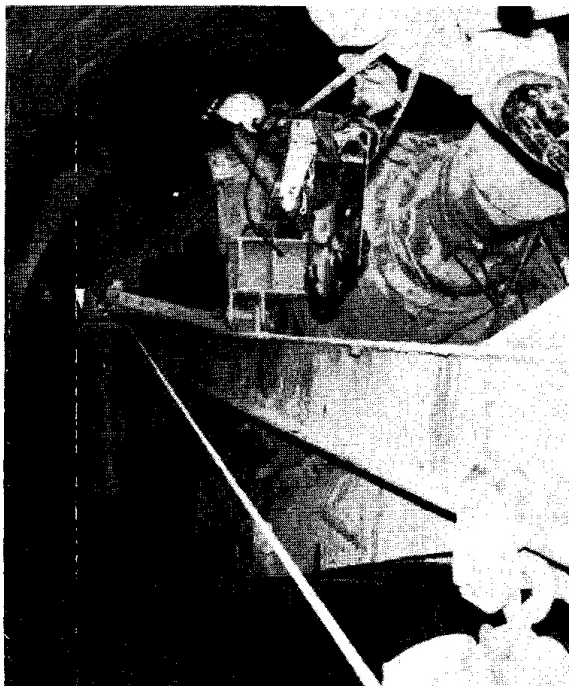
ISSN 0046-5828

# GEOTECHNICAL

# ENGINEERING

*Journal of*  
SOUTHEAST ASIAN GEOTECHNICAL SOCIETY

*Sponsored by*  
ASIAN INSTITUTE OF TECHNOLOGY



# GEOTECHNICAL ENGINEERING

## CONTENTS

### Photographic Feature:

Shield Driven Tunneling Method by M. SUGIMOTO.....	1
---	---

### Main Papers:

Improvement of Plasticity and Swelling Potential of Calcareous Expansive Clays by S.N. ABDULJAUWAD.....	3
Effect of Tail Void Closure on Ground Movement During Shield Tunnelling in Sandy Soil by C.Y. OU and J.C. CHERNG.....	17
Soil Particle Migration through Slots in Drains, Part I - Unidirectional Flows by B. TAHAR and T.H. HANNA.....	33
Soil Particle Migration through Slots in Drains, Part II - Reversing Flows by B. TAHAR and T.H. HANNA.....	51
Strength Characteristics of Sabkha Soils by O.S.B. AL-AMOUDI and S.N. ABDULJAUWAD.....	73
Effect of Bitumen Content and Curing Condition on Strength Characteristics of Asphalt Stabilized Soils by A.A. BASMA, A.S. AL-HOMOUD, T.S. KHEDAYWI and A.M. AL-AJLOUNI.....	93
Discussion by S.B. TAN and T.K. LIM.....	105
Paper Entitled "Hyperbolic Method for Evaluation of Settlement of Ground Pretreated by Drains and Surcharge" by S.A. Tan, Geotechnical Engineering, Vol. 25, No. 1, June 1994	

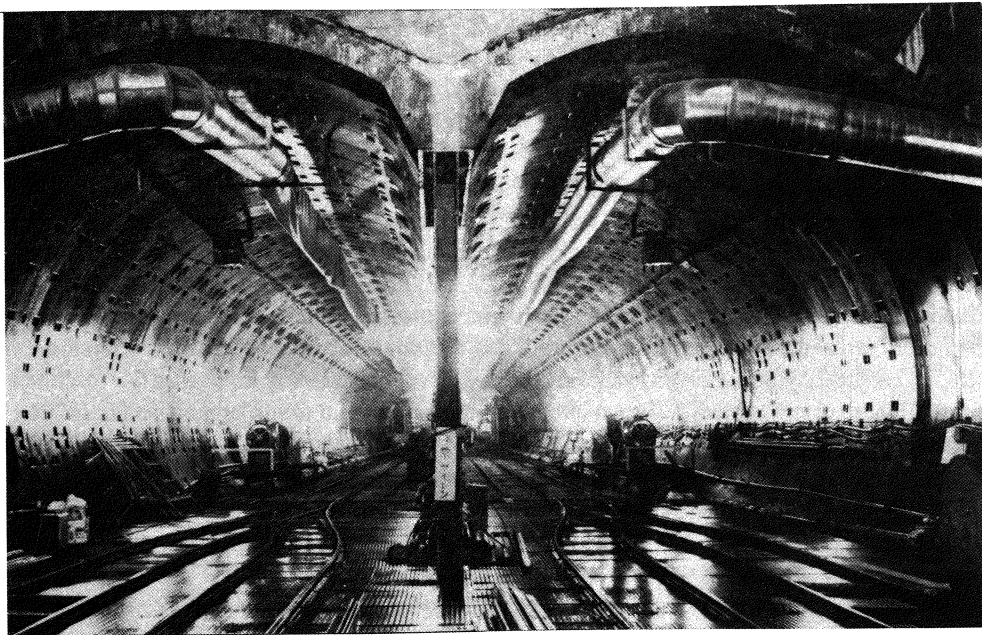
## PHOTOGRAPHIC FEATURE

# SHIELD DRIVEN TUNNELING METHOD

M. Sugimoto<sup>1</sup>

The demand of infrastructure network, such as, water supply, sewage, subway, road, electric supply, telecommunication cable, and soon, have increased due to the rapid urbanization of many cities in South East Asian region. The shield driven tunnel is one of the solution to construct the infrastructure network at the center of big city located on soft ground. This photograph shows the cross section of first multi-face shield (MF shield) driven tunnel for two track railway of Keiyou line in Tokyo, Japan.

Shield driven tunneling method was innovated in 1818 by Sir M.I. Brunel, UK. After the development of closed type shield in Japan and Germany in 1960-1970, shield driven method became popular to construct the infrastructure network in urban area on soft ground. Recently the number of the technology innovation related with shield driven method have increased, such as MF shield, HV shield, NOMST method, Automatic Control System, and so on. Euro tunnel between UK and French is one of the result of recent development.



---

<sup>1</sup> Associate Professor of Geotechnical Engineering, School of Civil Engineering, Asian Institute of Technology, GPO Box 2754, Bangkok, 10501, Thailand

# IMPROVEMENT OF PLASTICITY AND SWELLING POTENTIAL OF CALCAREOUS EXPANSIVE CLAYS

S.N. Abduljawwad<sup>1</sup>

## SYNOPSIS

This paper considers the effect of different treatment techniques on the plasticity and swelling potential of a calcareous expansive clay from Al-Qatif area in the eastern province of Saudi Arabia. These techniques are compaction, mixing with various proportion of local dune sand and treatment with commercial lime and potassium nitrate. The percentages of the stabilizers (3, 5 and 8% of dry weight) and the curing time (1, 7, 30 and 90 days) are the variables which were considered in this study. Results indicate that lime is very effective in reducing plasticity and swelling potential of the investigated soil. A lime fixation point was observed at 3% lime for swelling potential rather than the plastic limit as reported in the literature. Potassium nitrate is not as good as lime in improving the plasticity but its fixation between the smectite sheets was very effective in increasing the osmotic suction and reducing the percentages of swell and swell pressures. X-ray results reveal that in the lime treatment the pozzolanic reaction was the main factor in reducing the swelling potential of the calcium saturated clay, while in potassium nitrate treatment the smectite peaks almost disappeared and new peaks that correspond to muscovite are formed.

## INTRODUCTION

The arid climate, the geology and the severe weathering conditions in Saudi Arabia have produced a wide distribution of expansive soils (Fig. 1). In the Eastern part of Saudi Arabia the expansive soil is calcareous in nature and derived from argillaceous rocks of Permian, Cretaceous and Tertiary ages. The parent materials associated with expansive soils formations are dolomitic limestone and marls (Abduljawwad, et al., 1992; Okasha & Abduljawwad, 1992). This formation is aided by the presence of magnesium, calcium, sodium and iron cations and lack of leaching due to relatively low rainfall (Al-Sayari & Zotl, 1978). The damages due to this soil are enormous and manifest themselves in the following forms: cracking of masonry fences, reinforced concrete gates, interior and exterior masonry and stone walls and grade beams, and heave of slab-on-grade and pavement. Based on the economies and practicality of the operation, there are a number of methods which can be used to minimize heave of an expansive soil (Gromko, 1974). In this study, compaction control, mixing with various proportions of local dune sand and treatment with chemicals were utilized to reduce plasticity and/or swelling potential of the calcareous expansive clay.

---

<sup>1</sup> Associate Professor, Department of Civil Engineering, King Fahd University of Petroleum & Minerals, Box 608, Dhahran 31261, Saudi Arabia.

The chemicals used were locally produced commercial lime and potassium nitrate. The literature on the use of lime and lime-fly ash additives to improve the engineering properties of clayey soils is enormous (Hilt & Davidson, 1960, Clare & Cruchley, 1957, Mitchell & Hooper, 1961; Ho & Handy, 1963, Eades & Grim, 1960; Mateos, 1964; and Rowlands et al., 1987). The addition of lime initiates cation exchange, flocculation, carbonation and pozzolonic reactions. Some investigators indicated that the swelling potential of expansive soil is inversely proportional to the concentration of salts in the pore fluid (Mowafy et al., 1985). The most used salts are sodium and potassium chlorides (Frydman & Ehtenreich, 1977; Abduljawwad, 1991). The major problem with these salts is that they provide chloride ions which are very aggressive to the reinforced concrete structure. In this study potassium nitrate was selected as an alternative chemical additive to treat the calcareous expansive clays. The influence of different treatment techniques was investigated by comparing plasticity, mineralogy, physiochemical properties and swelling potential. The effect of curing time on plasticity and swelling potential was also examined.

### SOIL AND TESTING PROCEDURES

Figure 1 shows the site location in Al-Qatif, eastern province of Saudi Arabia. The site selection was based on reported structural damage in the area due to very active expansive soil. A test pit was used for obtaining good quality block samples, where undisturbed samples were carefully cut from the walls and bottom of the test pit. Geotechnical and physiochemical properties and mineralogical composition of this soil are shown in Table 1. The high percentage of soil grains passing No. 200 sieve, the high values of liquid limit

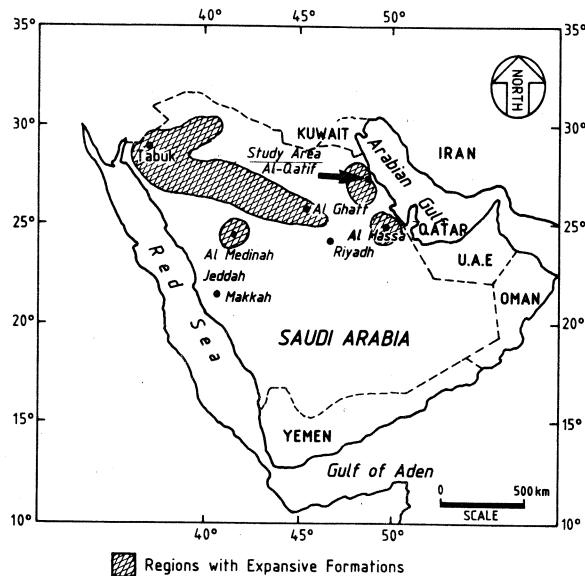


Fig. 1 Site Location.

*IMPROVEMENT OF PLASTICITY*

**Table 1 Properties of Calcareous Expansive Soils Tested**

Parameters	Values and Descriptions
Color	Greenish-brown
Specific gravity	2.77
Natural water content (%)	40
Dry density (g/cm <sup>3</sup> )	1.13
Optimum water content (%)	44
Maximum dry density (g/cm <sup>3</sup> )	1.15
% passing # 200 sieve	96
% smaller than 0.002 mm	72
Liquid limit (%)	173
Plastic limit (%)	49
Shrinkage limit	25
X-ray results	Smectite, Illite, Palygorskite, Quartz, and Gypsum
CEC (meq/1-ml)	106
pH	7.8

and plastic limit, the low value of shrinkage limit and the high value of cation exchange capacity, reflect the high plasticity and indicate the presence of active clay minerals. X-ray diffraction analysis indicates that the clay minerals present are smectite, illite and palygorskite and the non-clay minerals are quartz and gypsum. Smectite is considered as the main group of most active 2:1 clay minerals. The moisture density curve shown in Fig. 2 was obtained by using ASTM D-698 standard procedures. The compaction curve is flat and extends over a wide range of moisture content with the dry density being reduced significantly on the wet side in comparison with the dry one. This behavior is typical for high plasticity clay.

The soil was air dried and pulverized repeatedly until all soil aggregations were reduced to minus 40 sieve size. Soil was mixed with varying amounts of sand, lime and potassium nitrate (3, 5 and 8 percent of the dry weight) and distilled water was added in appropriate amounts to bring the mixture to a moisture content of 40 percent.

Samples after being mixed with additives were stored in sealed thermal plastic bags and placed in an oven under a constant temperature of 40°C to accelerate the chemical reactions. The moisture content was maintained at a constant value during the curing period. The swelling potential of treated samples was determined by the percentage of swell and swell pressure. The percentage of swell was determined by using the simple oedometer test, while the swelling pressure was estimated by using the constant volume test (Nelson & Miller, 1992). The treated samples were compacted directly into the ring to the natural density using static compaction.

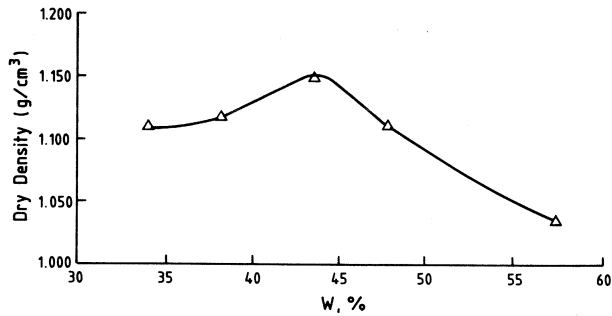


Fig. 2 Compaction Curve for the Investigated Soil.

### RESULTS AND DISCUSSION

#### Plasticity

The liquid limit and plasticity index of soil samples containing different percentages of additives and cured for various periods of time are shown in Figs. 3 and 4, respectively. The 8 percentage of lime with 90 days curing was the most effective treatment technique in reducing plasticity, while sand was the least effective in reducing the plasticity index. This is attributed to the small percentage of sand used in this study. It was observed that the liquid limit and plasticity index decreased with increasing additives content. The increase in liquid limit at small additions of  $KNO_3$  is in keeping with  $K^+$  ions being absorbed in the exchange complex. This effect decreases with time, due probably to higher quantities of added salt tending to reduce the liquid limit. The calcareous clay is largely calcium saturated. Since some cation exchange occurs on addition of additives, the effect of the chemicals may vary, depending on the extent to which pre-existing cations are exchanged.

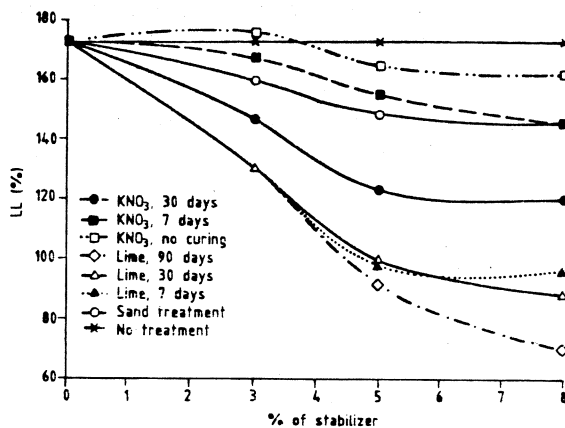
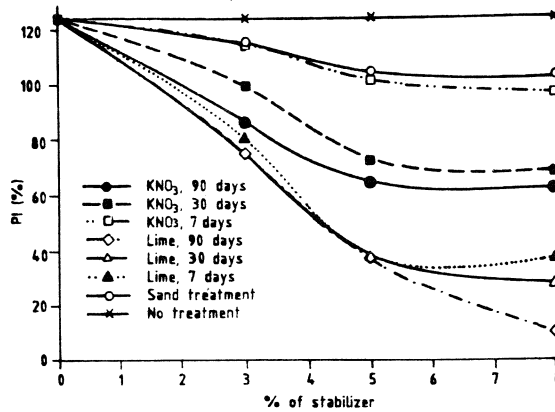


Fig. 3 Comparison of Liquid Limit for Different Treatment Techniques.

## IMPROVEMENT OF PLASTICITY



**Fig. 4 Comparison of Plasticity Index for Different Treatment Techniques.**

The addition of lime will cause the replacement of the exchangeable sodium, magnesium, or other cations previously held by the soil clay, by calcium cations. This will cause the calcareous clay to be more calcium saturated and have a substantially lower liquid limit than the same clay saturated with potassium due to the additions of potassium nitrate. The improvement in plasticity of the treated samples under different curing conditions, is shown on the plasticity chart (Fig. 5). The crossing of the A-line to the so called silty region occurred for most of the lime treated samples. The exceptions were the specimens with 3 percent lime that were immediately tested. The effect of the curing period was observed to cause a major reduction in plasticity and, hence, lower degree of expansivity. The addition of potassium nitrate does not cause significant change in plasticity and the A-line crossing took place only for samples treatment with 5 percent or more lime and cured for 30 days or longer.

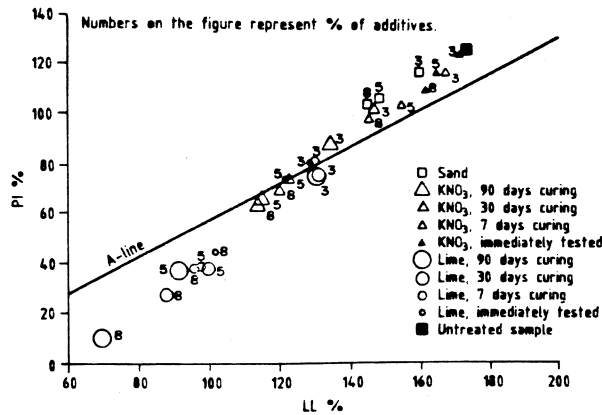


**Fig. 5 The Effect of Additives and Curing Time on Plasticity.**



Swelling Potential

The untreated and treated samples were subjected to swelling tests using the one-dimensional oedometer apparatus. Expansive clays were found to heave very little when compacted to low densities at high water content. Fig. 6 shows the effect of compaction on the percentage of swell. Samples were compacted dry of optimum, at optimum and wet of optimum. The effect of moisture content on swelling was verified by using the same dry density for samples compacted on the dry and wet side of the optimum. Samples compacted dry of optimum swell more when given access to moisture than wet-side compacted samples because they have a greater moisture deficiency and a lower degree of saturation, as well as more random particles arrangement.

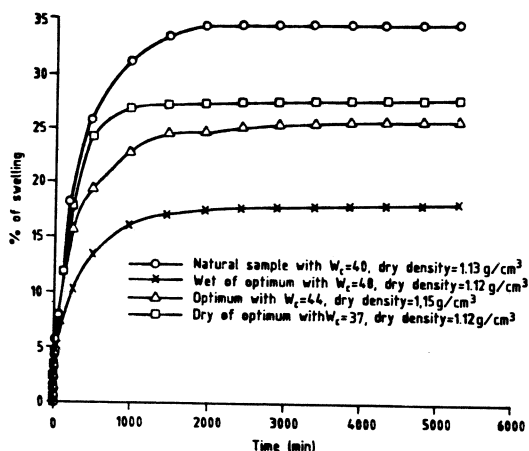
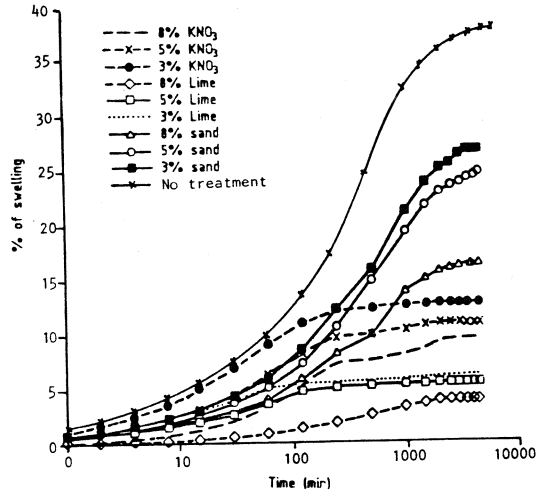


Fig. 6 The Effect of Compaction on Percentage of Swell.

Figures 7 and 8 show the percentage of swell and swelling pressures versus log. time for samples mixed with the different additives and cured for three months, respectively. Sand treatment was less effective than other additives, because of the small percentage of sand used in this study in order to be consistent with the amounts used for lime and potassium nitrate. The addition of sand to active clay will not generate chemical reactions and its effect mainly will be the reduction of clay content. A higher proportion of sand content, and corresponding lower clay content, will reduce the tendency of the clay to swell due to larger capillary canals in the soil pores and the corresponding reduction in the soil suction.

Figures 7 and 8 show also the effect of lime and potassium nitrate on the percentage of swell and swelling pressures by fixing the curing time to 3 months and varying the percentage of additives from 3 to 8%. Results indicate that lime is the most effective additive in reducing the swelling potential, where the major reduction in percentage of swell and swelling pressure occurred at 3% lime. This 3% is in agreement with lime fixation point

## IMPROVEMENT OF PLASTICITY



**Fig. 7 Percentage of Swell vs. Log. Time for Treated Samples.**

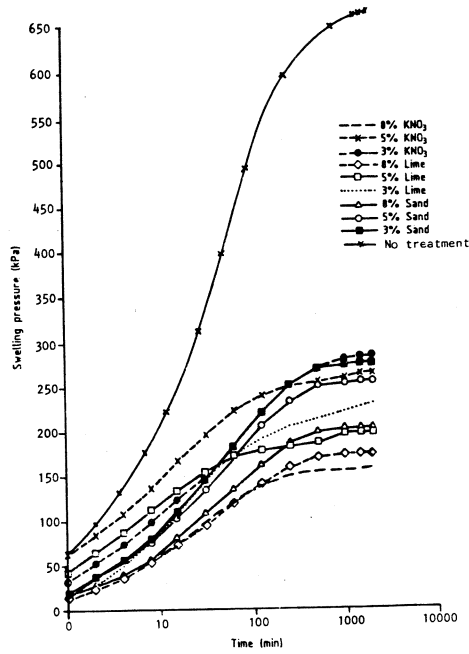


**Fig. 8 Swelling Pressure vs. time for Treated Samples.**

which was suggested by the research conducted at Iowa State University and supported by U.S. Army Corps of Engineers (Hilt & Davidson, 1960). In this study the fixation point is observed for swelling potential, while in Hilt and Davidson work it was observed for plastic

limit. A study of these two figures reveal that as the concentration of potassium nitrate increases, the percentage of swell and swelling pressure decreases for the same condition of initial water content, initial normal surcharge and density.

Figs. 9 through 12 show the effect of the percentage of additives and curing time on the percentage of swell and swelling pressure, respectively. As the curing time is increased from 1 day to 7, 30 or 90 days the percentage of swell and swelling pressure will continue to decrease. For samples treated with lime, the curing period of 30 days was the most effective in reducing the swelling potential, beyond which a small effect is observed. Similar behavior was also observed for samples treated with potassium nitrate. The water affinity of different mixtures was determined by measuring the soil suction using the filter paper technique (Snethen & Johnson, 1980). A comparison of initial suction, before the swelling test, and final suction, after the swelling test reveals that the lime stabilized soil absorbs less water than the untreated one (Table 2).

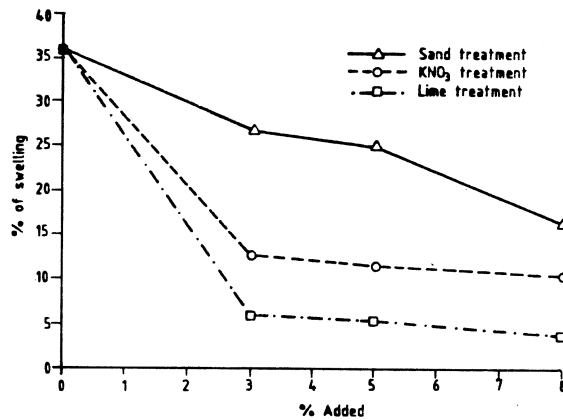


Fig. 9 Variation of Percentage of Swell with % of Additives.

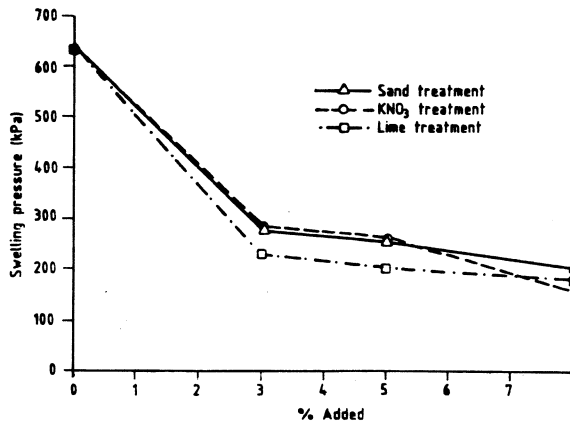
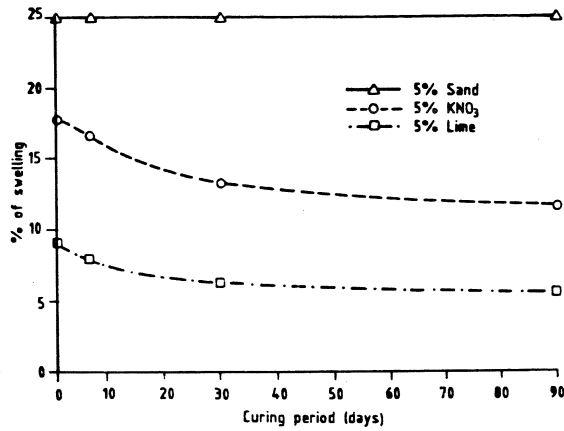
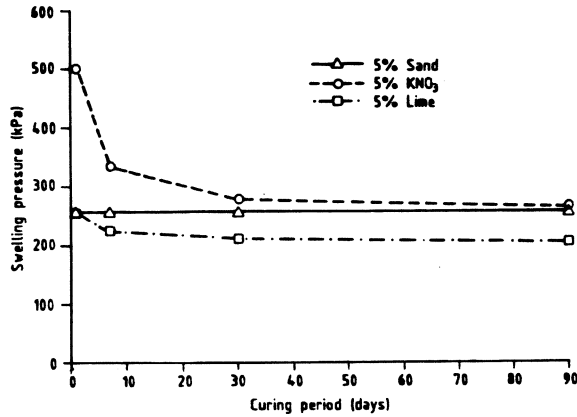


Fig. 10 Variation of Swelling Pressure with Percentage of Additives.

## IMPROVEMENT OF PLASTICITY



**Fig. 11** Variation of Percentage of Swell with Curing Time.



**Fig. 12** Variation of Swelling Pressure with Curing Time.

**Table 2** Total Suction and pH of Soil Samples

Sample descriptions	Initial suction (PF)	Final suction (PF)	pH
Untreated sample	4.61	3.70	7.75
Sample treated with lime and cured for 3 months	4.65	3.95	8.54
Sample treated with KNO <sub>3</sub> and cured for 3 months	4.96	4.44	8.12

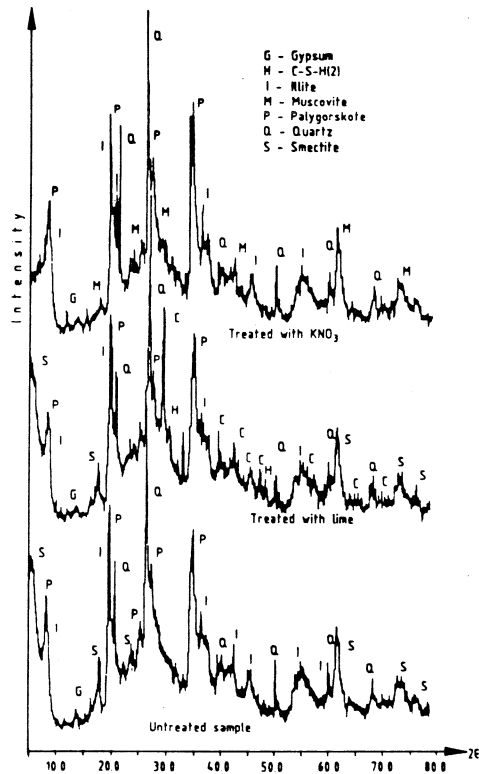
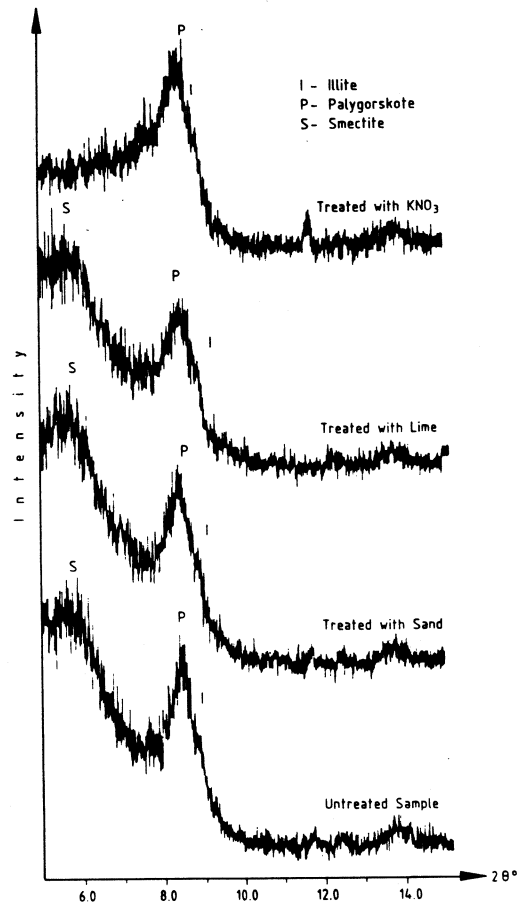


Fig. 13 X-ray Diffraction Patterns.

X-ray diffraction traces presented in Fig. 13 indicate the major peaks of the untreated sample were significantly altered. For lime treatment, there was no change in the smectite (ca-montmorillonite) peaks. This is because the natural soil is calcium saturated and cation exchange, replacement of exchangeable cations including sodium, magnesium, and others by calcium cation derived from the lime, can be eliminated as a serious explanation for the stabilizing effect of lime on soil. The new peaks of calcite can be attributed to the carbonation. The reaction of lime with carbon dioxide to form calcite produces short-term cementing action. X-ray results were for samples cured for 3 months. So, they should reveal the long-term (Pozzolanic) reactions which cause the formation of new phases including tobermorite gel, calcium silicate hydrates, C-S-H (1) and C-S-H (2) and calcium aluminate hydrates. Unfortunately, these phases are invariably poorly crystallized (amorphous) and difficult to detect. This is also because the peaks of these phases will interfere with peaks of the highly crystalline minerals (illite and palygorskite). However, small new peaks, correspond to C-S-H (2), were detected for the lime treated samples. Fig. 14 shows X-ray results for low scanning angles ( $5^{\circ}$  to  $15^{\circ}$ ), which reflect the effect of different treatment techniques on the smectite peak at about  $6^{\circ}$  angle. The peak has not affected by the sand treatment and was a little bit flatter due to lime treatment, and almost

## IMPROVEMENT OF PLASTICITY



**Fig. 14 Comparison of X-ray Diffraction Patterns at Low Scanning Angles.**

disappeared in the case of KNO<sub>3</sub> treatments. Furthermore, an examination of scanning electron microscope (SEM) micrography in Plates 1 and 2 indicate the flocculation of the calcareous clay and the consequent increase in effective grain size due to the addition of lime. This will produce further reductions in swelling potential of this clay as a result of lime treatment. The SEM micrography were taken in split screen mode, the left side showing the morphology at magnification printed on the micrograph while the right side is 5x zoomed imaged.

Due to the presence of smectite, the potassium provided by potassium nitrate not only becomes adsorbed but also may become fixed by the soil colloids. The potassium ions fit in between layers in the crystals of these expanding calcareous clays and become an integral part of the crystal. Potassium in this form cannot be replaced by ordinary exchange methods and consequently is referred to as nonexchangeable potassium. This has been

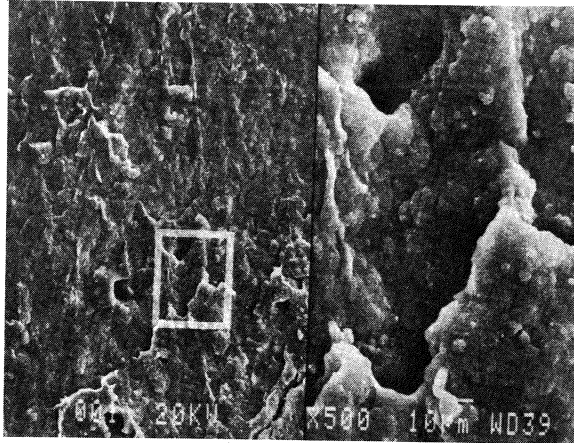


**Plate 1. SEM Micrograph for Natural Sample.**

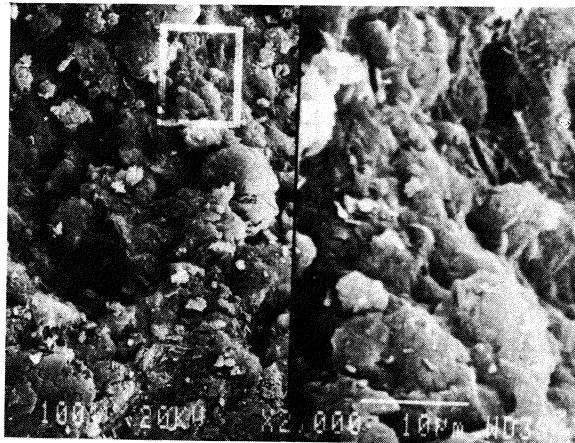


**Plate 2. SEM Micrograph for Sample Treated with 5% Lime (3 Months Curing).**

confirmed by the X-ray results which indicate that the smectite peaks reduced in intensity where 15 Å peak almost disappeared, and the presence of new peaks due to the formation of muscovite. The SEM micrography shown in Plate 3 indicates the flocculation and the formation of new phases due to the addition of potassium nitrate. The charges on the surface of clay particles play an important role in the stability of colloids that require the presence of small concentrations of electrolytes. The addition of potassium nitrate produces a large amount of electrolytes that precipitate with the effect of rapidly flocculating the colloids. Furthermore, upon flooding the sample with water to initiate the swelling process, the potassium nitrate is ionized into  $K^+$  and  $(NO_3^-)$ . The nitrate ions are absorbed between the sheets of smectite to form calcium nitrate. The calcium nitrate prevents water from entering

## IMPROVEMENT OF PLASTICITY



**Plate 3. SEM Micrograph for Sample Treated with 5% Potassium Nitrate (3 Months Curing).**

between the sheets and thus decreases the swelling ability of the active calcareous clay. The addition of  $\text{KNO}_3$ , caused an increase in the osmotic suction leading to an increase in the total suction from 3.7 pF for untreated sample to 4.44 pF for the treated one.

### CONCLUSIONS

Based on the results of laboratory tests, the following conclusions are drawn:

1. The addition of lime caused a major reduction in the liquid limit and plasticity index of the calcareous expansive clay. The curing time and percentage of lime are the major factors which control the behavior of the treated soil. The lime fixation point was observed at 3% for swelling potential but not for plastic limit.
2. The crossing of the A-line from the high plasticity clayey region to the silty region occurred for most of the lime treated samples, while the addition of potassium nitrate did not cause significant change in plasticity and the A-line crossing took place only for samples treated with 5% or more and cured for 30 days or longer.
3. The calcareous clay in the Eastern province of Saudi Arabia is largely calcium saturated. Carbonation, flocculation and pozzolonic reactions are effective in reducing plasticity and swelling potential. These reactions were verified by X-ray and SEM results.
4. Potassium nitrate was very effective in reducing the swelling potential of expansive clay. Fixation of potassium ions between the smectite sheets, flocculation due to precipitation of electrolytes and the formation of calcium nitrate which partially block the water from entering between sheets were very efficient in reducing the swelling potential of the calcareous expansive clay. The increase in the final total soil suction from 3.7 pF to 4.44 pF due to  $\text{KNO}_3$  treatment indicates that a smaller amount of water will be adsorbed by the treated samples leading to a reduction in swelling potential.



## ACKNOWLEDGEMENT

This work is part of an ongoing research project sponsored by King Abdulaziz City for Science & Technology (KACST) under grant No. AR-10-061. The author is grateful to KACST for providing support for this research and to the King Fahd University of Petroleum & Minerals for providing the laboratory space and facilities.

## REFERENCES

- ABDULJAUWAD, S.N. (1991). "Characteristics and Chemical Treatment of Expansive clay in Al-Qatif, Saudi Arabia." *J. Eng. Geology*, 30, pp. 143-158.
- ABDULJAUWAD, S.N, HAMEED, R.A., AL-SULAIMANI, G.J., BASUMBUL, I.A., and SAFAR, M.M. (1992). "Expansive soils in Eastern province of Saudi Arabia." *Proc. Seven Int. Conf. on Expansive Soils*, 1, Dallas, TX, pp. 426-431.
- Al-Sayarri, S.J., and Zotl, J. G. (1978). "Quaternary Period in Saudi Arabia." Springer-Verlag, Wein, Austria.
- CLARE, K.E., and CRUCHLEY, A.E. (1957). "Laboratory Experiments in the Stabilization of Clays with Hydrated Lime." *Geotechnique*, 7, pp. 97-111.
- EADES, J.L. and GRIM, R. (1960). "Reactions of Hydrated Lime with Pure Clay Minerals in Soil Stabilization." *Highway Research Board Bull.* 262, pp. 51-63.
- FRYDMAN, S. and EHTENREICH, T. (1977). "Stabilization of Heavy Clay with Potassium Chloride." *J. Geot. Eng.*, 8, pp. 95-108.
- GROMKO, G.J. (1974). "Review of Expansive Soils." *J. Geot. Eng. Div., ASCE*, 100(6), pp 667-687.
- HILT, G.H., and DAVIDSON, D.T. (1960). "Lime Fixation in Clayey Soils." *Highway Research Bull.* 262, pp. 20-32.
- HO, C., and HANDY, R.L. (1963). "Characteristics of Lime Retention by Montmorillonitic Clays." *Highway Research Record No. 29*, pp. 55-69.
- MATEOS, M. (1964). "Soil Lime Research at Iowa State University." *J. Soil Mech. Found. Eng., ASCE*, 90(2), pp. 127-153.
- MITCHELL, J.K., and HOOPER, D.R. (1961). "Influence of Time between Mixing and Compaction on Properties of a Lime-Stabilized Expansive Clay." *Highway Research Board Bull.* 304, pp. 14-31.
- MOWAFY, Y.M., BAUER, G.E., and SAKEBS, F.H. (1985). "Treatment of Expansive Soils: Laboratory Study." *Trans. Res. Rec.*, 1032, Washington, D.C. pp. 34-39.
- NELSON, J.D. and MILLER, J.D. (1992). "Expansive soils: problems and practice in foundation and pavement engineering." John Willey Publication.
- OKASHA, T. M. and ABDULJAUWAD, S.N. (1992). "Expansive Soil in Al-Madinah, Saudi Arabia." *J. Applied Clay Science*, 7, pp. 271-289.
- ROWLANDS, G.O., ARABI, M. and DEPLAK, R. (1987), "Lime and the Plasticity of Clay." *J. Instit. Highway Trans.*, pp. 21-24.
- SNETHEN, D.R. and JOHNSON, L.D. (1980). "Evaluation of Soil Suction from Filter Paper." Paper No. GL-80-4, U.S. Army Corps Eng. Wat. Exp. Sta., Vickburg, Miss.

# EFFECT OF TAIL VOID CLOSURE ON GROUND MOVEMENT DURING SHIELD TUNNELLING IN SANDY SOIL

C.Y. Ou<sup>1</sup> and J.C. Cherng<sup>2</sup>

## SYNOPSIS

The complete modelling of the tunnelling process for the finite element analysis should include;(1) gravity, (2) advance-heave and advance-release, (3) tail void closure, (4) lining installation and activation and (5) long-term consolidation. Except for the factor of shield machine operation, the tail void closure is the major cause of ground movement in the sandy soil deposit. The initial stress, which heavily affects the result of finite element analysis, will change as the results of a shield machine advancing and passing a particular point along the tunnel alignment. This is in nature a three-dimensional problem. However, the cost of three-dimensional analysis with nonlinear soil behavior is simply prohibitive. A converting procedure was developed to simulate the heaving effects produced by the shield advancing process. Plane strain analysis rather than three-dimensional analysis was used in the simulation. An example analysis for an actual shield tunnel is presented for the complete modelling of the tunnelling process. The same procedure can be applied in the case where the tail void closure is the major cause of ground movement.

## INTRODUCTION

The empirical method and the finite element method are two common methods of predicting ground surface settlement induced by shield tunnelling. Basically, the empirical method constitutes all factors contributing to ground settlement because it is normally derived on the basis of final measured values. A major advantage of the empirical method is that ground settlements in a project similar geological and construction environments can be easily and accurately predicted. However, the empirical method cannot be used as an evaluation tool for designing an auxiliary construction method that will reduce ground settlement, since it would not be possible to understand the mechanisms involved.

On the other hand, the finite element method has the advantage of providing an understanding of the settlement mechanisms and it can also be used to investigate the degree by which certain factors can affect the settlement due to shield tunnelling. As long as the geological condition and the construction sequence are known, predicting ground

---

<sup>1</sup> Professor, Department of Construction Engineering, National Taiwan Institute of Technology, Taipei, Taiwan, R.O.C.

<sup>2</sup> Engineer, Trinity Technology Consulting Engineers Co., Taipei, Taiwan, R.O.C.

settlement and designing a method for reducing ground settlement can be achieved using the finite element method.

There are two key factors affecting the reliability of finite element analysis of shield tunnelling. The first is the stress-strain modelling of the soil, and the second is the simulation of the tunnel construction sequence. A modified version of the computer program JFEST (Finno, 1983) is used in this paper. In the program, a nonlinear elastic approximation of soil response, as proposed by Duncan & Chang (1970), is used to model the behavior of both cohesive and cohesionless soils. The idea of this model is to characterize the stress-strain responses by an empirical equation, where the nonlinear stress-dependent hyperbolic curve is used for loading and a linear stress-dependent response is used for unloading and reloading. At any given stress level, a tangent modulus to the equation is used to predict the stress-strain relationship for the next loading increment. The convergence between predicted and actual responses is achieved by a number of small loading increments and special iteration techniques. All of the parameters for this model can be obtained directly from conventional triaxial tests.

The complete simulating of tunnel construction sequence should include the following steps: (1) gravity, (2) advance-heave and advance-release, (3) tail void closure, (4) lining installation and activation and (5) long-term consolidation as schematically illustrated in Fig. 1. Three-dimensional movements are usually induced in the soil around the shield face during the tunnelling operation. A three-dimensional analysis, therefore, is actually required to simulate the full tunnelling process. However, the cost of three-dimensional

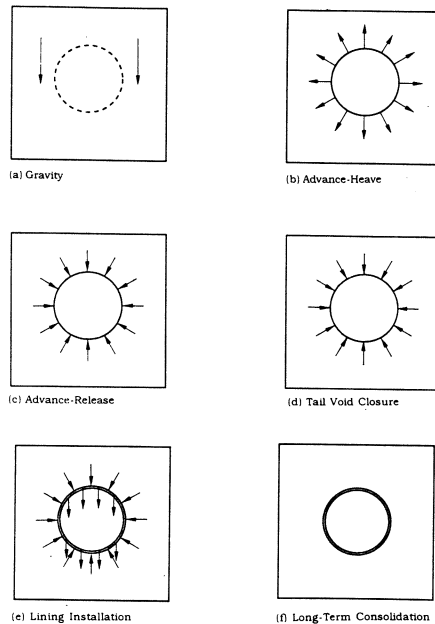


**Fig. 1 Modelling of Tunnelling process**

## EFFECT OF TAIL VOID CLOSURE

analysis with nonlinear material behavior is prohibitive. Therefore, the work described here is a plane strain analysis for the construction phase. Since the closure of tail void is a major cause of ground movement, the analysis of the tail void closure is also studied in detail.

### ADVANCE-HEAVE AND ADVANCE-RELEASE

The initial gravity stress will change as the result of a shield machine advancing toward and passing a particular point along the tunnel alignment. Most of the published finite element works which have been applied to soil tunnelling do not take into account the heaving effect due to shield advance. This is a three-dimensional problem. Under the considerations of simplifying 3-D analysis to plane strain analysis, Finno (1983) applied elliptical pressure distribution on the edge of the tunnel to simulate the heaving effect. The magnitude of the elliptical pressure was based on the field measurement of horizontal displacement of the soil element near the tunnel. This analytical procedure requires field measurements as a prerequisite. It should be noted that Finno studied this problem using longitudinal plane strain analysis which may not model the actual tunnelling process exactly.

In an idealized tunnel construction, any transverse section cut across the tunnel axis may experience the same amount of maximum pushing force by the shield. The induced ground surface heave and the change of initial stresses in the soil for each transverse section should therefore be the same. The pushing force acting on a transverse section may decrease to zero as the shield machine passes and moves away from the section. The total amount of decreasing force should be the same as the pushing force. For any element, this is a loading-unloading process, but the deformed soil mass will not recover because of the nonlinear property of soils. Thus, it is reasonable to model the process of shield advance using plane strain analysis for the section as long as the change of initial stress for the section due to the advancement of the shield is evaluated.

As shown in Fig 2, the pushing pressure,  $p_b$ , is defined as the net increase of lateral earth pressure over the cross sectional area of shield during the tunnelling process in the three-dimensional space; the heaving pressure,  $p_h$ , is defined as the equivalent distributed pressure applied on the periphery of the tunnel in the plane strain simulation procedure.

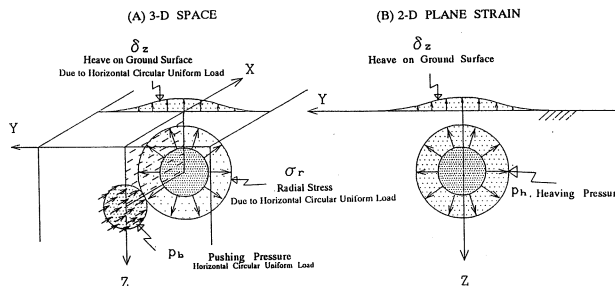
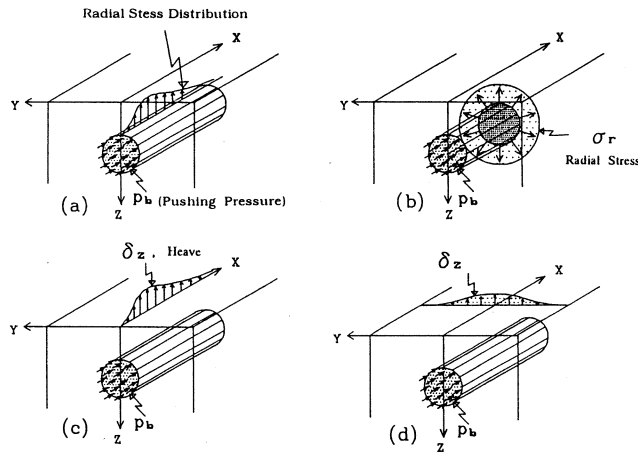


Fig. 2 Pushing Pressure and Heaving Pressure

During tunnelling, both the earth pressure in the cutter frame and the pushing force of the propulsion jack are measured simultaneously to determine the flow rate of soils and the propulsion rate of the shield machine. By subtracting the sum of lateral earth pressure at rest and water pressure from the total propulsion force, the pushing pressure can then be determined. If the relationship between the pushing pressure and heaving pressure is established, the plane strain analysis for the effect of advance-heave and advance-release of the shield becomes feasible.

The radial stress,  $\sigma_r$ , at the periphery of any transverse section of the tunnel and the accompanying ground surface movement under the application of the pushing pressure ( $p_b$ ) are calculated by using the second form of Mindlin's problem in this paper (Poulos & Davis, 1974). Gaussian Quadrature is used to integrate the horizontal pushing pressure over the cross sectional area of the tunnel.

As shown in Fig. 3, four problems have been studied to convert pushing pressure into heaving pressure by using Mindlin's elastic solution in three-dimensional space. For convenience, both the magnitudes of Young's modulus and the horizontal pushing pressure are set equal to one in the analysis. All other geometry are also set non-dimensional.



**Fig. 3 Three Dimensional Advance-Heave Problems**

Problem (a) assesses the variation of stress distribution at the crown of the tunnel in the longitudinal section with the ratio of tunnel depth to tunnel diameter ( $Z/R$ ) and Poisson's ratio,  $\mu$ , as illustrated in Fig. 3 (a). It is found that the maximum stress at the crown of the tunnel occurs at  $0.2 \leq X \leq 0.5$ ; the magnitude of the radial stress varies with  $\mu$  and distance,  $X$  (Fig. 4).

Problem (b) assesses the relationship between radial stress distribution ( $\sigma_r$ ) at the periphery of the tunnel and distance  $X$ ,  $\mu$  and  $Z/R$ , as illustrated in Fig. 3(b). It is seen that for given values of  $\mu$  and  $X$ , the shape of the radial stress distribution is close to a circle if

## EFFECT OF TAIL VOID CLOSURE

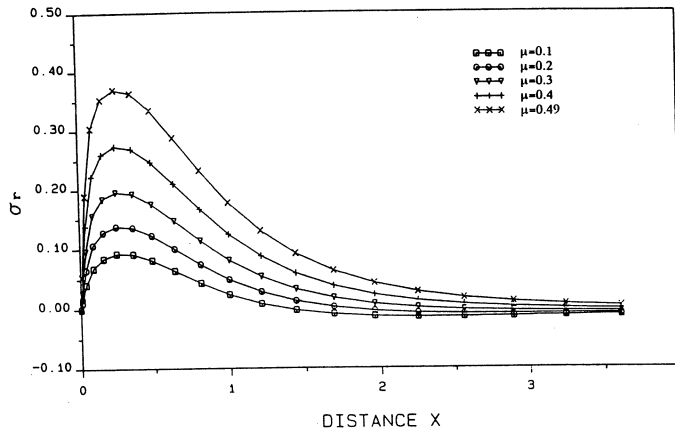


**Fig. 4 Radial Stress Distribution for Problem (a),  $Z/R = 7$ ,  $Y = 0$**

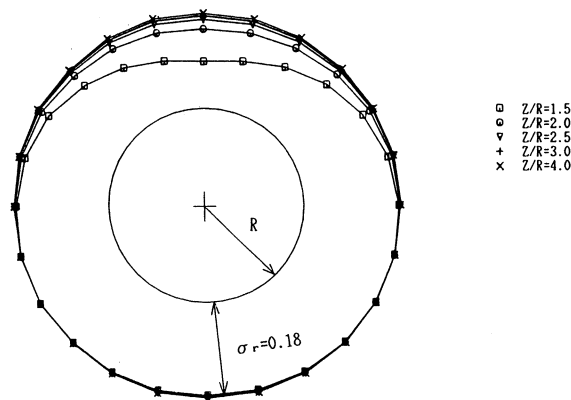


**Fig. 5 Radial Stress Distribution for Problem (b),  $X = 0.5$ ,  $\mu = 0.3$**

$Z/R$  is greater than two (Fig. 5). Therefore, as long as  $Z/R$  is large (i.e. greater than two) it seems appropriate to apply a heaving pressure,  $p_h$  with circular distribution to the periphery of the tunnel in simulating the advance heave of the soil due to the pushing pressure exerted by a shield machine. The distribution radius becomes smaller with increasing  $X$  for given values of  $\mu$  and  $Z/R$  (Fig. 6). The ratio of the maximum radial stress to the pushing pressure,  $\sigma_r/p_b$  (at  $0.2 \leq X \leq 0.5$ ) for each  $\mu$  is summarized in Table 1.

Problem (c) assesses the variation of ground surface heave,  $\delta_z$  along the direction of the tunnel with  $Z/R$  and  $\mu$  (Fig. 3(c)). It is found that the distance of the maximum ground surface heave ahead of the shield face increases with  $Z/R$ . However, it does not change with the variation of  $\mu$  for a given value of  $Z/R$ . The magnitude of  $\delta_z$  decreases with increasing  $Z/R$ .

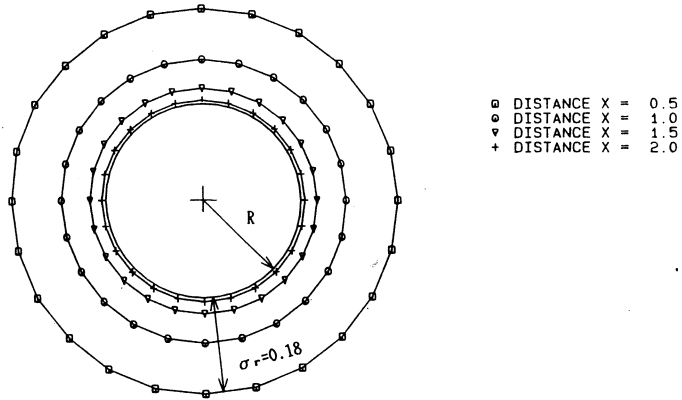


Fig. 6 Radial Stress Distribution for Problem (b),  $Z/R = 7, \mu = 0.3$

Table 1 Relationship of  $p_b, \sigma_r, p_h$  and  $\mu$

	$\mu$			
	0.2	0.3	0.4	0.49
$\sigma_r / p_b$	0.12	0.18	0.25	0.34
$p_h / \sigma_r$	1.8	2.1	3.2	25.0
$p_h / p_b$	0.22	0.37	0.8	8.5

Problem (d) assesses the variation of ground surface heave distribution in the direction perpendicular to the tunnel axis with the values of  $Z/R, \mu$  and  $X$  (Fig. 3(d)). Fig. 7 shows the distribution of ground surface heave with the variation of  $Z/R$  and  $\mu$ . It shows that the value  $Y$  where  $\delta_z$  approaches zero is about the same for all  $X$ . In other words, the width of

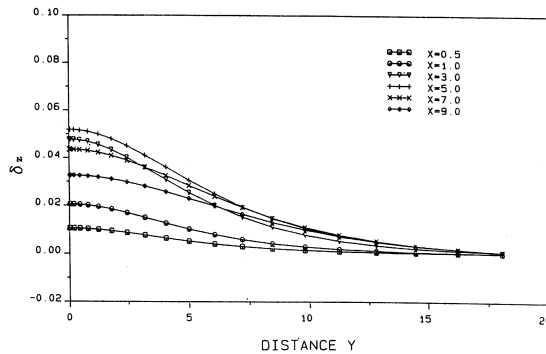


Fig. 7 Heave Distribution for Problem (d),  $Z/R = 7, \mu = 0.3$

## EFFECT OF TAIL VOID CLOSURE

the heave occurring is independent of  $X$  and  $\delta_z$ . This findings are significant in the use of plane strain analysis for simulating the tunnelling process.

As described in the previous paragraphs, the magnitude of radial stress, which is independent of  $Z/R$  if  $Z/R$  is greater than two, is in proportion to the magnitude of the heaving pressure. Consequently, values of  $Z/R$  greater than two have no significant influence on the magnitude of the heaving pressure. For simplification, a value of  $Z/R$  equal to seven is arbitrarily selected in order to convert pushing pressure in three-dimensional space to heaving pressure in plane strain analysis.

Fig. 8 gives the finite element mesh for plane strain analysis with  $Z/R = 7$ . Both the radial stress and heaving pressure are independent of  $Z/R$  if  $Z/R > 2$ , as demonstrated previously. The equivalent heaving pressure, whose magnitude is initially assumed to be the maximum radial pressure occurring at  $X = 0.5$ , is applied on the periphery of the tunnel in a circular shape distribution. The ground surface heave obtained from plane strain finite element analysis is then compared with the maximum ground surface heave from Mindlin's solution in three-dimensional space. The heaving pressure is adjusted until the result from the plane strain finite element analysis and from Mindlin's solution is in close agreement. For given values of  $\mu$ , the relationship between the heaving pressure and radial stress ( $p_h/\sigma_r$ ) is obtained and shown in Table 1. Finally, the relationship between the heaving pressure and pushing pressure ( $p_h/p_b$ ) can be established as shown in Table 1.

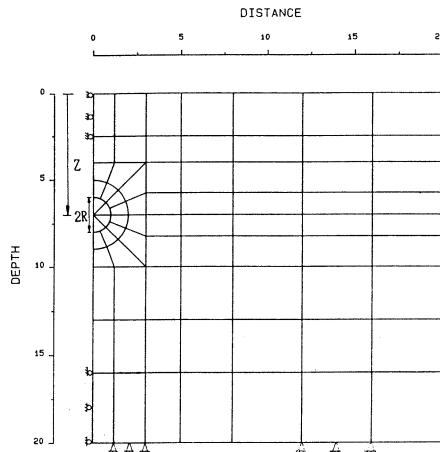


**Fig. 8 Finite Element Mesh for the Shield Tunnelling Problem with  $Z/R = 7$**

## TAIL VOID CLOSURE

During the tunnelling process, a tail void is created between the lining and the outer edge of the shield. After the lining is separated from the shield, the shield is normally allowed to fall down the bottom of the tunnel. The soil around the tunnel then moves



into the void, which in turn causes the ground surface settlement. In an idealized tunnel construction, the maximum ground surface settlement, at the limit, can be equal to twice the average length of the tail void.

Generally, two analytical methods can be adopted to study the effects of tail void closure on ground surface settlement. These methods are summarized as follows:

- (1) The unloading pressures with circular or elliptical distribution, with magnitude equal to the initial stresses at the depth of the tunnel, are applied on the periphery of the tunnel based on the concept of lining design.
- (2) The equivalent nodal forces induced by the elimination of the elements in the excavated zone are calculated as follows:

$$[F] = \int_v [B]^T [\sigma] dV - \int_v [N]^T \gamma dV \quad (1)$$

where  $[F]$  denotes the vector of the equivalent nodal forces;  $[B]$  denotes the strain-displacement matrix;  $[\sigma]$  is the vector of excavated element stresses;  $[N]$  is displacement shape function;  $\gamma$  is gravity. The equivalent nodal forces are then applied on the outer edge of the tunnel, and the ground surface settlement is calculated through the finite element routines.

Both of the two methods use unloading pressure as a simulation of tail void closure; therefore, excessive movements of the soil around the tunnel may occur due to the free movements of the boundary. It is necessary to limit the magnitude of soil movements during analysis in order to meet the real condition, where the actual soil movements do not exceed the total amount of tail void. This limitation greatly increases the difficulty in finite element simulation. Finno (1983) and Clough et. al. (1985) used the first method to study the effects of tail void closure. They applied the loading increments on the soil elements around the tunnel to cause the soil to deform inwardly. The lining elements do not activate until the displacement at the crown of the tunnel equals the tail void. Under such circumstances, no excess soil movements around the tunnel will occur. It is found that for this method, two uncertainties need to be overcome: (1) If the increment of unloading pressure is too large, the movement of the soil around the tunnel may exceed the tail void. On the other hand, it may require too much computation time if each unloading increment is too small, and (2) The soil masses connected to the lining elements will undergo large deformation when they approach failure. Therefore, there is no guarantee that the lining elements can keep their original shape before they activate. It is found that the accuracy of analysis is greatly affected when it is carried out using irregular shapes for the lining elements. It is also found that for the second method, the tunnel has a clear upward movement under the action of unloading pressure, which contradicts field observation. For these reasons, the tail void closure is simulated in this study by moving each nodal point connected to the tunnel inwardly to a new position, where the soil masses can finally settle. Therefore, reasonable simulation for tail void closure may be obtained as long as a suitable amount of tail void is selected.

For free field conditions, the closure of the tail void can be determined by using an equal-angle movement (Fig. 9) or closure potential, but it must be determined through

## EFFECT OF TAIL VOID CLOSURE

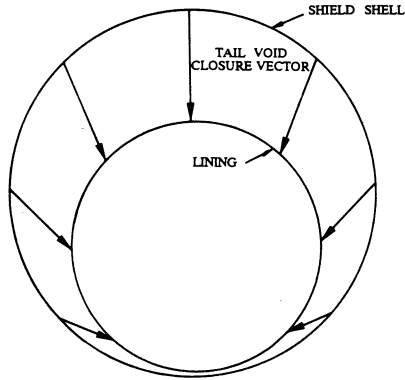


**Fig. 9 Normal Closure Vector of Tail Void**

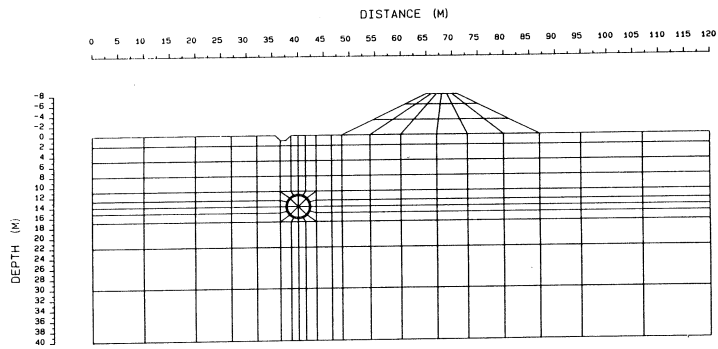


**Fig. 10 Finite Element Mesh for the Case Study**

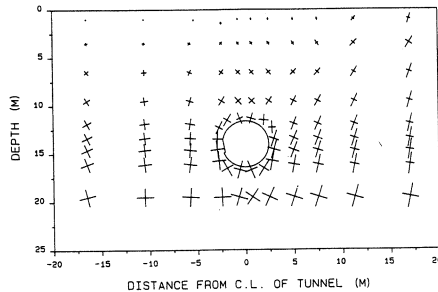


**Fig. 11 Magnitude and Orientation of Principal Stresses due to the Effect Advance-Heave and Advance-Release**

closure potential for non-free field condition. The closure potential is defined as the most possible tendency of closure, which can be obtained by plotting displacement contours either from field observations as shown in Fig. 11, or from finite element analyses. However, there is no information available regarding ground settlement before a tunnel is

excavated. Consequently, the closure potential can be estimated through the calculated displacement from the viewpoint of rational analysis.

### ANALYSIS EXAMPLE

In an idealized tunnel construction, tail void closure is the major cause of the ground movement. However, imprudent construction actions such as pitching and yawing of the shield machine may result in considerable increase of ground movement. Ground movement resulting from operational defects is not predicted in this analysis. It will be minimized in the future as the tunnel construction technology improves. Currently it is difficult to obtain a shield tunnelling case study from the literature where ground movement is dominated solely by the tail void closure. Therefore, an actual shield tunnelling is analyzed here to illustrate how the analysis procedure can predict the effect of tail void closure on the ground movement.

A sewage tunnel located near the Ell-Chong Flood Way in Taipei was constructed 12 m below the ground surface using slurry shield (Lee et al, 1990). The shield machine has 4.83 m outer diameter. The outer and inner diameters of the lining are 4.7 m and 3.80 m, respectively. The average length of the tail void is 65 mm. Adjacent to the tunnel alignment at ground surface is an 8 m high, trapezoidal embankment constructed with gravelly soil. The top and the base of the embankment are 6.0 m and 39.0 m, respectively. The embankment runs parallel to the tunnel at 9.0 m horizontal distance. A small ditch, 3.0 m wide and 1.0 m deep, is located above the tunnel. The ground condition and the basic material properties at the monitoring site are shown in Table 2.

#### Gravity

The magnitude of the initial stresses has a major effect on the results of analysis during nonlinear analysis. This is because the stiffness matrix of a finite element is dependent on the stress state within the element. The full finite element mesh, considering the existence of the embankment and the ditch, is shown in Fig. 10. The 8-node isoparametric

**Table 2 Soil Properties at the Monitoring Site**

Depth (m)	Soil type	N-value (blow/ft)	$W_n$ (%)	LL (%)	PI (%)	$G_s$	Silt Content (%)	$\gamma$ (t/m <sup>3</sup> )
2	silty sand (SM)	8-12	15	-	NP	2.72	25	1.95
5	silty clay(CL-ML) or clayey silt	1-6	30-45	34	12	2.70	78	1.84
17	silty sand (SM)	4-20	20-31	-	NP	2.72	25	1.93
40	silty clay(CL)	2-9	25-32	27	9	2.74	75	1.87

$W_n$ : water content; LL: plastic limit;  $\gamma$ : unit weight of the soil  
PI: plastic index;  $G_s$ : specific gravity

## EFFECT OF TAIL VOID CLOSURE

quadrilateral element is used for the study. Except for the embankment element, for all other elements the effective horizontal stress is equal to the effective vertical stress multiplying the coefficient of lateral earth pressure at rest ( $K_0$ ). The total stresses are equal to the sum of the effective stresses and pore water pressure. The embankment is then analyzed by the simulation of three construction increments. The change of the stress is then added into the initial stress in each element.

### Advance-Heave and Advance-Release

According to the principles of cutting face stability of the slurry shield, the relationship between the pushing pressure and the lateral earth pressure is

$$P_b = P_c - P_o \quad (2)$$

$$P_a < P_c < P_p \quad (3)$$

where  $P_a$  = the sum of Rankine's active pressure and water pressure

$P_o$  = the sum of lateral pressure at rest and water pressure

$P_c$  = propulsion pressure

$P_p$  = the sum of Rankine's passive pressure and water pressure

$P_b$  = pushing pressure

The values of  $p_a$ ,  $p_o$  and  $p_p$  are  $16.8 \text{ t/m}^2$ ,  $20.7 \text{ t/m}^2$  and  $65.0 \text{ t/m}^2$ , respectively as derived using the parameters listed in Table 3. To prevent passive failure of the soil and satisfy the requirements of stability for the cutting face, the pushing pressure must be less than  $44.3 \text{ t/m}^2$ .

For the purpose of balancing the earth pressure, the total propulsion force of the jacks in the shield machine should generally be larger than the lateral earth pressure at rest but less than the passive pressure. The allocation of the jacks depends on the soil condition, the cross sectional area of the tunnel and the required propulsion force. A typical jack in a shield machine usually provides 100 t of the maximum propulsion force and brings a 40% ~60% capacity of the maximum force during the advancing process. The shield machine having nineteen propulsion jacks can produce  $54.6 \text{ t/m}^2$  of propulsion pressure over the 4.83 m diameter of the shield. The value of pushing pressure,  $p_b$  is derived to be  $33.9$

$\text{t/m}^2$  by subtracting the earth pressure at rest from  $54.6 \text{ t/m}^2$ . According to the relationship in Table 1, the heaving pressure,  $p_h$  is obtained equal to  $12.6 \text{ t/m}^2$  for  $\mu = 0.3$ . The heaving pressure is then applied at incremental loads of  $2.5 \text{ t/m}^2$  on the edge of the tunnel with each load increment iterated twice for the purpose of increasing the accuracy of analysis. Finally, the same amount of unloading pressure would be acting on the edge of the tunnel, and the displacements and stresses in each element due to the effects of advance-heave and advance-release can be obtained.

The magnitude and orientation of the principal stresses for each element are shown in

Fig. 11. This figure indicates that the magnitude of the ground surface heave which is less than 2 mm is very small. The possible influence range of the Rankine's active pressure estimated based on the parameters listed in Table 3 due to shield advance is approximately 16 m to 30 m ahead of the shield face. The field measurements for the ground surface heave within this range are very limited. Except that 8 mm and 3 mm ground surface heaves are obtained at 36.2 m and 22.2 m ahead of the shield face, respectively, all other settlement points did not yield significant measurements of ground surface heave. The results of the analyses are reasonably close to the observation. Therefore, the simulation of heaving effects due to shield advance using the plane strain finite element analysis based on the relationships shown in Table 1 appears reasonable.

Table 3 Soil Parameters used in the Finite Element Analysis

Soil Layer	Depth (m)	$c$ (t/m <sup>2</sup> )	$\phi$ (deg)	$R_f$	$K$	$K_{ur}$	$n$	$\mu$
Embankment	-8	0	39	0.7	600	800	0.4	0.3
1	2	0	35	0.7	600	800	0.4	0.3
2	5	1.7	0	0.9	150	200	0.90	0.49
3	17	0	35	0.7	600	800	0.25	0.3
4	40	1.5	20	0.7	150	200	0.45	0.49

### Tail Void Closure

When the shield machine passes through the silty sand layer (SM), the tail void has the tendency to close immediately due to lack of cohesion. Back grouting, which is carried out after installation of three to five segments of lining, may not be effective in preventing the closure.

Fig. 12 shows the displacement vector of each nodal point obtained by applying the equivalent nodal forces generated by eliminating the excavated soil elements on the edge of the tunnel with free support system. The magnitude and orientation of principal stresses are shown in Fig. 13. It is shown that the main closure vectors come from the top of the tunnel and that the closure potential is larger for the embankment side. It is noted that the closure potential obtained from the analyses has the same trend as that of the field observation.

In this case, the average length of the tail void is 65 mm. According to the preceding discussion, it is reasonable to use twice the average length of tail void as maximum closure, which is equal to 130 mm, in the analysis. The direction of the movement of the soil elements around the tunnel should be adjusted with respect to a certain angle,  $\theta$  due to the existence of the embankment. Fig. 14 shows the closure direction based on the soil displacements shown in Fig. 12. After the determination of the closure vector, the analysis is performed by moving the soil connected to the shield inwardly with four increments of loading with

## EFFECT OF TAIL VOID CLOSURE

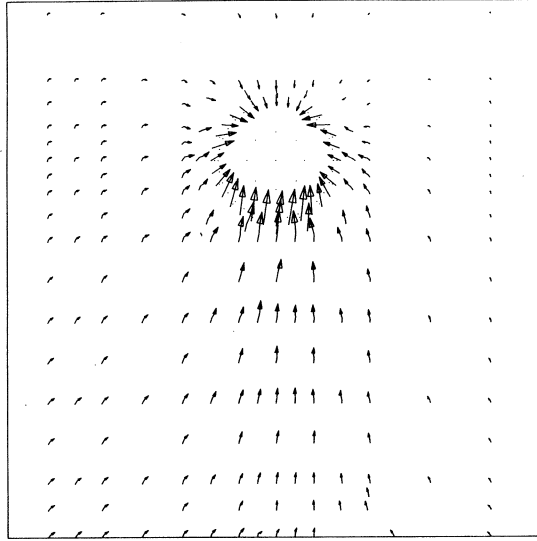


**Fig. 12 Closure Closure Obtained from the Finite Element Analysis**

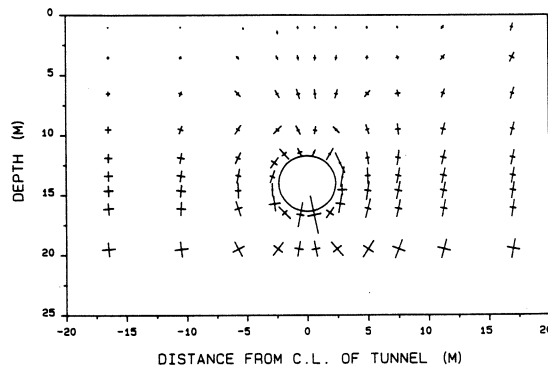


**Fig. 13 Magnitude and Orientation of Principal Stresses due to Tail void Closure**

each loading increment iterated twice. The initial stresses at this stage are obtained from the results of the analysis on the shield advance process.

### Lining Installation and Activation

The lining will activate and deform at the time the tail void is closed. The lining deformation, which may cause additional ground settlement, is also taken into account in the analysis. This is done by replacing the soil material at the position of the lining element with lining material. The equivalent nodal forces generated due to the removal of soil

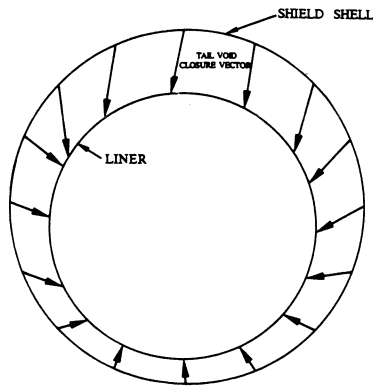


**Fig. 14 Vector of Closure Potential**

elements in the excavated zone are then applied on the lining. The effect of the dead weight of the lining is also included in the analysis. The results of the analysis show that the vertical and horizontal compression of the circular lining are  $10\text{ mm}$  and  $6\text{ mm}$ , respectively. The corresponding compressibility is  $0.2\%$  and  $0.11\%$ , respectively. Therefore, it can be concluded that the lining deformation has a negligible effect on the ground surface settlement.

### **Long-Term Consolidation**

The shield machine passes through the sandy soil layer which has relatively higher permeability where the excess pore pressure can dissipate quickly. The behavior is therefore typically drained. As indicated in Table 3, the thicknesses of the clay layers are relatively thin, and therefore the consolidation settlement should be very small. This consolidation effect is not considered in the analysis.

Figure 15 shows the comparison of the settlements obtained from the field measurements with those from the finite element analyses for various depths. As illustrated in the figure, the embankment side yields the larger settlement. The maximum amount of settlement obtained from the analysis at  $1\text{ m}$  above the tunnel (i.e. mainly coming from the tail void closure) is  $130\text{ mm}$  which is very close to the observed value. However, the observed settlements at  $5\text{ m}$  below the ground surface as well as that at the ground surface are larger than the calculated values. It is noted that the observed magnitudes of settlement at shallower depths above the tunnel are larger than that immediately above the tunnel. Such behavior is unlikely in the idealised situation. It may be due to the other (operational) factors such as the pitching and yawing of the shield machine during its advancement, which cause additional settlements. It is difficult to simulate operating factors of the shield machine or poor construction during idealised analysis. In such circumstances, the ground settlement is better calculated by empirical method of Peck (1969) as indicated in Fig. 15,

## EFFECT OF TAIL VOID CLOSURE

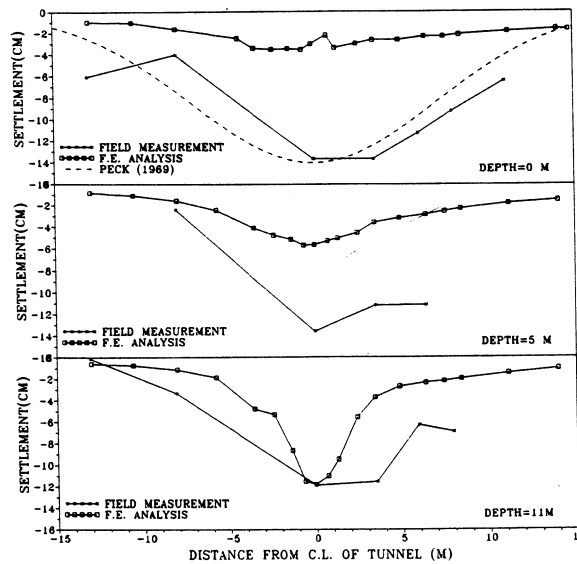


**Fig. 15 Calculated Settlements and Measured Settlements**

where the distance of inflection point from centerline of the tunnel ( $i$ ) is equal to 7.1 m.

Fang & Lin (1992) observed ground surface settlement caused by blind shield tunnelling through the Taipei silt in a sewage disposal project. This case is considered to have good construction quality. The tunnel depth is about 8.5 m. Since the shield has 65 mm of average tail void, the maximum tail void closure should be as much as 130 mm. In this case, only 59 mm of the maximum settlement at the ground surface was observed. The ratio of maximum settlement to maximum tail void closure is about 0.45 (tunnel depth = 8.5m). In the case of this paper the ratio from finite element analysis is only 0.3. This value seems reasonable because the case in this paper has greater tunnel depth (12.5m).

## CONCLUSIONS

Except for unusual construction effects, the tail void closure is the major cause of ground movement in the sandy soil. Additional ground movement may be induced by poor construction technique, which is unpredictable. The result of the finite element analysis of tail void closure is heavily affected by the magnitude of initial in situ stresses. The initial stress will change as the results of a shield machine advancing and passing a particular point along the tunnel alignment. This is a three-dimensional problem, however, the cost of three-dimensional analysis with nonlinear soil properties is prohibitive because of the complex pre-processing, post-processing works and enormous computation time required. In this paper, a converting procedure simulating the heaving effects produced by the advancement of the shield machine was developed. Plane strain analysis rather than



three-dimensional analysis can therefore be used in the simulation. Using boundary displacement whereby the closure direction was determined through the closure potential was found to be suitable for the analysis of tail void closure. The results observed using this analysis method are indirectly confirmed by a case study comparison .

#### **ACKNOWLEDGEMENTS**

Financial support for these studies was provided by a grant from the National Science Council at Taiwan under Grant No. NSC80-0410-E011-22. This support is gratefully acknowledged.

#### **REFERENCES**

- CLOUGH, G.W., SHIRASUNA, T. and FINNO, R.J. (1985). "Finite Element Analysis of Advanced Tunneling," Proceeding of the 5th International Conference on Numerical Methods in Geomechanics, Nagoya, Vol. 2, pp.1167-1174.
- CORDING, E.J. and HANSMIRE, W.H. (1975). "Displacements Around Soft Ground Tunnels," Proceeding of the 5th Pan-American Conference on Soil Mechanics and Foundation Engineering, Buenos Aires, pp. 571-633.
- DUNCAL, J.M. and CHANG, C.Y. (1970). "Nonlinear Analysis of Stress and Strain in Soils," Journal of the Soil Mechanics and Foundations Division, ASCE, Vol. 94, No. SM5, pp. 637-659.
- FANG, Y.S. and LIN, G.J. (1992). "Settlement Caused by Blind Shield Tunnelling through Taipei Silt," Tunnels and tunnelling, November, pp. 22-24.
- FINNO, R.J. (1983). "Response of Cohesive Soil to Advanced Shield Tunnelling," Ph.D. Dissertation, Department of civil Engineering, Stanford University, California.
- LEE, C.C., YAU, S.L. and UENG, B.(1990). "Shield tunnelling and Ground Settlement," Mining Technology, Vol.28, No.1, Taiwan (in Chinese).
- PECK, R.B. (1969). "Deep Excavation and Tunnelling in soft Ground," Proceedings of 7th International Conference on Soil Mechanics and Foundation Engineering, Mexico city, State-of-the-Art Volume, pp. 225-290.
- POULOS H.G., and DAVIS, E. H. (1974). "Elastic Solution for Soil and Rock Mechanics," Wiley and Sons, New York, New York.

# SOIL PARTICLE MIGRATION THROUGH SLOTS IN DRAINS - I, UNIDIRECTIONAL FLOWS

B. Tahar<sup>1</sup> and T.H. Hanna<sup>2</sup>

## SYNOPSIS

The silting of drains is a well known phenomenon. Attempts are made to prevent soil particle migration by the use of a filter surround. A special apparatus is used to simulate, in a realistic manner, the flow in the vicinity of a slot which is believed to be representative of an opening or crack in a drain. The soil loss through the slot was recorded as a function of time, for several values of applied water head and slot width. Three sand filters - fine-to-medium, fine-to-coarse and gap-graded were used.

The critical slot width can be related to the  $D_{85}$  size and values of slot width/ $D_{85}$  size ratio are in the range 2 to 4, much less than currently used values. For gap-graded soil the same limits apply provided that the coarser material does not allow the finer fractions to migrate.

## INTRODUCTION

It is now recognised by the construction industry that the development of voids in the ground surrounding structures can be of critical significance when the integrity of the structure is being evaluated. Examples which come to mind are the migration of soils through openings in walls (sheet piled, contiguous bored, soldier pile and timber lagged), through openings and cracks in drains, sewers and tunnels, through the joints between the facings of reinforced earth and through joints between paving slabs. In general, soil migration is only likely to be of significance where there is water flow. The general subject of void stability has been addressed by many studies particularly those related to tunnel openings, Atkinson & Potts (1977), Atkinson & Mair (1981).

In contrast to the problems posed by the formation of voids near to civil engineering structures, the question of how soil in contact with an opening in a structure may behave, as water flows towards or away from the structure, has to be addressed. Some or all of the adjacent particles may migrate through the opening in the structure to cause loss of support to nearby services and foundations. The structural member (eg drain, wall facing) may remain substantially intact yet ground movement and possible collapse of facilities (eg road surfaces) may occur solely as the result of soil migration. This general subject is not a new one but the emphasis of this paper, and a companion paper (Tahar & Hanna, 1995), is on a general experimental study of soil particle migration through openings due to hydraulic flow.

---

<sup>1</sup> Institut National de L'Enseignement Superieur D'Hydraulique de Chlef, Clef, Algeria.

<sup>2</sup> Professor Emeritus, 288 Ecclesall Road South, Sheffield, S11 9PT, UK.

It has been reported by the Water Research Council (1983) that many clay sewer pipes built before 1920 have lost their jointing because puddle clay was used to seal the joints. Brick sewers lose their mortar leaving the bricks loose and, as a consequence, the sewers leak. It is well known that all sewer systems suffer from leakage and infiltration. This problem is not confined to the UK but occurs world-wide. Early studies were in progress in the US over thirty years ago into leaks in drains, Nettles & Schomacher (1967).

As part of a more general study into ground volume changes caused by construction-related activity, an investigation has been in progress for some time into the behaviour of soil surrounding buried pipes with an opening in the pipe wall. Both unidirectional and reverse water flows through the opening have been simulated. This paper considers unidirectional flows.

### **PREVIOUS RELATED STUDIES**

The prevention of soil migration is an essential feature of the design of subsurface drains, well casings, rock-fill dams, break-waters and protective filters.

All soil granular materials comprise a range of particle sizes and a range of constriction sizes. A distinction must be made between pore size and constriction size. The constriction size is the opening between and connecting two pores, the size being the diameter of grain which will pass through a particular constriction. Kenney et al (1985) discuss constriction size. The primary purpose of filters is to prevent soil particles being transported through the pores of the filter by water flow, yet permits the easy flow of water. In general, the larger particles in the filter (in this paper the soil material adjacent to the opening is referred to as the filter material) gradually block the larger entry openings and, thereafter, the filter is stable. Many studies of filter stability are reported, primarily in the USA. Useful recent reports summarise the findings of these early works, draw attention to their limitations and chart a possible route, Sherard et al (1984). An even more comprehensive review is given by Kenney & Lau (1985) of the grading stability of compacted granular materials. In some of their tests the specimens were subjected to downwards seepage and vibrational forces to encourage particles to move towards the bottom of the specimen. At the end of the test the grain size distribution at various levels was determined and compared with the initial grading.

The flow of water through a granular soil may "pipe" the soil particles away and, consequently, filters are used in the belief that they provide internal stability. However, internal stability cannot be corrected by the use of external filters, Kenney et al (1985), Kenney & Lau (1985). The subject of conventional piping is covered in most standard textbooks, Terzaghi & Peck (1967). To prevent the mechanism of a pipe developing the "erodible" soil must never be in direct contact with an opening larger than some of the coarser particles. The question is - what size is necessary to retain the first eroded particles? A different form of soil movement due to water flow is described by Wittmann (1979) and has been under study for many years, Kovacs (1981). Mixtures with a gravel skeleton may allow the transport of sand-size particles through the gravel skeleton, the phenomenon

## SOIL PARTICLE MIGRATION THROUGH SLOTS-I

being referred to as “suffusion”, where a net transport out of the skeleton occurs, and “col-matation” where transport into the coarse skeleton occurs.

The design of filters has been based upon a ratio relating a certain size of the filter to some size of the material to be protected, the base, and to the size of the perforation in the structure (the drain, for example). The USCE (1953) carried out studies in the 1940's on wooden pipes perforated with slots and circular openings. They concluded: (i) if the size opening/ $D_{85}$  ratio  $< 0.83$ , no washout will result; (ii) more soil was lost through slots than circular openings; (iii) the filters were stable as related to the openings in the well screen if the 0.5 inch hole size opening/ $D_{85}$  ratio was 0.83 to 0.7. Unfortunately, in these tests, the filter materials around the well screen were not compacted in a controlled manner. Other similar criteria are quoted by Cedergren (1967). Further work is reported by Nettles and Schomacher (1967) to determine the susceptibility of filter materials passing into drains through openings in joints. They concluded: (i) the factors which affected soil infiltration were opening size, grain size, plasticity, density and the nature of the flow path through the opening; (ii) the critical ratios of the width of the joint opening to  $D_{85}$  were  $< 0.36$  for fine-to-medium sand,  $< 0.48$  for uniform sand; (iii) total washout generally occurred in silts well compacted, with openings  $> 2.67$  mm; (iv) for fine soils (plasticity index  $> 12$ ), there was no infiltration for compaction  $> 85\%$  maximum density.

Many studies are reported for filter stability and useful reviews will be found in Karpoff (1955), Thanickachalam & Sakthivadirel (1974) and Sherard et al (1984).

From an examination of the reported data, and after further discussion with the construction industry, the following variables were identified for detailed study:

1. the opening size of the slot in the drain wall;
2. a range of filter gradings;
3. a range of unidirectional flow conditions with the capability of recording the rate of soil loss with flow time;
4. the ability to simulate reverse flow conditions.

### THE TEST SIMULATION

The simplest form of simulation was a rectangular box formed of thick perspex. A sketch of the apparatus shows all the main features, Fig. 1. The inner dimensions were  $150 \times 270$  mm cross-section and 400 mm high. The top and bottom end were detachable perspex sheets. The bottom plate had a 60 mm diameter conical funnel attached to collect the washed-through particles. A set of three perspex plates, two fixed and one moveable, enabled horizontal gaps up to 10 mm to be formed, the size of the gap being monitored by dial gauge. Three sets of apparatus were prepared, each with the facility for unidirectional or reverse flow. The layout of the water pressure control system is shown in Fig. 2.

Sand was placed in the upper compartment of the apparatus by pouring from a fixed

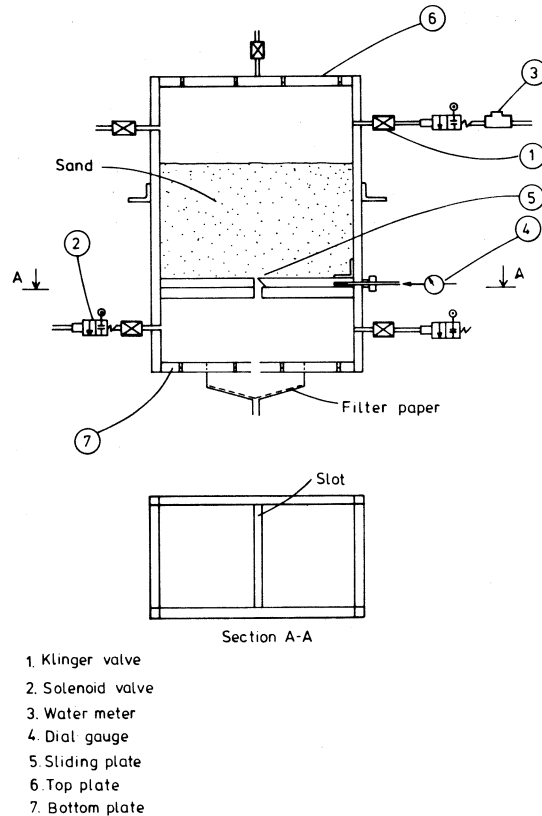


**Fig. 1 The Test Apparatus Sand Container and Slot Opening Arrangement.**

height. The sand could also have been compacted to any required denseness by a special drop hammer. By regulation of the height of drop, a constant relative density of 80% was achieved.

The water head system comprised a header tank with a head of 2.1 m. The variable heads were maintained at constant values by means of overflow outlets at the base of each moveable tank. In the unidirectional flow tests, water entered the top of the apparatus, flowed through the specimen and exited through the slot in the sliding plate, carrying fines through to be collected in a special filter box beneath the bottom plate. The apparatus also had a reverse flow capability and simulated a surge passing along a drain with the water pressure inside greater than the external pressure. Under this condition, water would flow back through the slot. This reverse flow was believed to cause a "sieving action" whereby the water would flow in different directions after short time intervals. The reverse flows were controlled by solenoid valves. The variable head required was connected to the inlet through one solenoid valve and the tank which contained the outlet through the second

## SOIL PARTICLE MIGRATION THROUGH SLOTS-I

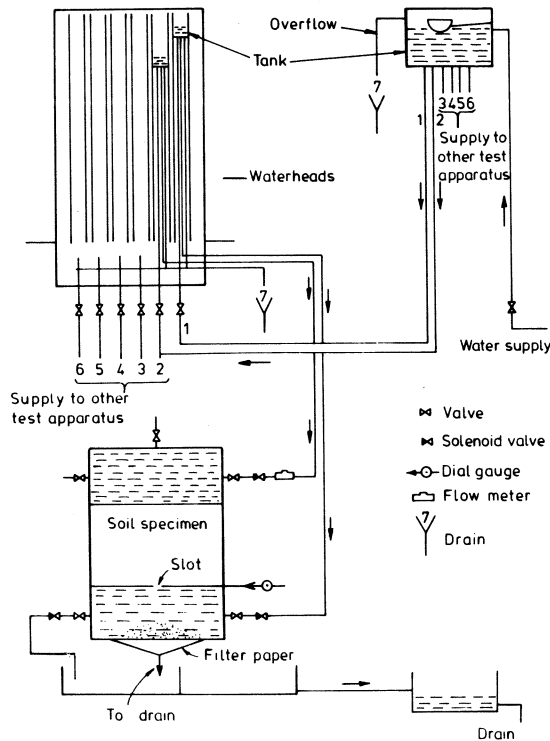


**Fig. 2 The Water Flow System.**

solenoid. The water valve controller could provide a range of cyclic heads and time intervals with both manual and preset control up to 100,000 cycles of reverse flows. The flows through the samples (such measurements were taken only in a few tests) were measured by a volumetric water meter, the soil loss being recorded on a filter paper trap below the bottom of the exit opening. The size of the gap opening was verified throughout the test by reference to the dial gauge and at the end of the test by precise feeler gauge measurement.

Details of the set-up and precautions taken are given by Tahar (1987). All specimens were placed at a relative density of 80%. The specimens were saturated from the bottom by applying a back pressure to the bottom of the specimen, which forced most of the air out of the sand through the top plate valve. Initially the back pressure, equivalent to 0.01 m head, was maintained for 40 minutes to ensure equalization of the level of water head in the supply tank and the apparatus. The back pressure was then increased to 2.5 kN/m<sup>2</sup> and the specimen was considered to be saturated when the level of water above the soil specimen was equal to the level in the supply tank. A surcharge pressure equal to the head of water was placed on the surface of the specimen via a perforated plate to prevent an increase of volume during the saturation process. After having completed the saturation phase, the

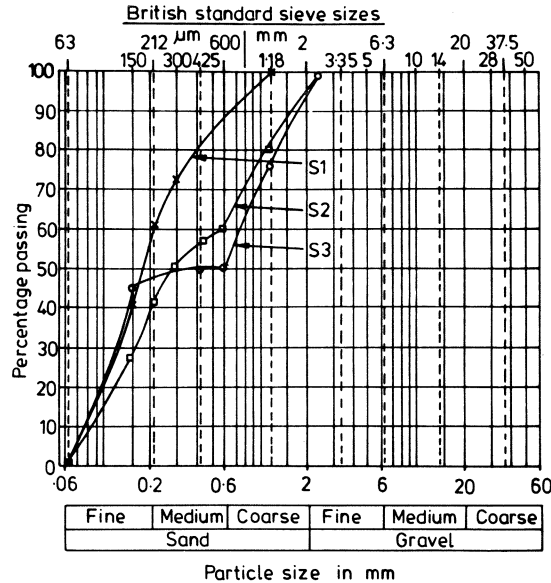


Fig. 3(a) Grain Size Distribution Curves for Test Sands.

upper part of the container was filled with water and the water was drained from the lower part. The side valve, attached to the constant head supply, was opened to start the test. The soil loss from the specimen was collected in the filter trap and the quantity recorded as a function of time. The tests were run for a period of at least 60 minutes or until a complete washout occurred.

Test Materials

Sub-rounded Leighton Buzzard sand was used, different gradings being blended to produce three specimens with gradations similar to those used as filter back-fill around drains. The grading curves of the specimens, Fig. 3 (a), show well-graded fine-to-medium sand ( $s_1$ ), well-graded fine-to-coarse sand ( $s_2$ ) and gap-graded sand ( $s_3$ ). Values of  $D_{85}$ ,  $D_{50}$ ,  $D_{10}$  and  $D_5$  are given in Fig. 3 (b).

The fine-to-medium sand was placed by a pluviation technique. The other two sand types were placed in layers and gently tamped, detail being given by Tahar (1987).

The tests:

Several series of preliminary tests were conducted in which the same specimens ( $s_1$ ) were subjected to increasing heads until either damage to the back-fill occurred or the maximum test head, 2.1 m, was reached. In general the cumulative soil loss through the opening became static after a short period of time but most of the tests continued for at least an hour thereafter. The primary purpose of these tests was to assess the suitability of the

## SOIL PARTICLE MIGRATION THROUGH SLOTS-I

	Specific Gravity	D85 mm	D50 mm	D10 mm	D5 mm
S1 Fine to medium sand	2.660	0.50	0.16	0.11	0.09
S2 Well-graded sand	2.665	1.50	0.30	0.09	0.08
S3 Gap-graded sand	2.670	1.70	0.60	0.08	0.07

**Fig. 3(b) Properties of The Test Sands**

apparatus, to evaluate the effects of test duration, head applied and opening width and to check the experiment repeatability. The remainder of the tests were conducted on the three soil types (Figure 3) and were a continuation of earlier work of Nettles & Schomacher (1967). The applied head was 1.2 m and the opening size was related to the specimen  $D_{85}$  value, Fig. 3 (b).

## RESULTS

### Preliminary Tests

Tests P2 and P3 were used to verify the cumulative soil loss values of the test P1. The results, Fig. 4, are very similar with the exception that there are small difference during the first five minutes of test. Beyond that time period, excellent agreement resulted. The repeatability of test was assessed, as defined in BS 812, British Standards Institution (1984) for  $r_1 = 2.8 v_r$ , where  $v_r$  is the repeatability variance and  $r_1$  the value of repeatability below which the absolute difference between two single results may be expected to lie with a probability of 95%. For the three test results, and taking the cumulative soil loss figures for the time 25 minutes, the repeatability value.  $r$ , is 106 which is greater than the maximum absolute difference between the cumulative soil loss values for tests P1 and P2. It is concluded that the soil loss in the test apparatus is reproducible under the same test conditions.

The additional preliminary tests, P4 and P5, assessed the effect of the head of water causing flow, the opening size being constant. In each test the water head initially was low and its value was gradually increased until either a washout occurred or the head capacity of the apparatus was reached. The test duration was varied with the head being held constant until the soil loss was zero. The results of these tests (Table 1) show that for each increase in applied water head a further small quantity of soil was washed through the opening, presumably being the result of the larger hydraulic gradient caused. For all tests, the majority of the migrated soil was produced during the early stages of a test with 80 to 90% occurring within the first 10 minutes. Also, if migration of particles through an



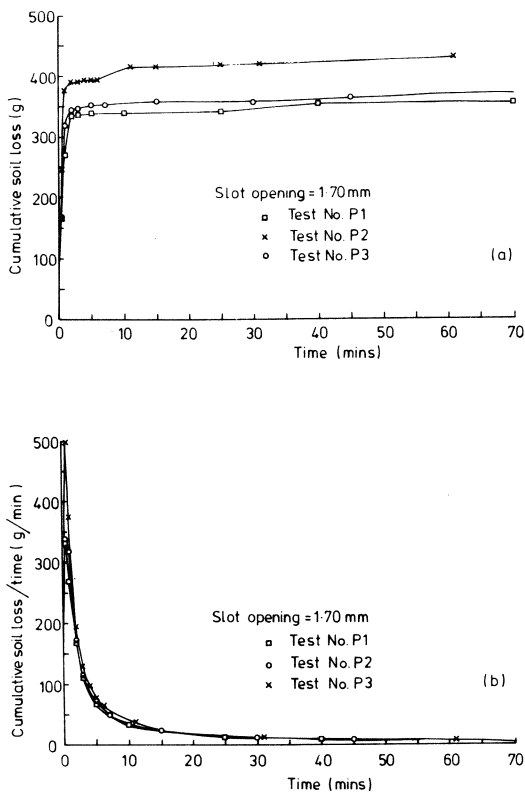


**Fig. 4 Preliminary Test Data Showing.**  
**(a) Cumulative Soil Loss V Time.**  
**(b) Repeatability of Testing.**

opening occurs, it happens within the first few minutes of test.

**Unidirectional Tests:**

The primary purpose of the main series of test was to assess the influence of time, opening size and the nature of the flow on the migration of soil particles and also to determine the critical value of the slot width/ $D_{85}$  ratio to compare it with published values. In all tests, the applied head was 1.2 m and the opening size was related to  $D_{85}$  size because other investigators had concluded that, if the slot size be small enough to hold  $D_{85}$  size particles, then the filter would be stable. The hydraulic gradient in the specimen is not static but varies with the distance from the opening slot as discussed later - (see Fig. 8).

*(i) Fine-to-medium sand ( $s_1$ )*

Six tests were performed with the slot opening increments of 0.05 mm between 1.70 and 1.95 mm. The  $D_{85}$  size of the soil  $s_1$  was 0.50 mm, as determined by dry sieving. The

*SOIL PARTICLE MIGRATION THROUGH SLOTS-I*

**Table 1 Preliminary Tests**

Test No	Slot width (mm)	Test head (m)	Test period (min)	Sand loss (gm)	Remarks
P <sub>1</sub>	1.70	1.20	60	345	
P <sub>2</sub>	1.70	1.20	60	460	
P <sub>3</sub>	1.70	1.20	60	360	
P <sub>4</sub>	1.50	0.65	505	65.1	A small loss occurred for a short time after each change in water head
	1.50	1.50	190	4.5	
	1.50	2.60	565	2.4	
P <sub>5</sub>	1.70	1.00	385	345	moderate infiltration occurred on applying each head increase
	1.70	1.50	120	11	
	1.70	2.70	1057	17	

test with a slot opening of 1.05 mm suffered a total washout after head application of 1.2 m and no data were recorded. The results of the other five tests are plotted in various forms in Fig. 5. The effect of varying the slot width is shown in Figure 5(a) as a function of time. A major cumulative soil loss had occurred before 5 minutes, thereafter the amount of soil loss was very small. For example, for a 1.80 mm slot width, 896 gm of soil were lost during the first five minutes of test with a further loss of 110 gm during the next 3593 minutes. From a practical point of view it may be concluded that, after the initial period of high migration rate, the particles stabilised for this slot width and self-filtering ensued. This stabilisation is shown in Figure 5(b) where the cumulative soil loss/time is graphed against time and in Figure 5(c) where the rate of soil loss/unit time data are given. The cumulative soil loss increased with slot width increase. Figures 5(d) and (e) show the influence of slot width on soil loss for different cumulative periods of water flow. The cumulative soil loss remained constant after five minutes but the rate of soil particle migration increased with slot width increase and time decrease.

*(ii) Fine-to-coarse sand (s<sub>2</sub>)*

Three tests were performed and the results are presented in Figure 6 and summarised in Table 2. The change in cumulative soil loss as a function of time and opening size, in general, was similar to that of the fine-to-medium sand tests. Figure 6(a) shows that the cumulative soil loss increased at the start of a test with slot width increase but, after a period of flow of 5 minutes, the slot widths of 3.0 and 3.1 mm gave similar results. It will be noted that, with the slot width of 3.2 mm, the cumulative soil loss increased with time indicating a total washout condition was developing. However, when these data were plotted as cumulative soil loss/time against elapsed time, a pattern very similar to the s<sub>1</sub> series test data

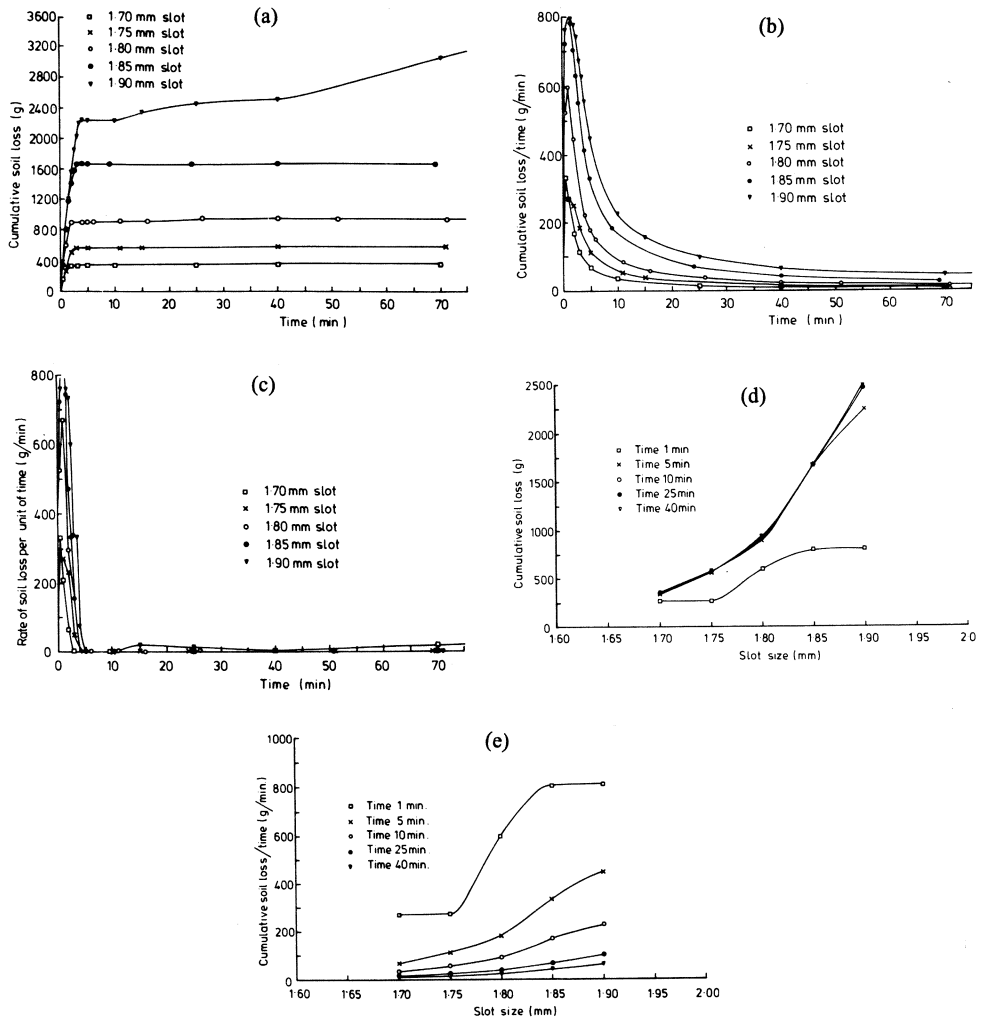


**Fig. 5 Fine-to-medium Sand Tests:**  
**(a) Cumulative Soil Loss V Time.**  
**(b) Cumulative Soil Loss/Time V Time.**  
**(c) Rate of Soil Loss/Unit Time V Time.**  
**(d) Cumulative Soil Loss V Slot Width.**  
**(e) Cumulative Soil Loss/Time V Slot Width.**

emerged, Figure 6(b). The rate of soil loss/unit time data, Figure 6(c), show very high losses during the first 10 minutes of test but, thereafter, the rate was relatively constant for all slot widths. The cumulative soil loss, for a given flow time, increased with slot size increase, Figure 6(d, e). As the fine particles are gradually removed leaving a matrix of coarser sizes

## SOIL PARTICLE MIGRATION THROUGH SLOTS-I

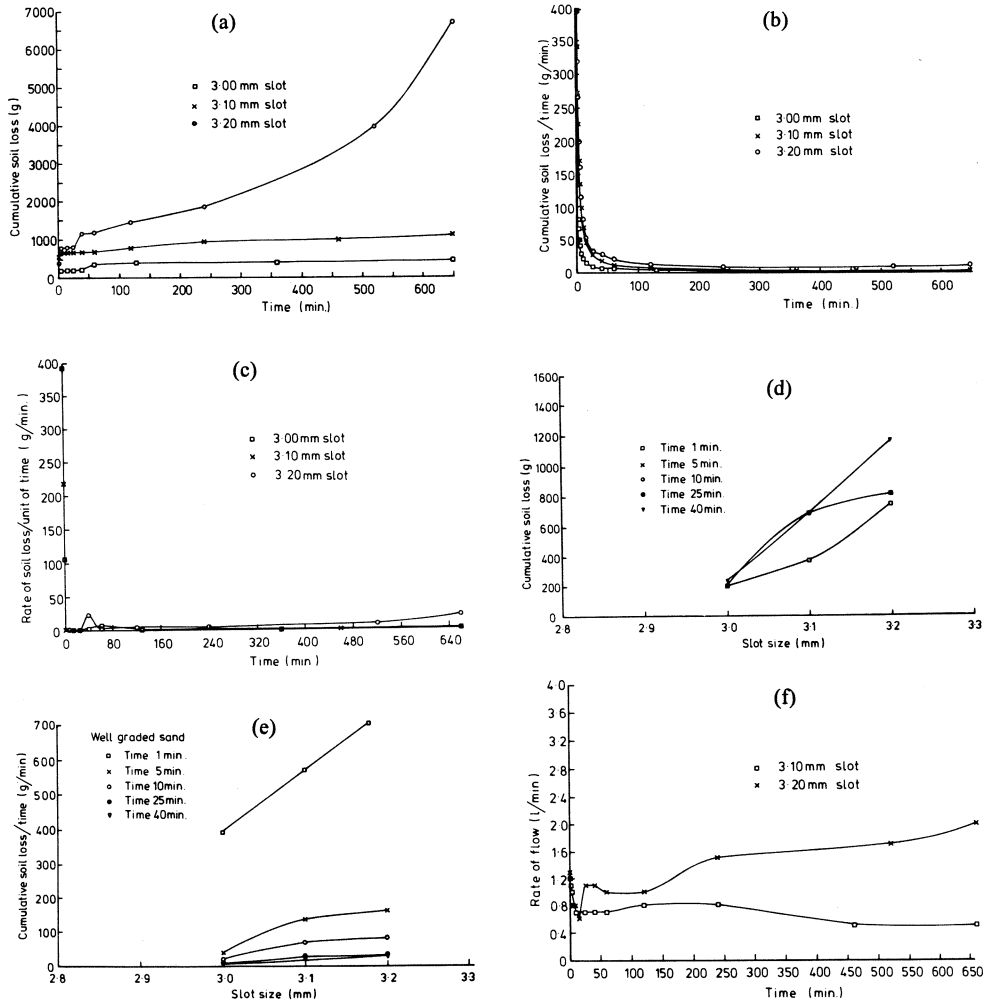


**Fig. 6 Fine-to-Coarse Sand Tests:**

- (a) Cumulative Soil Loss V Time.
- (b) Cumulative Soil Loss/Time V Time.
- (c) Rate of Soil Loss/Unit Time V Time.
- (d) Cumulative Soil Loss V Slot Width.
- (e) Rate of Water Flow V Time.

the flow rate increased, Figure 6(f), and for the 3.20 mm slot which eventually failed by complete washout (during the test programme it was not possible to record flow rates for sands  $s_1$  and  $s_3$ ). In contrast with a slot width of 3.10 mm, the water flow rate decreased with time reflecting the stabilization of the filter with time. Unfortunately, during the testing programme flow rates were not recorded for the slot width of 3.0 mm.

**Table 2 Fine-to-coarse Well Graded Sand Tests ( $s_2$ )**

Test No	Slot width (mm)	Test head (m)	Test period (min)	Sand loss (gm)	Remarks
w <sub>1</sub>	3.00	1.20	4302	565	Partial wash out
w <sub>2</sub>	3.10	1.20	3540	2765	
w <sub>3</sub>	3.20	1.20	660	6864	Total wash out

**Table 3 Gap-Graded Sand Tests ( $s_3$ )**

Test No	Slot width (mm)	Test head (m)	Test period (min)	Sand loss (gm)	Remarks
G <sub>1</sub>	1.80	1.20	60	22.6	Very small soil loss
G <sub>2</sub>	2.00	1.20	60	13.6	
G <sub>3</sub>	2.00	1.20	60	28.8	
G <sub>4</sub>	3.00	1.20	4170	118	After 60 min soil loss equals 110 gm
G <sub>5</sub>	3.10	1.20	120	453	Partial wash out on application of water
G <sub>6</sub>	3.15	1.20	60	498	head
G <sub>7</sub>	3.20	1.20	60	1276	
G <sub>8</sub>	3.25	1.20	5	3215	Total wash out occurred

*(iii) Gap-graded sand ( $s_3$ )*

The gap between the coarse and fine particle sizes was 0.45 mm, Figure 3(a). The results from the eight tests performed are presented in the same format as those for sands  $s_1$  and  $s_2$ , Figure 7 and Table 3. The cumulative soil loss, Figure 7(a), cumulative soil loss/unit of time, Figure 7(b), the rate of soil loss/unit time, Figure 7(c), are similar to the trends observed with sands  $s_1$  and  $s_2$ . Other features of the results are considered in the next section.

**DISCUSSION**

An examination of the limited data presented will show that the stability of a soil filter adjacent to a slot opening is influenced by the size of the slot. For the fine-to-medium sand filter ( $s_3$ ) the cumulative soil loss increased with increase in the slot width (Figure 5), but only a small loss occurred with a 1.70 or a 1.75 mm opening. A partial washout occurred with openings in the range 1.80 to 1.90 mm. A total washout occurred rapidly (almost in-

## SOIL PARTICLE MIGRATION THROUGH SLOTS-I

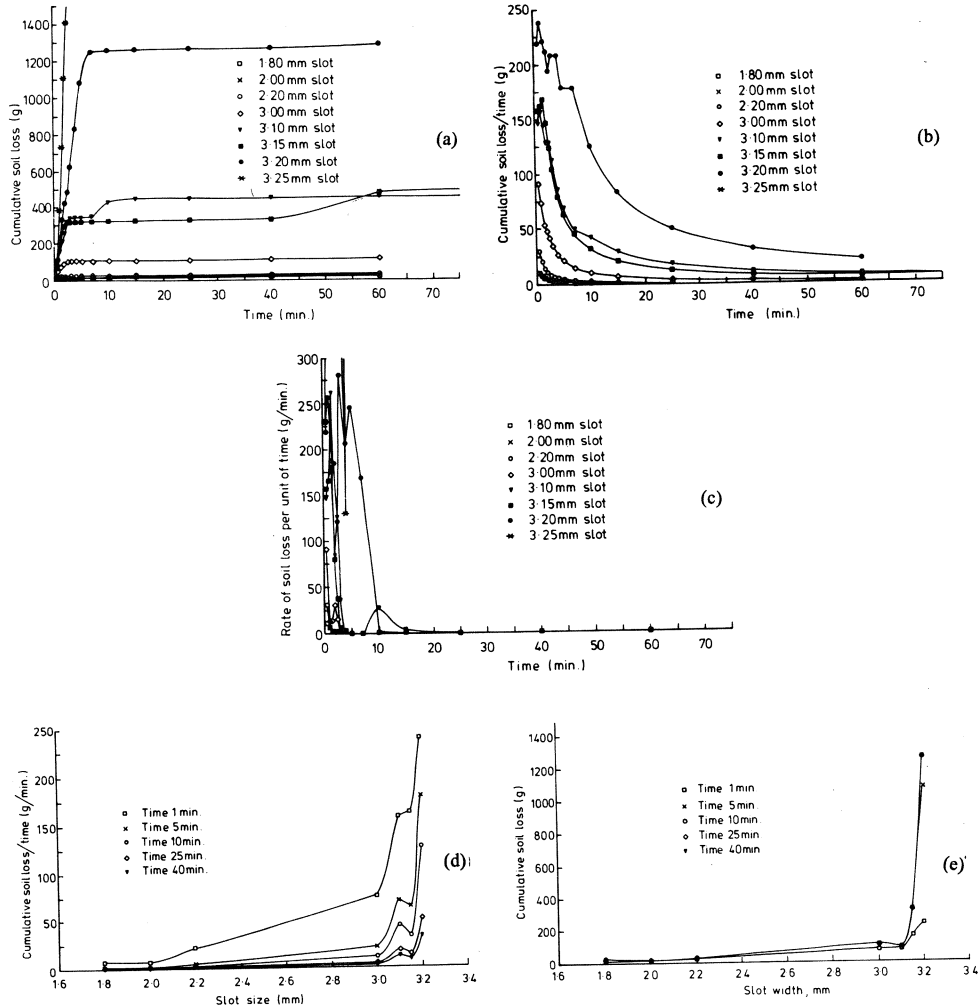


**Fig. 7 Gap-Graded Sand Tests:**

- (a) Cumulative Soil Loss V Time.
- (b) Cumulative Soil Loss/Time V Time.
- (c) Rate of Soil Loss/Unit Time V Time.
- (d) Cumulative Soil Loss V Slot Width.
- (e) Cumulative Soil Loss/Unit V Slot Width.

stantaneously) on application of 1.2 m head with a slot opening of 1.9 mm. The  $D_{85}$  size of this filter sand was 0.5 mm. The slot opening/ $D_{85}$  ratio, at which complete washout resulted, was 3.84. The filter was stable when the ratio was less than 3.84. The test data published by Nettles and Schomacher (1967) are in agreement. They gave critical ratios of 3.6 and 4.8 for fine-to-medium and uniform sands, respectively.

For the fine-to-coarse filter sand ( $s_2$ ), total washout occurred with a slot opening of 3.2 mm. The  $D_{85}$  size of the filter was 1.5 mm. The slot opening/ $D_{85}$  ratio at washout was 2.13. In two of the tests, with openings of 3.00 and 3.10 mm, respectively, a partial washout occurred at the beginning of the test but the filter subsequently became stable. It is considered that such a situation is acceptable.

For the gap-graded filter ( $s_3$ ), stability resulted for slot sizes up to 3.1 mm. Between 3.1 and 3.2 mm opening size, a partial washout occurred at the beginning of the test but, thereafter, the filter became stable, Figure 7(d). At an opening of 3.25 mm, a total washout was observed during the first five minutes of test. The  $D_{85}$  of this filter was 1.7 mm resulting in a critical slot opening/ $D_{85}$  ration of 1.92.

The critical ratios found for the three filters tested are much greater than the 0.83 value established by the USCE (1953) for slotted wood well screens and the value of 0.5 given by the USBR (1955). The work of USCE (1953) and USBR (1955) did not control the compaction of the filter. The results of Nettles & Schomacher (1967), for the fine-to-medium sand, are in good agreement with the present findings.

The unidirectional flow tests all gave a similar pattern of soil loss behaviour with 80% or more of the soil loss occurring during the first 10 minutes of test. After the first or primary stage of the test a constant pattern emerged with very small losses, that is the filter system had become stable. In four of the tests, 1.85 mm opening (fine-to-medium sand), 3.00 mm opening (gap-graded sand), 3.00 and 3.10 mm opening (fine-to-coarse sand) the flow was continued for periods of 3598, 4170, 4302 and 3540 minutes. The amount of soil loss recorded after the initial loss (i.e. after 5 to 10 minutes) was negligible compared to the loss during the first 5 to 10 minutes of the test. This experimental observation is well supported by contemporary literature. Based on extensive tests on uniform sand filters, Sherard et al (1984) concluded that if little or no base material was lost during the first minute of flow, little or no further loss would result from long-term flow. They also found that if any significant quantity of soil loss occurred during the first minute of flow then this loss would continue to penetrate the filter until failure and at a near constant rate. Other researchers have noticed that there is always a finite amount of soil loss through a filter during its early life, see Bertram (1948), Soares (1980), Hoare (1984).

During the present tests, it was noticed that, as the continuous migration of fine particles was under way at an early stage of the test, the coarser particles gradually blocked the larger entry openings to cause physical binding. This binding was established with some of the coarse particles filling the slot opening by a bridging or arch action and retaining the finer particles. After binding, the filter became stable and no further movement of soil particles resulted. This general mechanism was confirmed by the plots of the rate of soil loss/unit of time against time (Figures 5(c), 6(c), 7(c)) which showed that the rate values tended to zero after about 5 minutes. After all of the tests, the apparatus was carefully dismantled and different horizontal sections through the sand were examined visually. They showed that there was a homogenous distribution of the sand sizes except for the sand in the immediate vicinity of the slot opening. In this central area there was clear evidence of a concentration of "coarse" particles. It is believed, therefore, that the infiltration

*SOIL PARTICLE MIGRATION THROUGH SLOTS-I*

processes are controlled by the coarse particles. There is a considerable body of experimental evidence on the effects of infiltration of sand particle bridging around openings. The US Corps of Engineers (1953) placed very uniform sand specimens above thin metal plates with circular holes of diameter 3.18, 6.35 and 12.7 mm. For a range of hydraulic gradients, visual observations were made in the vicinity of the circular holes to assess the effect of soil particle bridging. In one case, a hole approximately four times the mean diameter of the sand particles held the material. With decrease in void ratio, the bridging effect became less efficient. Soares (1980) arrived at a somewhat similar conclusion that particles with a diameter between  $D_{85}$  and  $D_{60}$  could protect the base soil from migration through the pores in the filter by bridging action.

The present test data showed that the filter remained stable provided that the slot openings were less than 1.85 mm for fine-to-medium sand, 3.10 mm for fine-to-coarse sand and 3.10 mm for gap-graded sand. These values are 4 times the  $D_{80}$  value for the fine-to-medium sand, the  $D_{65}$  for the fine-to-coarse sand and  $D_{65}$  for the gap-graded sand. This particular observation might suggest that bridging may be controlled by particles of size smaller than  $D_{60}$ . Clearly further tests are required to confirm this.

Consider the flow net for a small opening (slot). It seems reasonable to make the simplifying assumption that the part of the seepage near to the slot is similar to flow into a cylinder-shaped hole, of a diameter equal to the slot width, in an infinite soil mass, Fig. 8. The major head loss occurs very near to the slot, the hydraulic gradient being ap-

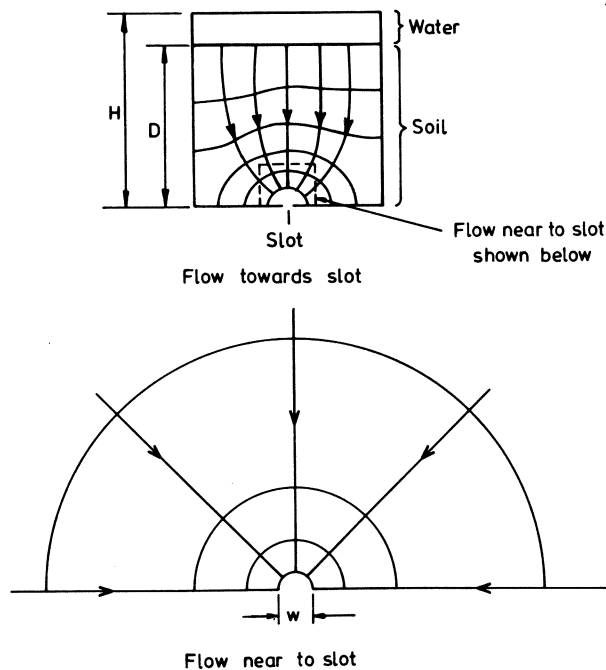


**Fig. 8 Flow Net Near Soil Opening.**



proximately inversely proportional to distance from the slot. Close to the slot the hydraulic gradient is very large. Because the coarser soil particles are capable of forming a bridge or arch over the slot opening, it is to be expected that the critical width of the crack will be independent of the applied water head,  $H$ . To cause the arch to fail, very high heads would be necessary to generate seepage forces required to crush the arch-forming particles. The heads of water found in practice will have no influence on soil particle migration provided the critical slot width has not been exceeded. Figure 6(f) presented data on water flow rates which showed a reduction in flow rate with time for a 3.1 mm slot and an increase in flow rate for a 3.2 mm slot. The reason for the slight reduction in flow rate, when the slot width was somewhat less than the critical value, was the bridging action and the holding of fines behind these bridges.

The tests on the gap-graded sand are of particular interest and use in understanding the mechanics of preventing particle migration. The most important feature of the grading is the range of sizes absent, the gap, and the position of the gap relative to the percentage of material passing. The gap-graded sand,  $s_3$ , has a gap at 50% to define coarse and fine materials of 50% of the whole sample, Fig. 3(a). The missing material at the gap was the medium sizes in a sample covering the full range of sand sizes. All of the relevant literature shows that the process of self-filtering is essential if the migration of fine soil particles through the slot opening via the large pores in the coarse sizes is to be prevented. The difference with a gap-graded material is the presence of two distinct materials, a coarse material and a fine material both of which possess self-filtering capability. From a conceptual view point, the coarse fraction may be considered as a filter to protect the finer material which may be considered to act as a base. By use of this idealization, two quantities of importance can be identified,  $D_{15f}$ , the 15% size for the coarse material (the filter) and  $D_{85b}$ , the 85% size for the fine material (the base). The values are  $D_{15f} = 0.15$  mm and  $D_{85b} = 0.70$  mm. The practical size ratio used to prevent the migration of base sizes into the filter is  $D_{15f} < 5 D_{85b}$ . This ratio has been used for several decades and based on the extensive early studies of Terzaghi and the USCE (1953). In drawing up the sample gradation, this criterion was followed because it seemed reasonable to expect a gap-graded soil not to be susceptible to soil migration if two conditions were met - (i) the  $D_{85}$  size/slot width ratio of the total sample was less than the critical ratio and (ii)  $D_{15f} < 5 D_{85b}$ . From an inspection of the cumulative soil loss through the various slot sizes tested, Fig. 7(e), it is clear that the loss of material was very small until the critical slot width was reached. This conclusion is also supported by the rate of water flow measurements which indicated a constant flow behaviour, indicative of a constant permeability. When the critical slot width was reached, a significant increase in water flow was noted. It is clear that the gap size in the grading curve was sufficiently small for the coarser fraction to act as an efficient filter to the finer fractions yet allow self-filtering processes to operate and avoid migration of fine sizes through the "gap". With this condition fulfilled, the stability of the whole specimen, with respect to migration through the slot, was regulated by the  $D_{85}$  size of the whole sample.

From these very simple tests the general principle of soil migration through a slot opening in a structure can be stated, although further testing is warranted to examine specific details. The critical slot width to cause loss of fines was independent of the applied

## SOIL PARTICLE MIGRATION THROUGH SLOTS-I

water head. The slot width/ $D_{85}$  ratio was found to be in the range 2 to 4 for the three soils tested. A wider range of material sizes needs to be tested including silt and clay sizes as well as several gap-graded materials. Three-dimensional-shaped openings require further study and can be simulated in the test apparatus. The maximum size of slot width or opening in a drain system can only be established by field observations. Fractured pipes may have crack widths up to 10 mm although brickwork sewers may have larger openings where the mortar joints are missing. The longitudinal pulling of joints in drains caused by severe differential settlements can post major problems as can collapsible soil types and soils which partly dissolve due to water flow. Research on all of these topics is warranted.

Current practice appears to be conservative relative to the present study findings. For subsurface drains, both UK and USA practice relates to the  $D_{85}$  size where slot width  $< 0.83 D_{85}$  and hole diameter  $< D_{85}$ . For well casing design, the heterogeneity of the soil is considered and generally, for a uniformity coefficient  $> 6$ , the maximum slot width is either  $D_{70}$  or  $D_{50}$  size, depending on the state of compaction of the soil. For more homogeneous soils, these values fall to  $D_{60}$  (compacted) and  $D_{40}$  (poorly compacted). Current practice does not make appropriate allowance for erodible soils, a subject of great importance in several regions of the world, Sherard et al (1976). Layered soils, similar to those discussed by Wittmann (1979), have not been tested. Reverse flows through soil create new problems and the companion paper (Tahar & Hanna, 1995) is directed to this topic.

### CONCLUSIONS

The main conclusion to be drawn from the unidirectional flow tests is that the susceptibility of granular soils to migration through a slot depends primarily on the shape of the grading curve and the slot width relative to the  $D_{85}$  size. The experimental test system works well giving repeatable results. Based on the limited range of soils tested, present filter design criteria are conservative for both well screens and subsurface drains and consequently a margin of safety on the critical washout condition is provided. The critical slot width/ $D_{85}$  size ratio is in the range 2 to 4. Gap-graded soils fall within these limits provided the coarser material does not allow the finer fractions to migrate.

### ACKNOWLEDGEMENT

The authors thank the Water Research Centre, UK, for the provision of the basic test equipment which has been modified and developed for the test programme.

### REFERENCES

- ATKINSON, J.H. and POTTS, D. M., (1977). "The Stability of a Shallow Circular Tunnel in Cohesionless Soil", *Geotechnique*, Vol. 27, No. 2, pp. 203-215.
- ATKINSON, J.H. and MAIR, R.J., (1981). "Soil Mechanics Aspects of Soft Ground Tunnelling.", *Ground Engineering*, Vol. 14, No. 5, pp. 20-28.

- BRITISH STANDARDS INSTITUTION, (1984). "Guide to Sampling and Testing of Aggregates", BS 812, Part 101, London, 1984.
- CEDEGREN, H.R., (1967). "Seepage, Drainage and Flow Nets", John Wiley and Sons, New York.
- HOARE, D. J., (1984). "Geotextiles as Filters", *Ground Engineering*, Vol. 17, No. 2, pp. 29-43.
- KARPOFF, K.R. (1955). "The Use of Laboratory Tests to Develop Design Criteria for Protective Filters", *Proceedings ASTM*, Vol. 55, pp. 1183-1195.
- KENNEY, T.C. CHAD, R., OFOEGBU, G.I., OMANGE G.N. and UME, C.E.,(1985). "Controlling Constriction Sizes of Granular Filters", *Canadian Geotechnical Journal*, Vol. 22, No. 1, pp. 32-43.
- KENNEY, T.C. and LAU, D., (1985). "Internal Stability of Granular Filters", *Canadian Geotechnical Journal*, Vol. 22, No. 3, pp. 215-225.
- KOVACS, G., (1981). "Seepage Hydraulics", Elsevier Scientific Publications, Amsterdam.
- NETTLES, E.H. and SCHOMACHER, N.B., (1967). "Laboratory Investigation of Soil Infiltration through Pipe Joints", *Highway Research Record*, No. 203, pp. 37-56.
- SHERARD, J.L., DUNNIGAN, L.P. and TALBOT, J.R., 1984. "Basic Properties of Sand and Gravel Filters", *Proceedings ASCE*, Vol. 110, No. 6, pp. 684-700.
- SHERARD, J. I., DUNNIGAN, L.P., DECKER, R.S. and STEELE, E.F., (1976). "Pinhole Test for Identifying Dispersive Soils", *Proceedings ASCE, Journal of the Geotechnical Engineering Division*, Paper 11846.
- SOARES, F.H., (1980). "Experiments on the Retention of Soils by Filters", M. Phil Thesis, London University.
- TAHAR B., (1987). "The Behaviour of Soil Surrounding Buried Pipes with an Opening in the Pipe Wall", M. Phil Thesis, University of Sheffield.
- TAHAR B., & HANNA, T. (1995). "Soil Particle Migration Theory in Slots in Drains - II Reversing Plan," *Geotechnical Engineering*, Vol. 26, No. 1.
- THANICKACHALAM, V. and SAKTHIVADIREL, R., (1984). "Rational Design Criteria for Protective Filters", *Canadian Geotechnical Journal*, Vol.21, No. 2, pp. 312-314.
- TERZAGHI, K. and PECK, R.B., (1967). "Soil Mechanics in Engineering Practice", John Wiley and Sons, New York.
- USBR, (1955).-quoted by Cedegren H.R.
- U.S. ARMY CORPS OF ENGINEERS (USCE), (1953). "Filter Experiments and Design Criteria", Waterways Experiment Station, Vicksburg, Technical Memorandum No. 3 - 360, 52 pp.
- WATER RESEARCH CENTRE (WRC), (1983). "Sewerage Rehabilitation Manual", Vol.2.
- WITTMANN, L., (1979). "The Process of Soil Filtration - its Physics and Approach in Engineering Practice", *Proceedings 7th European Conference on Soil Mechanics and Foundation Engineering*, Brighton, UK, Vol. 1, pp. 303-310.

# SOIL PARTICLE MIGRATION THROUGH SLOTS IN DRAINS - II, REVERSING FLOWS

B. Tahar<sup>1</sup> and T.H. Hanna<sup>2</sup>

## SYNOPSIS

The soil loss through a slot in a simulated drain was observed for a range of reversing flow conditions. The soil loss was related to the magnitude of the surge during the reverse flow, the number of surges and the slot dimension relative to the filter grain size. The test data supplement the results reported in a companion paper for the case of uni-directional flow.

## INTRODUCTION

There is a growing awareness world-wide that the stability of cracked sewers and drains depends on the level of lateral support which the surrounding ground can provide. It is known that soils in contact with cracks, pulled joints and holes may migrate into the drain as water flows through the opening in the drain wall from the surrounding ground. These deformations may cause damage to the drain system and lead to loss of support of nearby structures such as shallow foundations, wall footings and manholes. In the companion paper, Tahar & Hanna (1995), the case of unidirectional water flow through three filter types were examined. This paper considers an extension of that work using reversing flows. The term "reversing flow" is used generally although strictly speaking only one of the flow conditions simulated a reverse flow. The two other flow states studied are varying unidirectional flows where the surge applied varies between preset limits of fluctuating or pulsating head. Because the difference between a steady unidirectional flow and a fluctuating flow which could cause a local or a general reversal of flow direction in part or all of the soil mass was under study, the term "reversing flow" has been adopted to distinguish the flow from the more common steady and unidirectional flow. In many cases a surge of water passes along a drain. If the pressure in the surge is greater than the static water pressure in the surrounding ground, water flows out of the drain through the opening and into the surrounding ground. The quantity of flow will depend on the slot width, the soil permeability and the duration of the surge and the surge head relative to the static ground water level. After the surge passes along the drain, water will drain back through the slot until an equilibrium condition is reached. Water surges along drains of domestic dwellings are frequent. Damage to such dwellings on occasions is reported yet the causes of the damage are seldom attributed to the erosion of soil adjacent to the drain but to other causes

---

<sup>1</sup> Institut National de L'Enseignement Supérieur D'Hydraulique de Chlef, Chlef, Algeria.

<sup>2</sup> Professor Emeritus, 288 Ecclesall Road South, Sheffield, S11 9PT, UK.

such as faulty foundation or faulty ground strengthening works.

### The Test System

The apparatus used for the unidirectional flows was modified to simulate the surges in the following manner. Two solenoid valves were controlled by a water valve controller and connected to the base part of the test apparatus, Fig. 1. The water valve controller comprised a 12-volt output via a transformer, a timer (range 0 to 5 minutes) with cyclic switch (on/off) and manual and electrical preset counters with reset facility to record the number of surges. Figure 2 shows the general layout. The solenoid valves were of the two-way shut-off type with one inlet and one outlet and were normally closed. All other instrumentation was also used for the unidirectional tests. To cause a reverse flow, a pressure of water was applied to the bottom compartment causing water to flow upwards through the slot. By gradually varying the applied bottom water pressure ( $H_b$ ) and keeping the water pressure head in the top compartment ( $H_t$ ) constant, the water flowed upwards and then downwards through the samples. The cyclic pressure on the bottom compartment was recorded by piezometer as the pressure changed from a high to a low value. The pressure/time relationship produced is shown in Fig. 3. The top compartment head,  $H_t$ , was 1.2 m and the head in the bottom compartment could be cycled between 0 and 1.80 m.

With the sample fully saturated and the system completely filled with water, all valves were closed. The filter to collect the soil loss was placed on the mesh plate in the drain tank, Fig. 1. The solenoid valves were connected to the water valve controller. The klinger valves were opened and the applied water heads were controlled by the solenoid valves. A preset number of flow cycles was chosen and the soil loss collected. At the end of the number of cycles chosen, records were taken of the soil loss collected, the quantity of water passing through and the number of cycles of flow. The above operations were then re-

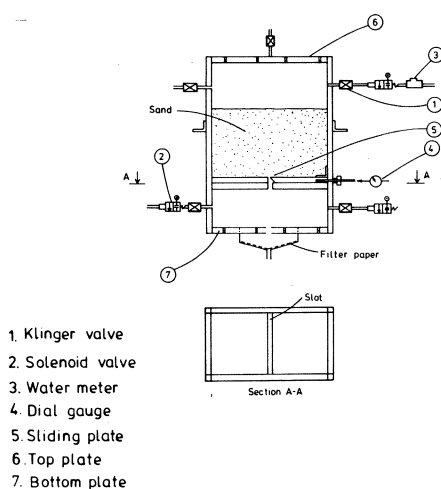


**Fig. 1 Sketch of The Test Apparatus.**

## SOIL PARTICLE MIGRATION THROUGH SLOTS-II

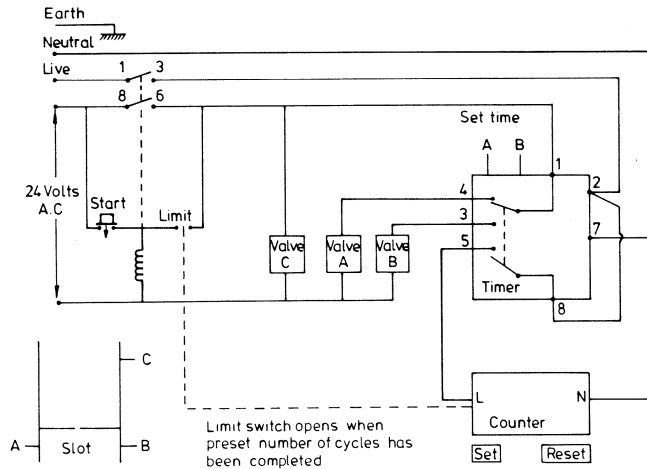


**Fig. 2 Water Valve Controller.**

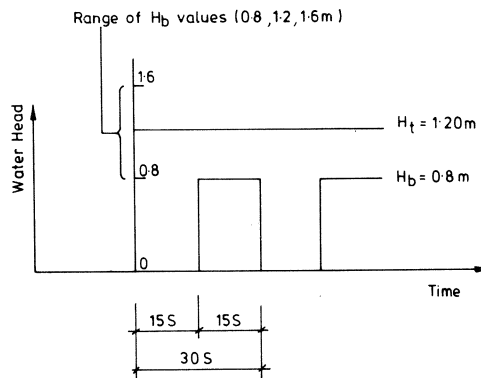


**Fig. 3 Cyclic Pressure/Time Relationship.**

peated until either a “washout” occurred or flow stability resulted. The soil loss was recorded as a function of the number of flow cycles.

Three series of tests were performed on each of the test samples. Details are given in Table 1. The test samples were a fine-to-medium sand, a fine-to-coarse well-graded sand and a gap-graded sand. Details of these materials are given in the companion paper, Tahar and Hanna (1995), along with a full description of the test apparatus and the philosophy of the test set-up to simulate an opening in the wall of a drain.

### TEST RESULTS

#### Series 1 ( $H_b > H_t$ )

During the first series of tests the cyclic head at the base of the sample,  $H_b$ , was varied

**Table 1 Programme of Reverse Flow Tests**

Material Used	Opening (mm)	Second Series		Third Series		Fourth Series	
		Head (m)	Test No	Head (m)	Test No	Head (m)	Test No
Medium to fine sand	1.80	Ht = 1.20	1	Ht = 1.20	19	Ht = 1.20	34
	1.70	Hb = 0-1.60	2	Hb = 0-1.20	20	Hb = 0-0.8	35
	1.60		3		21		36
	1.50		4		22		--
	1.40		5		23		--
	1.30		6		24		--
	1.20		7		--		--
	0.90		8		--		--
Gap-graded sand	3.10	Ht = 1.20	9	Ht = 1.20	25	Ht = 1.20	37
	3.00	Hb = 0-1.60	10	Hb = 0-1.20	26	Hb = 0-0.80	38
	2.90		11		27		39
	2.80		12		28		40
	2.60		13		29		41
	2.20		14		30		--
	1.60		15		--		--
Well-graded sand	3.00	Ht = 1.20	16	Ht = 1.20	31	Ht = 1.20	42
	2.80	Hb = 0-1.60	17	Hb = 0-1.20	32	Hb = 0-0.80	43
	2.60		18		33		--

between 0 and 1.60 m, the head applied to the sample top,  $H_t$ , being 1.20 m. Thus the bottom head,  $H_b$ , was greater than the top head,  $H_t$ , and, as a consequence, a sieving-type action was applied to the sand as the water flows were reversed every 15 seconds. The effect of the frequency of the cycles has not been investigated.

Eight reverse flow tests were performed on the fine-to-medium sand. The results of these tests are given in Fig. 4. Figure 4(a) shows the cumulative soil loss as a function of the number of cycles of flow. The rate of cumulative soil loss as a function of the number of cycles of flow is presented in Fig. 4(b). It will be noted in Fig. 4(a) that there are three distinct parts to each curve. During the first stage there is a proportionality between the cumulative soil loss and the log of the number of flow cycles, showing that only a small quantity of soil has been lost through the slot. During the second stage, there was an abrupt change in the behaviour with the cumulative soil loss increasing rapidly with the log of the number of flow cycles, which indicates the first stage of instability. In the third stage, a large amount of soil was washed through the slot. Washout has occurred for all slot widths except that of 0.90 mm.

With the same data plotted as rate of cumulative soil loss, Fig. 4(b), initially the rate of cumulative loss decreased and then remained nearly constant. As the number of flow cycles increased, there was a significant increase in soil loss as the condition for a washout

## SOIL PARTICLE MIGRATION THROUGH SLOTS-II

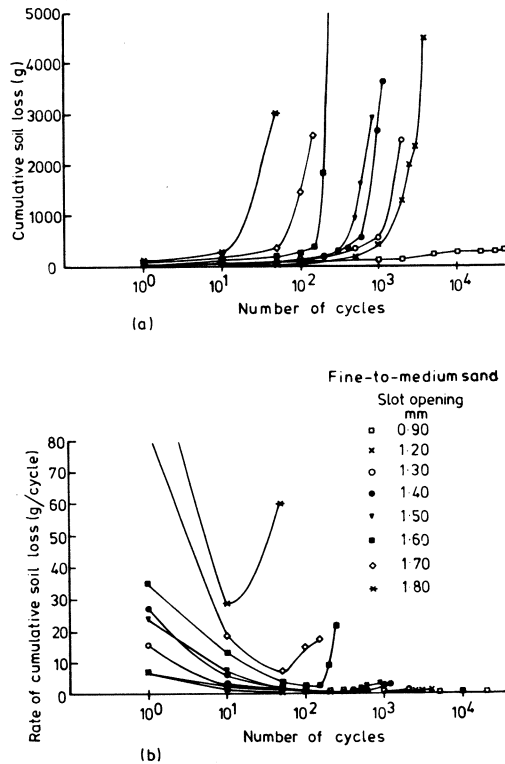


**Fig. 4(a) Cumulative Soil Loss/Number of Reverse Flows - Fine to Medium Filter.**  
**(b) Rate of Cumulative Soil Loss/Number of Reverse Flows.**

was reached. Stability of the filter material is shown by a decrease in the rate of cumulative soil loss from the beginning to the end of a test; see slot width opening 0.90 mm data. The length of the transition zone between the first stage, where the filter was stable, and the third stage, where washout had started, depended mainly on the slot width. For a decrease in the slot width from 1.80 to 1.20 mm the stability duration was prolonged from 20 to 2,000 cycles. For an opening of 0.9 mm the filter was stable for the duration of the test, 40,000 cycles. From the rate of cumulative loss data, Fig. 4(b), the rate of loss increased after dropping to a minimum value. This critical loss rate corresponds to the number of cycles when the filter starts to deteriorate.

For the gap-graded sand, seven tests were carried out with the slot widths in the range 1.60 and 3.10 mm. The cumulative soil loss data are given in Fig. 5(a). When the slot was wide (3.10 mm) there was a large cumulative loss with total washout after 75 cycles. For the 2.20 mm opening, washout resulted after 3,000 cycles. As expected, the number of water flow cycles to cause washout increased with slot width decrease. For the smallest slot tested, 1.60 mm, a loss of 1,400 gm occurred after 40,000 water flow reversals.



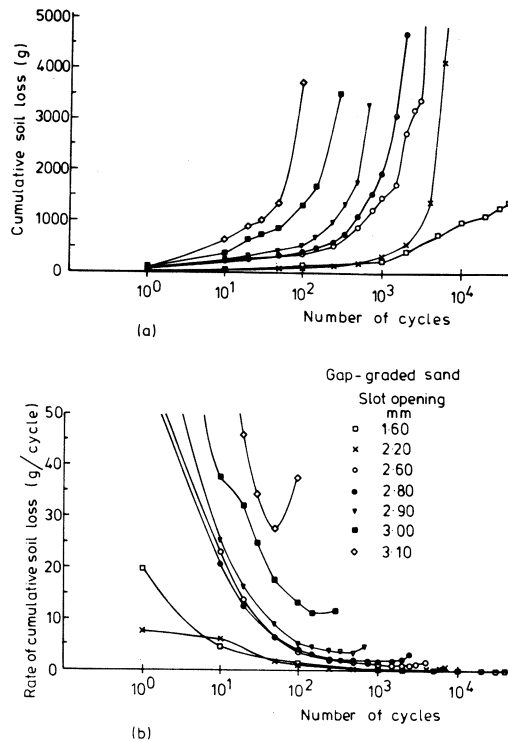


**Fig. 5(a) Cumulative Soil Loss/Number of Reverse Flows-Gap-Graded Filter.**  
**(b) Rate of Cumulative Soil Loss/Number of Reverse Flows.**

The soil losses were all recovered and grain-size distribution analyses performed. The sand loss with the 1.60 mm opening was composed of particles smaller than 0.3 mm size, Fig. 6.

The rate of cumulative soil loss, as a function of the number of water flow reversals, is given in Fig. 5(b). The stability of the filter may be deduced easily from these plots. The trends are similar to those for the fine-to-medium sand, Fig. 4(b). There is clear evidence of a deterioration of the filter for slot widths of 3.10, 3.00, 2.90 and 2.80 mm but, for slot widths of 2.60 and 2.20 mm, the decrease in the rate of cumulative soil loss throughout the tests is indicative of an improvement of the filter's stability.

With the bottom head,  $H_b$ , greater than the top head,  $H_t$ , the fine soil particles tended to follow the water flow path. At the start of a test, the fine particles migrated from the slot opening towards the top of the filter. The grading curves for soil losses after 750 and 2,000 water flow reversals, Fig. 6, show that the losses obtained during the early stages of the test were coarser than those from the later stages of the test.

For the tests with slot openings of 2.60, 2.20 and 1.60 mm the rate of water flow was recorded, Fig. 7. The rate of flow increased initially with increase in the number of water

SOIL PARTICLE MIGRATION THROUGH SLOTS-II

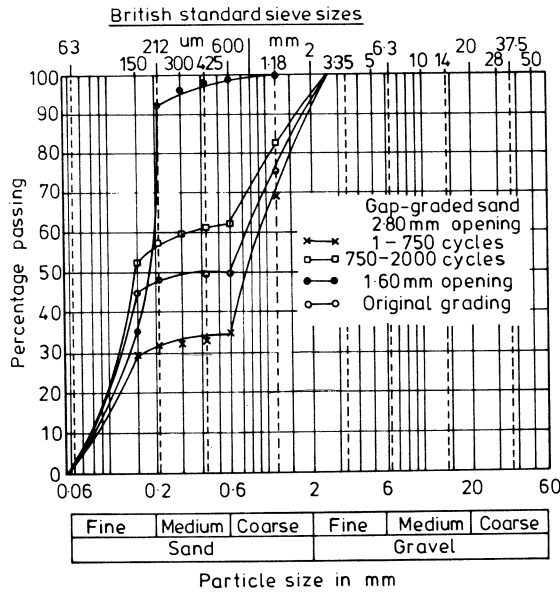


Fig. 6 Grain Size Distributions of Soil Lost Through Slot During Reverse Flow Testing - Gap-graded Filter ( $H^b > H^i$ ).

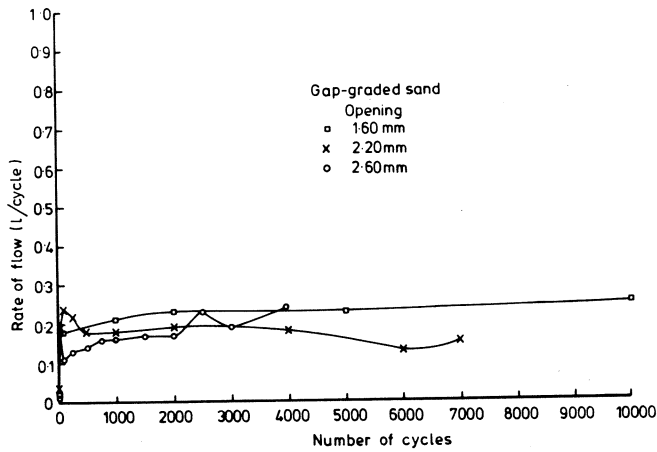


Fig. 7 Rate of Water Flows/Number of Reverse Flows - Gap-Graded Filter.

flow reversals but, for the 1.60 mm opening, the value was nearly constant thereafter. For the 2.20 mm opening the rate of flow decreased with time. The widest opening, 2.60 mm, gave a gradual increase in the flow rate with time.

The well-graded sand was tested at three slot widths, 2.60, 2.80 and 3.00 mm. For the

well-graded sand, trends were observed similar to those found for the fine-to-medium and gap-graded sands.

The relationships between the cumulative soil loss recorded and number of cycles of reversing flow are given in Fig. 8. By reducing the opening size from 3.00 to 2.60 mm the longevity of the filter was extended from 50 to in excess of 50,000 cycles. In this series of tests, although not for all test series, the water flowing through the soil was recorded. The data are presented in Fig. 9 where it is clear that the rate of flow increases initially with the number of flow reversals, and thereafter remains sensibly constant.

Series II ( $H_b = H_t$ )

In this series of tests the bottom water head was varied between 0 and  $H_t$ , the top head value (1.20 m). Material similar to those of Series I were tested for a range of slot widths.

The test results for the fine-to-medium sand are given in Fig. 10. Any increase in the number of water flow reversals or slot width led to increase in the cumulative soil loss. For a slot width of 1.70 mm, total washout occurred after 20 reversals but with an opening

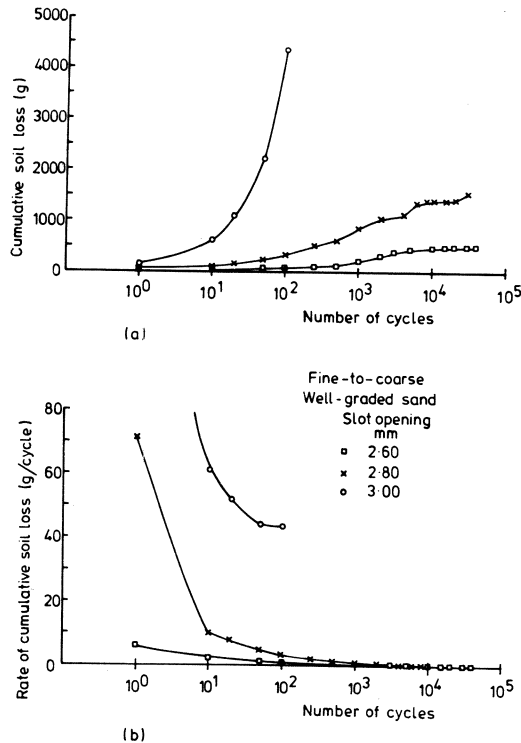


Fig. 8(a) Cumulative Soil Loss/Number of Reverse Flows - Fine to Medium Filter.  
 (b) Rate of Cumulative Soil Loss/Number of Reverse Flows.

SOIL PARTICLE MIGRATION THROUGH SLOTS-II

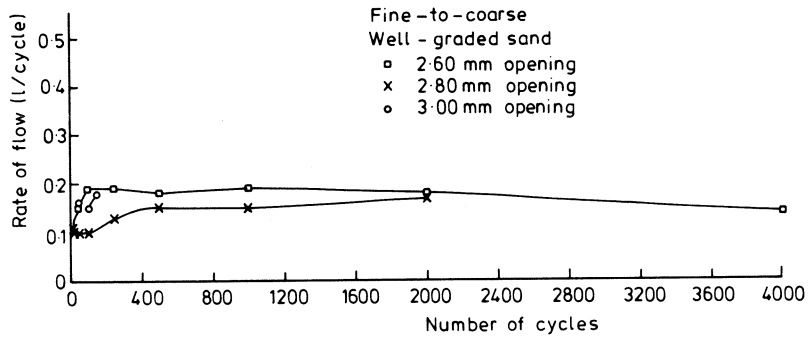
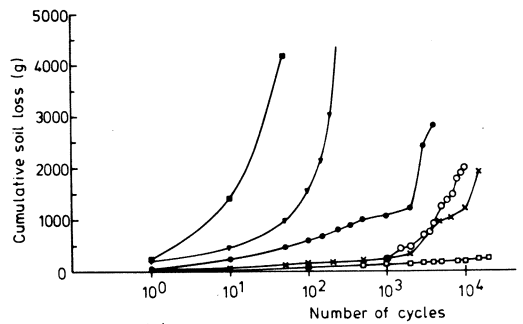
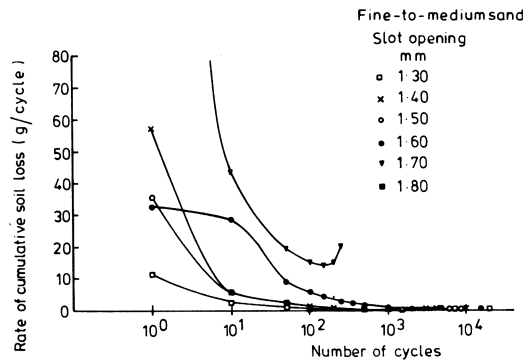


Fig. 9 Rate of Water Flows/Number of Reverse Flows - Fine to Medium Filter.



(a)



(b)

Fig. 10(a) Cumulative Soil Loss/Number of Reverse Flows - Fine to Medium Filter.  
(b) Rate of Cumulative Soil Loss/Number of Reverse Flows.

of 1.40 mm the life of the filter had increased to 10,000 reversals of flow. A further decrease in slot width to 1.30 mm gave a stable filter condition even after 20,000 water flow reversals.

For the gap-graded sand filter, Fig. 11, the results followed trends already established

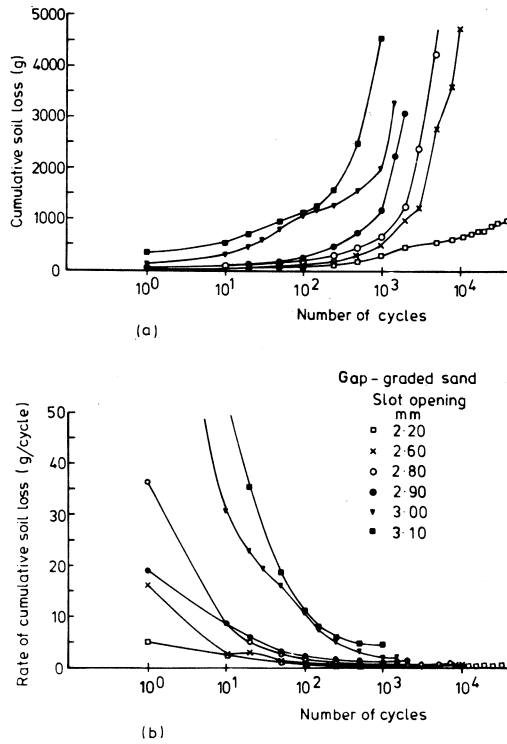


**Fig. 11(a) Cumulative Soil Loss/Number of Reverse Flows- Gap-Graded Filter.**  
**(b) Rate of Cumulative Soil Loss/Number of Reverse Flows.**

in the Series I tests but with differences of detail. A total washout occurred with a slot width opening of 3.10 mm. For the smallest slot width, 900 gm of very fine sand particles were collected during 40,000 flow reversals. Ninety percent of the soil particles lost were less than 0.3 mm size, Fig. 12. The rate of water flow was also recorded during this test. There was an increase in the flow with increase in the number of flow reversals, indicating that the permeability of the soil was increasing as the fine sizes slowly were removed, Fig. 13.

The well-graded sand filter behaved in a predictable manner with the 2.80 and 2.60 mm slot widths giving stability but washout occurring after 100 reversals for a 3.00 mm slot width, Fig. 14.

#### Series III ( $H_b < H_f$ )

The bottom water head was varied between 0 and 0.8 m; the top head was kept constant at 1.20 m.

The results of three reversing flow tests for the fine-to-medium sand filter are given in Fig. 15. For all three openings tested, the cumulative soil loss rate decreased with decrease

SOIL PARTICLE MIGRATION THROUGH SLOTS-II

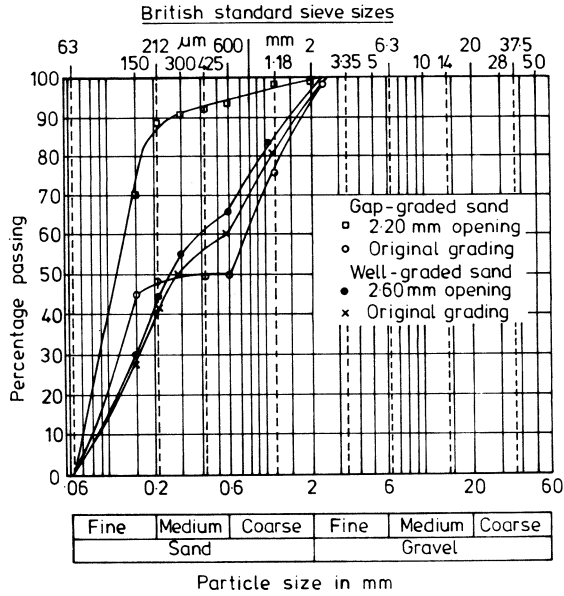


Fig. 12 Grain Size Distributions of Soils Lost Through Slot During Reverse Flow Testing- Gap-Graded and Well-Graded Filters ( $H^b > H^a$ ).

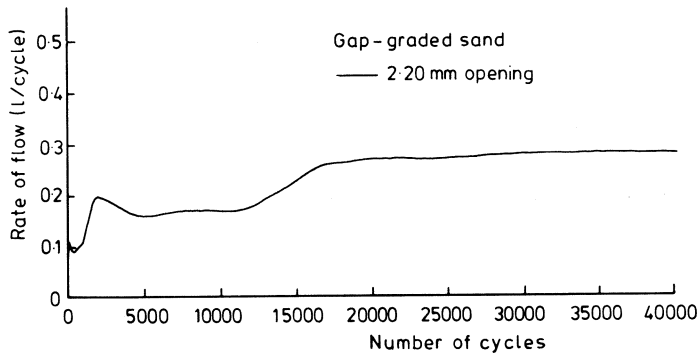
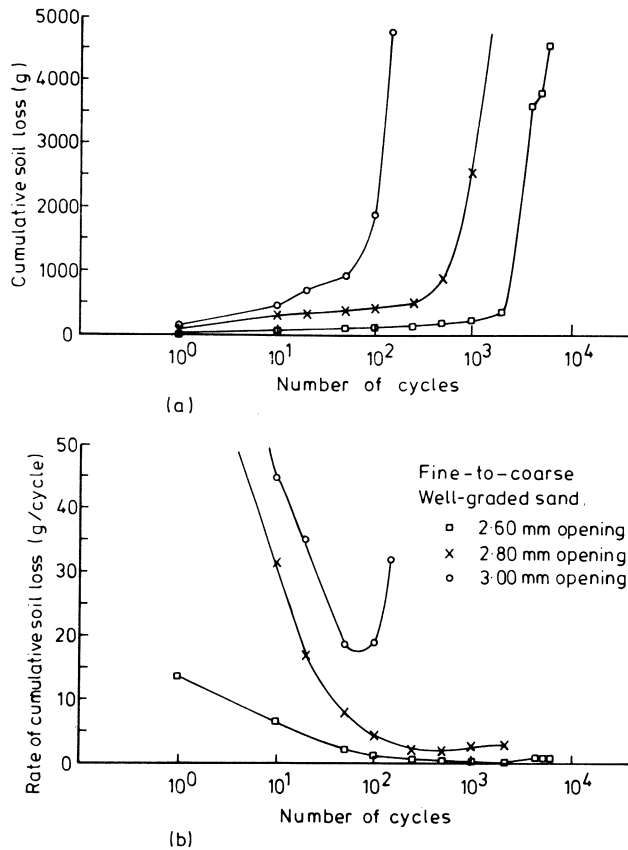


Fig. 13 Rate of Water Flows/Number of Flow Reversals - Gap-Graded Filter.

in the slot width. The life span of the filter increased dramatically from 600 flow reversals for an opening of 1.80 mm to more than 6,000 cycles for an opening of 1.60 mm.

For the gap-graded sand filter, all five tests were run for more than 10,000 reverse flow cycles to observe the migration of the fine sizes through the coarser sizes. The test data are given in Fig. 16. For the 2.60 mm slot width, the soil loss was only 800 gm after 10,000 flow reversals. With slot widths of 2.80 and 3.10 mm, the trends were very similar to the 2.60 mm slot. For all tests, the cumulative soil loss rate decreased as the number of



**Fig. 14(a) Cumulative Soil Loss/Number of Reverse Flows - Well Graded Filter.**  
**(b) Rate of Cumulative Soil Loss/Number of Reverse Flows.**

flow reversals increased. The soil materials washed through the slot were much finer than those initially forming the filter. The soil loss contained particles, 80% of which had a diameter less than 0.3 mm, Fig. 17.

Only two tests were performed on the fine-to-coarse well-graded sand filter. For a 3.00 mm slot width, total washout resulted after 5,000 flow reversals but, with a 2.80 mm slot width, the filter was stable for 40,000 flow reversals, Fig. 18, that is for the duration of the test. The soil loss had a gradation very similar to that of the original filter material, Fig. 19.

### OBSERVATIONS

A summary of all test results is given in Table 2. The number of reverse flows to

SOIL PARTICLE MIGRATION THROUGH SLOTS-II

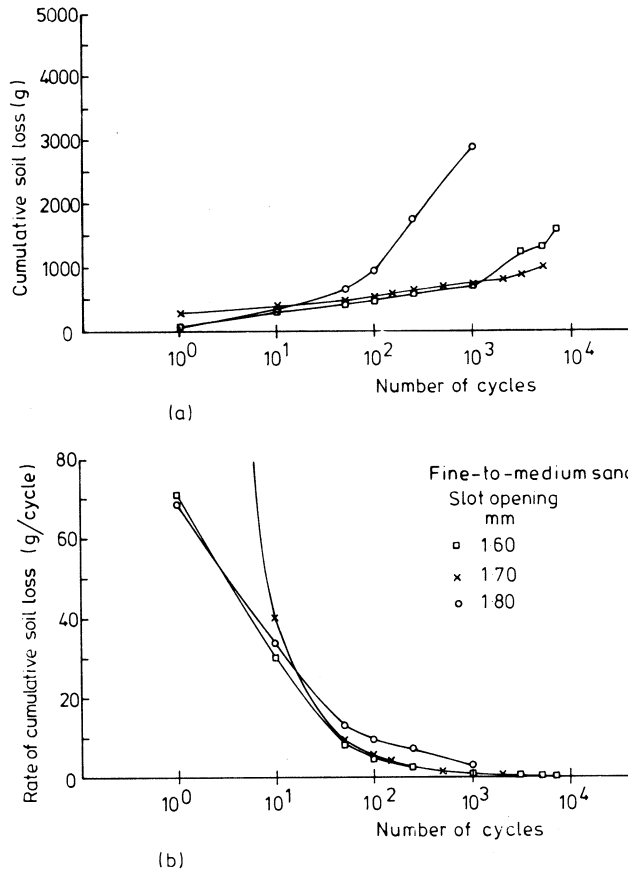
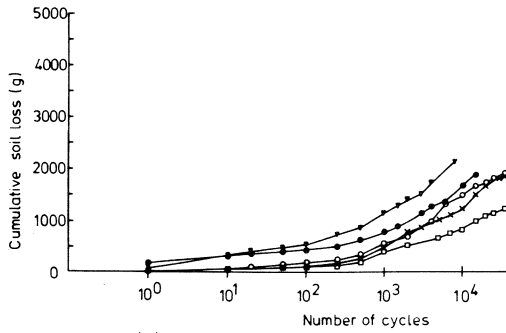


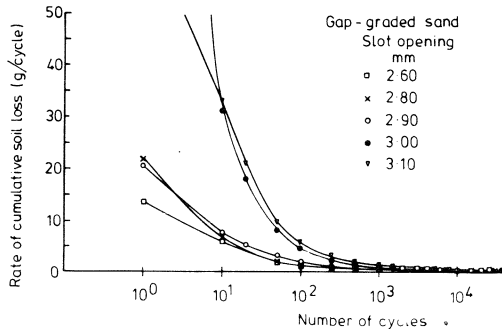
**Fig. 15(a) Cumulative Soil Loss/Number of Reverse Flows - Fine to Medium Filter.**  
**(b) Rate of Cumulative Soil Loss/Number of Reverse Flows.**

cause a total washout was related to the slot width. The development of the washout was derived from a breakdown of the soil filter structure. In the case for which the bottom head,  $H_b$ , was greater than the top head,  $H_t$ , the flow of water upwards through the sample and then downwards, all within a short time interval (30 seconds), caused a sieving-type action in which the fine particles were displaced from the vicinity of the slot opening towards the top of the filter at the beginning of a test. A close examination of the sample through the perspex side of the apparatus showed a concentration of fine particles near the top. The ability of the flow upwards to lift the particles and thus break the bridges of coarse particles depends on the local hydraulic gradient at the entry to the slot. In these tests, a very high gradient exists and, from visual observation, there was clear evidence of severe damage being caused to the soil structure near to the opening. With a 2.80 mm slot, the soil loss recorded for the first 750 cycles was coarser than for cycles 750 to 2,000. The action of the upward flow is to cause a loosening of the filter but, in the present tests, it was





(a)



(b)

**Fig. 16(a) Cumulative Soil Loss/Number of Reverse Flows - Gap-Graded Filter.**  
**(b) Rate of Cumulative Soil Loss/Number of Reverse Flows.**

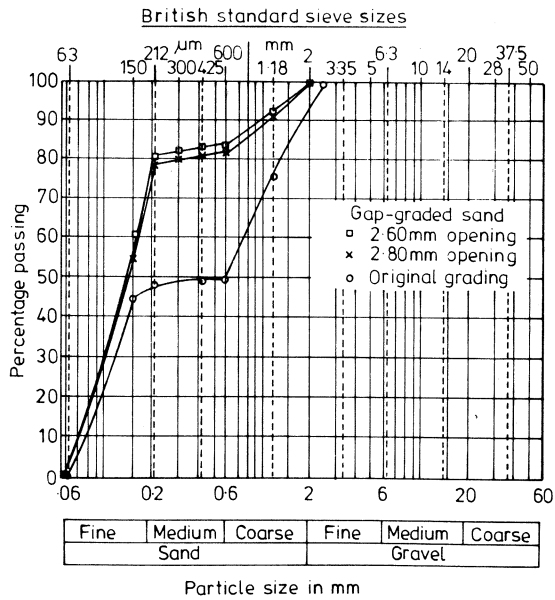


**Fig. 17 Grain Size Distributions of Soil Lost Through The Slot During Reverse Flow Testing - Gap-Graded Filter.**

SOIL PARTICLE MIGRATION THROUGH SLOTS-II

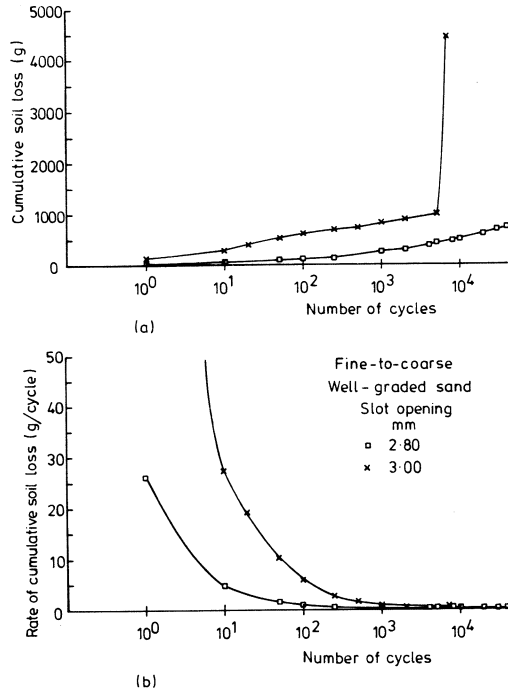


**Fig. 18(a) Cumulative Soil Loss/Number of Reverse Flows - Well Graded Filter.**  
**(b) Rate of Cumulative Soil Loss/Number of Reverse Flows.**

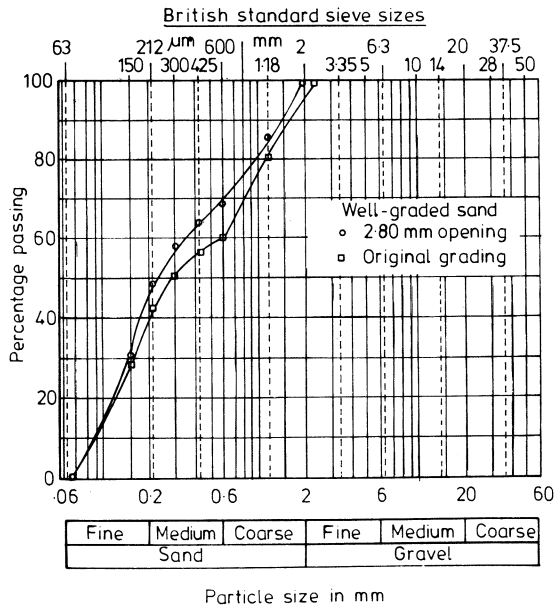


**Fig. 19 Grain Size Distributions of Soil Lost Through The Slot During Reverse Flow Testing - Well-Graded Filter.**

**Table 2 Summary of Reverse Flow Test Results**

Material	Opening (mm)	Number of Cycles Producing a Total Washout		
		Second Series Ht = 1.20m Hb = 0-1.60m	Third Series Ht = 1.20m Hb = 0-1.20m	Fourth Series Ht = 1.20m Hb = 0-0.80m
Medium to Fine Sand	1.80	20	50	250
	1.70	150	100	5,000
	1.60	180	3,000	7,000
	1.50	600	9,000	-
	1.40	800	15,000	-
	1.30	2,000	No Washout Occurred	-
	1.20	2,500	-	-
	0.90	No Washout Occurred		
Gap-Graded Sand	3.10	50	150	3,000
	3.00	150	250	10,000
	2.90	500	1,500	15,000
	2.80	750	3,000	35,000
	2.60	1,500	5,000	60,000 (No Washout Occurred)
	2.20	5,000	No Washout Occurred	
	1.60	No Washout Occurred		
Well-Graded Sand	3.00	100	100	7,000
	2.80	1,000	6,000	No Washout Occurred
	2.60	3,810	No Washout Occurred	-

not possible to confine the upper surface of the filter. In future tests, a confinement pressure could be applied. For  $H_b > H_t$  the stability of the filter was ensured when the slot width/ $D_{85}$  ratio 1.8 (fine-to-medium sand) and  $< 1.06$  (gap-graded sand). These ratios are about half those found in the unidirectional flow tests. In all cases, the filter near the slot opening was destroyed initially because the upwards flows displaced the fine particles upwards, then downwards, increasing the migration potential significantly.

When the top head,  $H_t$ , was equal to the bottom head,  $H_b$ , the stability life of the filter

## SOIL PARTICLE MIGRATION THROUGH SLOTS-II

was extended relative to the condition  $H_b > H_t$ . The curves of cumulative soil loss have three stages, a feature also noted in the unidirectional flow tests - in the first stage there is a relatively linear relationship between cumulative loss and log number of reverse flows. This stage was followed by a transition zone in which non-linearity occurs, indicating the early stages of a deteriorating situation leading to the commencement of a washout, the third stage. The number of cycles to produce a total washout increased as slot size decreased. For example, the life span of the filter was increased from 50 to 15,000 reversals, 150 to 5,000 reversals and 100 to 6,000 reversals by reducing the slot widths from 1.80 to 1.40 mm (fine-to-medium sand), from 3.00 to 2.80 mm (well-graded sand), from 3.10 to 2.60 mm (gap-graded sand). A close examination of the test data reveals that the filter material was stable for the following slot width/ $D_{85}$  ratios: fine-to-medium sand 2.63, well-graded sand 1.72 and gap-graded sand 1.30. It was clear from the tests that the sand particles were subjected to very severe loads from the flow reversals. With a slot width of 2.20 mm, 90% of the soil particles lost were less than 0.3 mm size, Fig. 12, yet, with the slot width increased to 2.60 mm, the soil gradation was similar to that of the original filter. By use of the method of analysis proposed by Kenney et al. (1985), based on the shape grading curve, it was found that the gap-graded sand was unstable, the data lying below the stable boundary in Fig. 20. The other two filters tested were shown to be internally stable. In this diagram F is the mass fraction smaller than a particle diameter, D, and H is the mass fraction measured for particles between D and 4D, Kenney & Lau (1985). The point

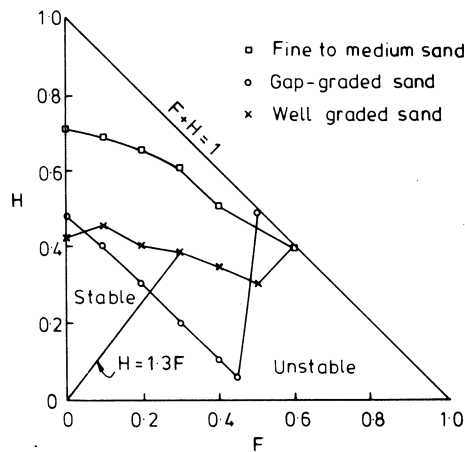


**Fig. 20 Shape Curves of Filter Materials Tested.**

representing the coarse end of the grading curve falls on the line  $F + H = 1$ , the shape of the transformed grading curve being independent of grain size but dependent on the geometrical form of the grading curve. According to the work of Kenney and Lau (1985) the line  $H = 1.3 F$  is the boundary between stable and unstable filters. This comparison indicates that the gap-graded filter was much more susceptible to infiltration than the other well-graded sands. The less severe case of  $H_b < H_t$  led to washout occurring at slot widths/ $D_{85}$

ratios of 3.03 (fine-to-medium sand), 1.89 (fine-to-coarse sand) and 1.54 (gap-graded sand).

From an examination of all of the data, the most important factor affecting soil infiltration was the magnitude of the bottom head,  $H_b$ , (the surge) relative to the top head,  $H_t$ . Extensive damage was caused to the soil fabric even with small slot widths when  $H_b > H_t$ . The differences in the life spans of the filters are shown in Fig. 21 where the slot width to cause washout is related to the log number of flow reversals. The critical ratios, slot width/ $D_{85}$ , are given in Table 3. The critical ratio is sensitive to the magnitude of the bottom head,  $H_b$ . A close examination of Fig. 21 shows that (i) the best filter was the fine-to-medium sand with the data for all three flow conditions plotted together and the most severe flow was  $H_b > H_t$ ; (ii) for the gap-graded filter, the data show a similar trend to the fine-to-medium sands but the slot sizes were much larger; (iii) the few points for the well-graded filter lie near to the data for the gap-graded filters; (iv) total washout for a given slot width occurred with the gap-graded and the fine-to-medium sands but seldom with the well-graded sand. It should be appreciated that only one relative density of sand has been simulated. It is believed, however, that the relative density will not have a significant influence on the life span of the filters when subjected to flow reversals, but controlled laboratory tests are required to confirm.

The critical slot width/ $D_{85}$  ratios found were larger than those reported by USCE (1953) and Karpoff (1955) which were 0.83 and 0.5 respectively. For the minimum ratio of 0.83, the slot size is 0.41 mm (fine-to-medium), 1.25 mm (well-graded) and 1.40 mm (gap-graded). Using these openings and referring to the test data presented, it will be noted that no soil movement occurred except for the gap-graded material where some very fine sizes migrated through the 1.40 mm slot. It is possible that the values quoted by these authors make allowances for a factor of safety.

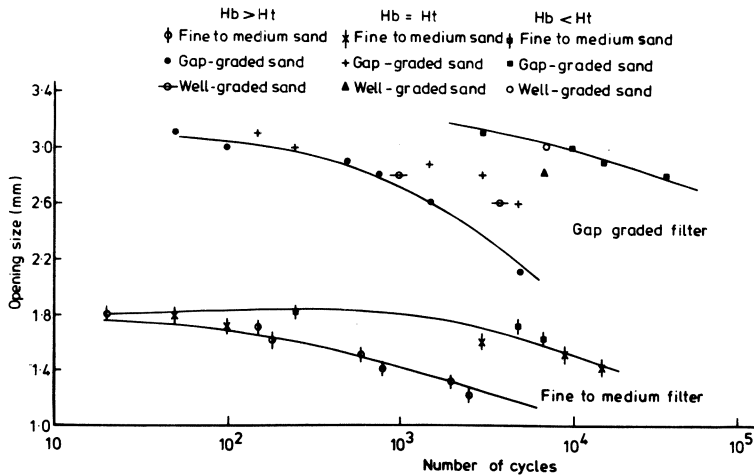


Fig. 21 Life Spans of Filters Causing Wash-Out/Slot Width.

## SOIL PARTICLE MIGRATION THROUGH SLOTS-II

**Table 3 Critical D85/Slot to Cause Washout**

	Medium to Fine Sand	Gap-graded Sand	Well-graded Sand
Unidirectional Flow	0.26	0.52	0.47
Hb = 1.6 m Ht = 1.2 m	0.56	0.94	--
Hb = 1.2 m Ht = 1.2 m	0.38	0.77	0.58
Hb = 0.8 m Ht = 1.2 m	0.33	0.65	0.53

In all tests there was a “significant” quantity of sand washed through the slot, a funnel of coarser material had accumulated directly above the slot with most of the fine sizes missing. The permeability of this funnel-shaped zone was much greater than the original soil mass. As the number of flow reversals increased, more and more fines were washed through and the size of the sand particle near the slot increased, the bridging mechanism and the self-filtering mechanism associated with one-way flow, Tahar & Hanna (1995), being prevented. In addition to the loss of fines from the filter, there was evidence of a zone of “segregated” sand extending upwards and outwards from the slot and this sand was in a loose to very loose condition.

### SIGNIFICANCE OF EXPERIMENTAL FINDINGS

Aggregate filters have been used extensively to prevent fine particles from being washed out of the natural soil. The design of filters is based on the concept of forcing loose fine soil particles and water to follow a tortuous path through the voids. Filters may be required to perform under (i) relatively steady unidirectional flow, (ii) slow reversing flows, (iii) fast reversing flows (not simulated in the present studies). Examples of each category are land drain filters, river and coastal protection filters and anti-pumping filters beneath rail track ballasts. Where the water flow is unidirectional near a slot there must be some loss of fines initially, especially near to the slot opening, leaving a zone of somewhat larger particles which bridge over the slot. These “larger” particles hold back the slightly smaller particles which, in turn, hold back even smaller sizes to cause a zone of graded filter material behind the slot, Fig. 22.

Where the pore constriction size is too large, then the fine soil sizes will pipe through leading to a washout. Where an internal erosion mechanism is involved, a large percentage of the sizes may be lost because the initial loss of sizes creates larger voids in which water

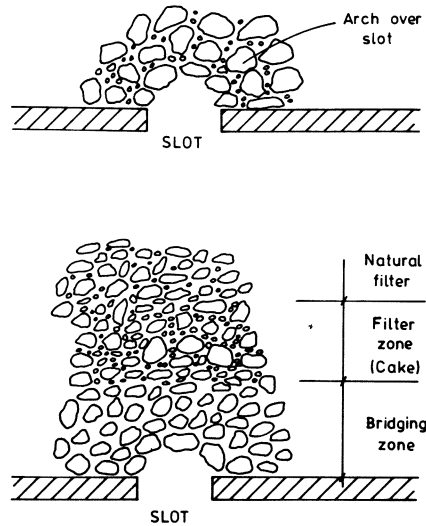


**Fig. 22 Representations of Soil Filter Arching Over A Slot Opening.**

flow is less restrained and more turbulent and erosive. The adjacent soil is more likely to erode which, in turn, furthers the process of soil loss. With the reversing flow condition the arch mechanism and associated bridging across the slot are prevented and, at the critical slot width, zones of segregated soil extend outwards from the opening and apparently the soil is of low density.

The present work shows that even very small changes in the slot width can have a major influence on the stability of the filter material under reversing flow conditions. Where the slot width cannot be maintained at less than the critical values, Table 3, designers should consider seriously the use of geotextiles. During the past decade, extensive studies have been made of the filtration capabilities of different geotextiles. Useful reviews are provided by Giroud (1982) and Ingold (1985).

## CONCLUSIONS

The behaviour of a filter material in the vicinity of an opening with reversing flow surges being passed through the opening, was characterised by three stages. First, there was an initial stable period followed by a short period when deterioration occurred with soil migration through the slot increasing. Finally, a rapid deterioration led to a washout. The rate of the cumulative soil loss as a function of the log of the number of flow reversals indicated how stable the filter material was, an increase in the rate indicating a trend towards instability and a decrease in the rate suggesting improvement in stability. The life span of the filter was increased by a reduction in the slot width and by a reduction in the value of the cyclic bottom head,  $H_b$ . The well-graded filter was more stable than the gap-

## SOIL PARTICLE MIGRATION THROUGH SLOTS-II

graded or the fine-to-medium filters. The slot widths relative to the  $D_{85}$  sizes varied depending on the relative values of the top head,  $H_t$  and the bottom head,  $H_b$ . The most severe flow condition was  $H_b > H_t$ .

Much further research, both field and laboratory, is needed to establish (i) the actual condition of drains and in particular the pulling of joints and dimensions of cracks and other imperfections; (ii) the amount of silting in drains; (iii) the extent of ground migration towards an opening in a drain or other foundation element such as a retaining wall; (iv) the tolerances of drains to differential movements; (v) the magnitude and duration of surges in drains. Coupled with these investigations there is the need to quantify the ground particularly gradation and denseness.

The primary purpose of the paper is to make civil engineers more aware of the damage which may be caused to the ground by water pressure surges in a drain with openings in its walls. The geotechnical significance of the phenomena does not appear to have been highlighted. Further study of the significance, if any, of the relative density of the filter and the frequency of the reverse flows appear justified before generally applicable slot width to  $D_{85}$  ratios can be recommended.

### REFERENCES

- GIROUD, J.P., (1972). "Filter Criteria for Geotextiles", Proceedings Second International Conference on Geotextiles, Las Vegas, Vol. 1, pp. 103-108.
- INGOLD, T.S., (1985). "A Theoretical and Laboratory Investigation of Alternating Flow Criteria for Woven Structures", Geotextiles and Geomembranes, Vol. 2, No. 1, pp. 31-46.
- KARPOFF, K.P., (1955). "The Use of Laboratory Tests to Develop Design Criteria for Protective Filters", Proceedings American Society for Testing and Materials, Vol. 55, pp. 1183-1195.
- KENNEY, T.C., CHAHAL, R., OFOEGBU, G.I., OMANGE, G.N. and UME, C.E., (1985). "Controlling Constriction Sizes of Granular Filters" Canadian Geotechnical Journal, Vol. 22, No. 1, pp. 32-43.
- KENNY, T.C. and LAU, D., (1985). "Internal Stability of Granular Filters" Canadian Geotechnical Journal, Vol. 22, No. 3, pp. 215-225.
- TAHAR, B. and HANNA, T.H., (1995). "Soil Particle Migration through Slots in Drains - I, Unidirectional Flows", *Geotechnical Engineering*, Vol. 26, No. 1.
- US ARMY CORPS OF ENGINEERS, (1953). "Filter Experiments and Design Criteria", Waterways Experiment Station, Vicksburg, Miss, Technical Memorandum, No. 3 - 360, 52 pp.





# STRENGTH CHARACTERISTICS OF SABKHA SOILS

O.S.B. Al-Amoudi<sup>1</sup> and S.N. Abduljawwad<sup>1</sup>

## SYNOPSIS

This is a study to assess the strength characteristics of a sabkha soil from eastern Saudi Arabia. A total of 24 undisturbed samples were tested under unconfined compression, direct shear, consolidated-drained and consolidated-undrained triaxial tests. These samples were tested either at their natural moisture content or initially saturated with either distilled water or sabkha brine. Moreover, 14 CBR tests were conducted in the field and laboratory under natural and soaked conditions to evaluate the response of undisturbed sabkha soil to penetration tests.

Results of this investigation indicate that sabkha possesses low strength in its natural condition and it is highly susceptible to collapse upon exposure to water. Furthermore, there is a strong correlation between the shear strength and the cemented structure of sabkha soil. Only those triaxially-tested samples which were saturated with distilled water and for which volume change measurements were measured suffered a reduction in the angle of internal friction. Direct shear test produced shear strength parameters ( $Q'$  and  $c'$ ) higher than those produced by the triaxial tests.

## INTRODUCTION

Depositional environments and subsequent geological histories sometimes combine to produce particularly difficult and in some respects unique ground conditions. Examples include the Canadian Champlain (Leda) and the Norwegian marine "quick" or sensitive clays. In the tropics, hot and arid climates, with considerably more evaporation than precipitation are most conducive to saline "evaporitic" soils (Renfro, 1974). Although attempts to formulate an index of the degree of aridity for purposes of climatic classification are somewhat difficult (American Geological Institute, 1974), arid regions are generally defined to have an annual rainfall of less than 100 mm and characterized by a net evaporation rate (El-Naggar, 1988). This naturally results in the concentration of various salts in the groundwater that may diagenetically lead to precipitating some minerals in the uppermost part of the soil profile as well as in the groundwater (Kinsman, 1969). Once salts have been deposited, the capacity of the sediments to transmit moisture upward is enhanced so that salt accumulation is accentuated (Fookes et al, 1985).

Many types of evaporite flats exist around the globe, particularly within the Tropical Zones. Local names for these evaporite associations are many and highly bewildering. Ellis (1973) presented some local names used in many countries. At the risk of gross over-

---

<sup>1</sup> Department of Civil Engineering, King Fahd University of Petroleum & Minerals, Dhahran 31261, Saudi Arabia

simplification, Fookes and Collis (1975) have reduced these names, for engineering purposes, to sabkha (a coastal salt marsh), playa (an ephemeral lake flat), salt playa (as playa but with salty surface due to evaporation of saline lake waters) and salina (a local depression with high watertable and capillary rise reaching the surface, with the formation of a salt crust).

Sabkhas are well-distributed in Saudi Arabia, particularly along the eastern and western coastal plains (Fig. 1) (Al-Amoudi et al, 1992b). These soils have generally been viewed as unconsolidated, heterogeneous, layered or unlayered sedimentological framework, bathed in highly concentrated subsurface brines. They normally have loose, rather porous and permeable, gritty structure (Al-Amoudi et al, 1991). Their outer surfaces are usually composed of hygroscopic salts, which can render the normally stable sabkha surfaces unstable when dampened. The sedimentary features, mineralogical composition and the chemistry of the interstitial brines in such coastal sabkhas vary greatly in both the horizontal and the vertical directions (Butler, 1969). Horizontal variations are expected to be related to proximity from the shoreline (Akili & Torrance, 1981), while vertical variations represent successive stages in the development of the sabkha cycle. These characteristics, added to the presence of highly concentrated brines, are the distinguishing features that have rendered the sabkha soils their hazardous geotechnical properties (Amoudi et al, 1991; Shehata et al, 1990).

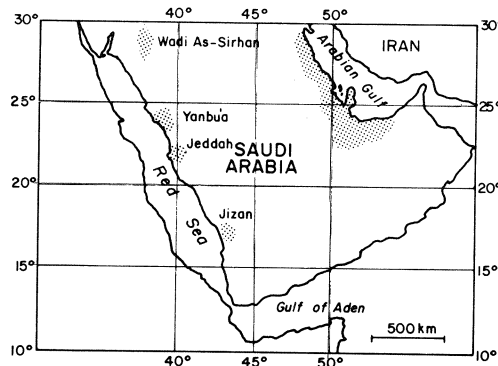


**Fig. 1 Distribution of Sabkha Soils in the Kingdom of Saudi Arabia (Al-Amoudi et al. 1992b)**

The shear strength of a soil is a measure of its resistance to deformation by continuous displacement of the soil individual particles. Soil shear strength is by far the most important property in foundation and embankment design, slope stability, etc., and unless it is properly assessed, misleading shear strength parameters will lead to spurious, unwarranted consequences. For the case of arid, saline soils, such as sabkhas, the degree of saturation presents an inevitable challenge that the geotechnical engineer has to deal with to properly evaluate the shear strength parameters of such cemented soils. This is so because of the weakly cemented structure of such soils and the source of saturation, whether

## STRENGTH CHARACTERISTICS OF SABKHA

from the highly saline groundwater or rain water, which might cause significant salt dissolution and/or salt precipitation, thereby endangering the cemented matrix of the soil.

This investigation was carried out to properly assess the strength characteristics of a surficial sabkha soil from eastern Saudi Arabia. Due to the complicated nature of sabkha, several tests, including field and laboratory CBR, unconfined compression, direct shear and triaxial tests, were conducted in order to provide an accurate assessment for the strength of this unusual soil.

### EXPERIMENTAL PROGRAM

In this investigation, surficial undisturbed sabkha samples were retrieved from Ras Al-Gar, eastern Saudi Arabia (Fig. 2). These samples were obtained using thin-walled PVC tubes that had been sharpened from their penetrating ends in order to reduce disturbance. Classical samplers made of steel or brass were not used due to the high salt content of sabkha which might cause rust problems. These tubes were made with two different sizes, 5 x 10 cm and 10 x 20 cm, both of them had an area ratio of 14%. Although well-designed samplers should have an area ratio of less than 10% to obtain undisturbed samples, the commonly-used thin-walled (Shelby) tube has an area ratio of 13.6% which is almost similar to that for the PVC tubes used in the present investigation. The 5 x 10 cm tubes were used to obtain undisturbed specimens used in unconfined and triaxial tests while the 10 x 20 cm ones were used to obtain the specimens used in direct shear tests.

To obtain the undisturbed sabkha samples, the PVC tubes were inserted manually to a depth of 22 to 42 cm from the ground surface. Through the use of a shovel and a knife,

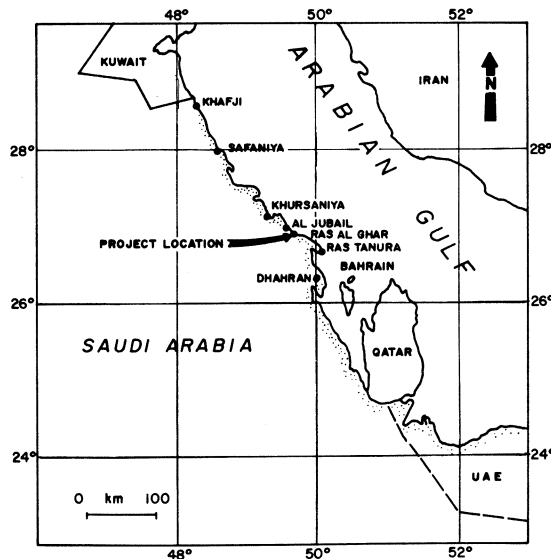


Fig. 2 Vicinity Map Showing the Ras-Al Ghar Location

the tubes were retrieved with great care in order to minimize disturbance. Each specimen was thereafter placed in a double nylon sheet along with a label indicating the date of sampling. As soon as the samples were brought to the laboratory, they were uncovered from the nylon and their top and bottom ends were sealed with wax and preserved until they were tested.

For the laboratory California bearing-ratio (CBR) tests, eight undisturbed specimens were retrieved from the same depth from which other samples were obtained in the special CBR moulds and covered with nylon sheets to prevent any moisture loss.

Direct shear tests were conducted in general accordance with ASTM D 3080 at a loading rate of 0.75 mm/min using a square shear box (6 x 6 cm). The normal stresses were 109, 218 and 435 kPa. Three undisturbed samples (5 x 10 cm) were used in the unconfined compression test at a constant loading rate of 0.5 mm/min in accordance with ASTM D 2166.

Five series of isotropically-consolidated triaxial tests (ASTM D 2850) were conducted on 5 x 10 cm undisturbed sabkha samples. In the first series, six specimens were tested at their natural moisture content using different confining pressures under consolidated-drained (CD) conditions with no measurement of the volume change. This series was intended to be as a "pilot" study for the other four series. In the second series, three samples were initially saturated with distilled water and tested under similar conditions to series # 1; however, volume change measurements were recorded. Saturation was achieved through firstly applying carbon dioxide (CO<sub>2</sub>) gas in order to expel gas in the pores; thereafter, back pressure was applied. The carbon dioxide has been used due to its high solubility in water which will lead almost to a fully saturated condition. It should be mentioned that a little amount of water was allowed to drain out during the saturation stage in order not to alter the initial fabric of these sabkha samples. In the third series, three specimens were initially saturated with distilled water and subjected to consolidated-undrained (CU) tests with continuous measurements of pore-water pressure. For the case of series # 4 and 5, similar tests to series # 2 and 3 were conducted on undisturbed sabkha samples, however, the specimens were initially saturated with sabkha brine that was brought from the same test pit from which the undisturbed samples were obtained. All triaxial tests were conducted at a loading rate of 0.5 mm/min.

The laboratory CBR tests were conducted in compliance with ASTM D 1883, at a penetration rate of 1.27 mm/min and the load and penetration readings were measured until a penetration of a slightly more than 13 mm was obtained. Four of the eight CBR specimens were tested at their natural state on the same day they were retrieved. The other four were flooded with distilled water under a surcharge of 5 kg, according to the standard procedure, for four days, with a gage attached to the specimens to measure any expansion due to water flooding. Moreover, six field CBR tests were conducted in a similar manner to the laboratory tests wherein the standardized plunger, having an end area of 19.4 cm<sup>2</sup>, was used. Three of these field tests were performed on sabkha at its natural condition while the other three were conducted under flooded "soaked" condition.

Data generated from the various laboratory tests conducted in this investigation

## STRENGTH CHARACTERISTICS OF SABKHA

were collected using a portable TDS-301 Tokyo Sokki data logger, which were, thereafter, analyzed and interpreted.

### RESULTS PRESENTATION

Results of a recent investigation have indicated that the present sabkha soil could be classified as A-2-4 and as SW-SP according to the AASHTO and USCS systems, respectively (Al-Amoudi, et al. 1992a). Its specific gravity was 2.73 and the permeability coefficient varied from  $1.24 \times 10^{-6}$  to  $3.15 \times 10^{-5}$  m/s depending on the type of permeability test (i.e., whether constant or variable head) and the percolating liquid (i.e., whether distilled water or sabkha brine). Figure 3 shows an X-ray diffractogram for the surficial sabkha. Semi-quantitative analysis indicates that the following mineral phases are present: quartz (44.2%), halite (15.3%), orthoclase (11.9%), aragonite (11.1%), calcite (9.1%), gypsum (6.5%), and traces of anhydrite (Al-Amoudi 1992).

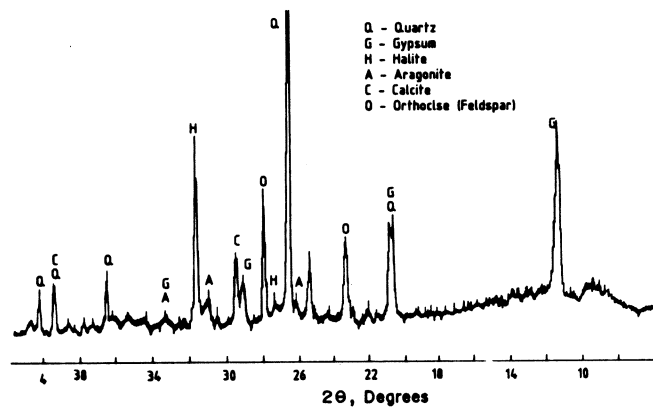


**Fig. 3 X-Ray Diffraction Pattern for Surficial Sabkha Soil**

Data developed using both field and laboratory CBR tests are summarized in Table 1. These data delineate the low strength of surficial sabkha layers at their naturally-existing conditions. These soils had very poor CBR values of only 3 and 4, and such poor values were even reduced by 50% when the sabkha was flooded with water. Table 1 also shows that the average CBR values for both the field and the laboratory tests agree well with each other and such a good correlation between the field and laboratory tests provides a better assessment for the strength of surficial sabkha soils than the individual CBR values. This is because the heterogeneity of sabkha necessitates that a large number of samples be tested to produce a representative average value that can be relied upon.

Results of the unconfined compression tests were presented in Fig. 4. These data indicate that the surficial, natural sabkha possesses very low strength of 14.9, 19.9 and 22.0 kPa, with an average unconfined compressive strength ( $q_u$ ) of 18.6 kPa (2.7 psi). Again,

**Table 1 Summary of Field and Laboratory CBR Test Results.**

Type of Test	Sample#	CBR at 0.1 inch		CBR at 0.2 inch		Corrected CBR Value <sup>+</sup>	Average CBR Value
		Pressure (psi)	CBR*	Pressure (psi)	CBR**		
Field CBR at Natural Condition	1	21	2.1	26	1.7	2.1	3.2
	2	43	4.3	60	4.0	4.3	
	3	21	2.1	47	3.1	3.1	
Field CBR at Soaked Condition	1	23	2.3	32	2.1	2.3	1.6
	2	17	1.7	25	1.7	1.7	
	3	8	0.8	13	0.9	0.9	
Laboratory CBR at Undisturbed Natural Condition	1	12.79	1.3	20.21	1.3	1.3	3.8
	2	41.96	4.2	65.26	4.4	4.4	
	3	16.24	1.6	23.37	1.6	1.6	
	4	40.12	4.0	50.27	3.4	4.0	
Laboratory CBR at Undisturbed Natural Soaked-Condition	1	31.30	3.1	42.95	2.9	3.1 <sup>++</sup>	1.7
	2	15.37	1.5	21.61	1.4	1.5	
	3	22.78	2.3	29.07	1.9	2.3	
	4	14.32	1.4	18.21	1.2	1.4	

\* CBR = Pressure/10.0

\*\* CBR = Pressure/15.0

+ This value equals to the highest of the two CBR values

++ This test was deleted due to disturbance.

Note: 1 psi = 6.9 kPa  
1 inch = 25.4 mm

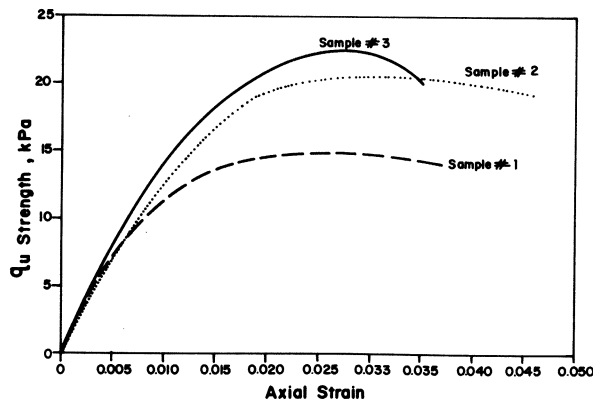


**Fig. 4 Unconfined Compressive Strength Test Results for the Undisturbed Sabkha Samples**

*STRENGTH CHARACTERISTICS OF SABKHA*

the variation in  $q_u$  test results reflects the heterogeneous nature of sabkha soils.

The direct shear test results are presented in Fig. 5, where part (a) presents the horizontal displacement vs. shear stress, while part (b) shows the Mohr-Coulomb failure envelope using the best fit for the normal and shear stresses at failure. This test yielded an angle of internal friction ( $\phi'$ ) of  $36^\circ$  and a cohesion intercept ( $c'$ ) of 50 kPa. This value of  $\phi'$  is much more than those reported by Abu-Taleb and Egeli (1981) for an eastern Saudi sabkha ( $\phi' = 0^\circ$  to  $22^\circ$ ), however, the methodology by which those values were determined were not reported. These  $\phi'$  values could have been developed for either some argillaceous sabkha soils at deeper strata or they were predicted using some correlations from field test results. Ismail, et al. (1986) have recently observed that prediction of the angle of internal

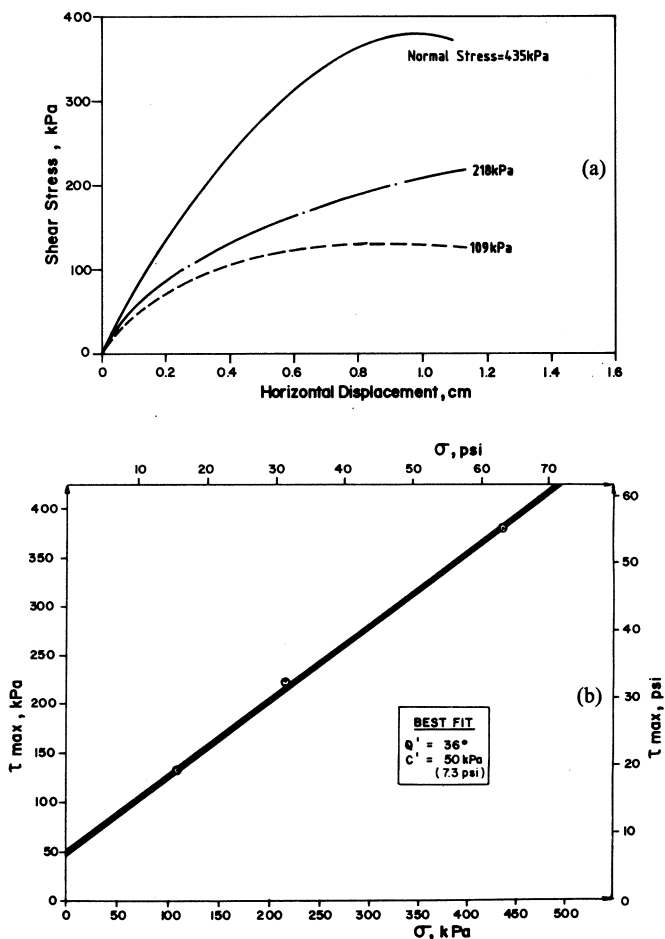


**Fig. 5 Direct Shear Test Results**  
**Fig. 5a Shear Stress-Horizontal Displacement Data**  
**Fig. 5b Mohr-Coulomb Failure Envelope**



friction ( $\phi'$ ) from SPT field tests conducted on cemented calcareous silty sands generally produce smaller values of  $\phi'$  than the ones obtained from both soaked and unsoaked direct shear tests. The present  $c'$  value was, nevertheless, on the upper range of Abu-Taleb and Egeili ( $c' = 0$  to 54 kPa).

Results of the CD triaxial tests in which volume change measurements were not recorded are shown in Fig. 6, where part (a) depicts the deviatoric stress-axial strain data and part (b) shows the Mohr-Coulomb failure envelope. Results of the CD triaxial tests in which the specimens were initially saturated with distilled water are presented in Figs. 7 (a, b and c), where parts a, b and c show the stress-strain curve, volumetric strain-axial strain curve and Mohr-Coulomb failure envelope, respectively. Similar results are presented in Figs. 8 (a, b and c) for those specimens which were initially saturated with sabkha brine. For the case of CU triaxial tests, Fig. 9 shows the results of tests carried out on undisturbed

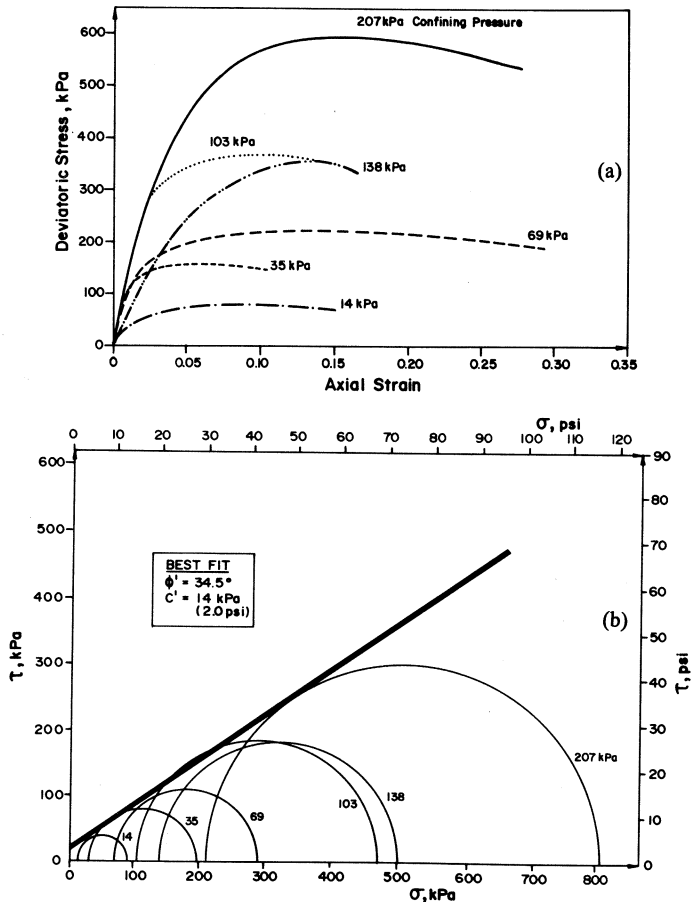
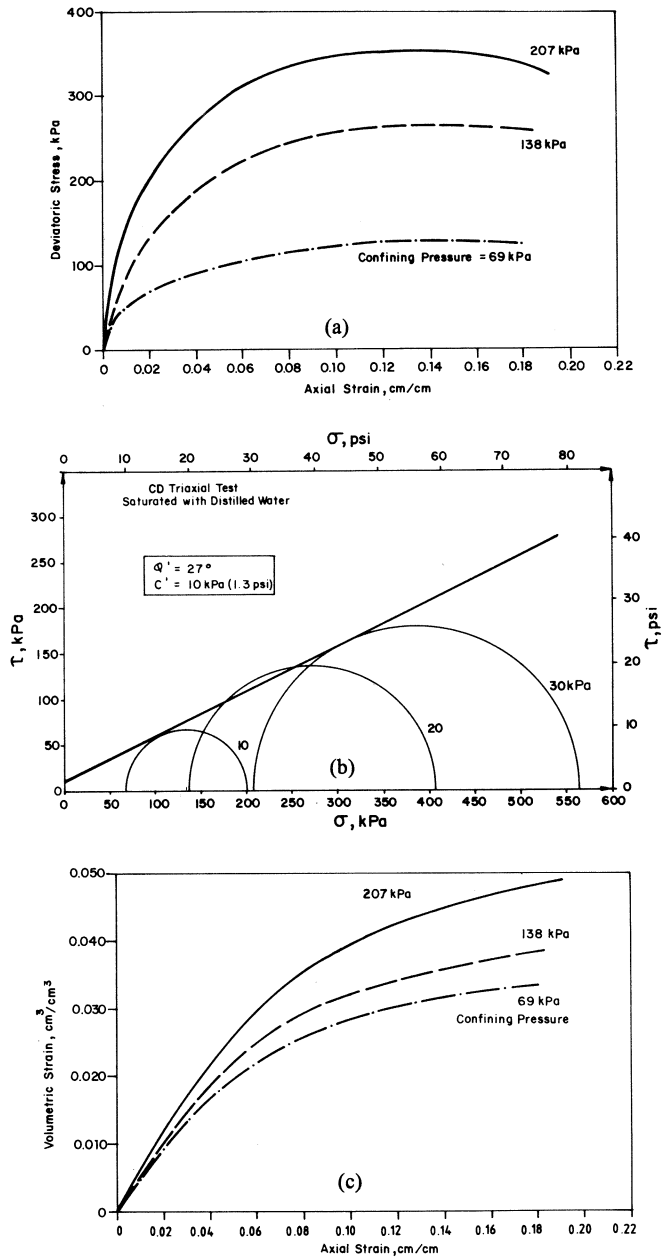


Fig. 6 CD Triaxial Test Results with No Volume Change Measurements  
 Fig. 6a Stress-Strain Data    Fig. 6b Mohr-Coulomb Failure Envelope

**STRENGTH CHARACTERISTICS OF SABKHA**



**Fig. 7 CD Triaxial Test Results with Initial Saturation with Distilled Water and Volume Change Measurements**

**Fig. 7a Stress-Strain Data      Fig. 7b Volume Change Measurement  
Fig. 7c Mohr-Coulomb Failure Envelope**

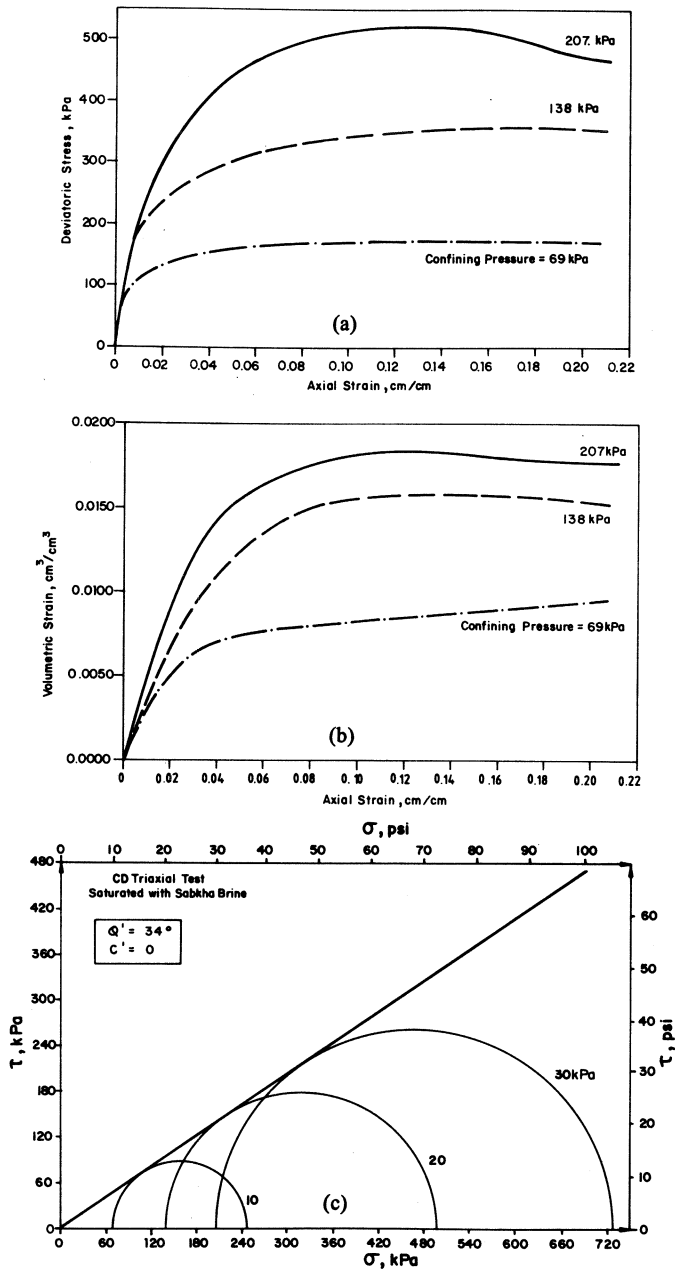


**Fig. 8 CD Triaxial Test Results with Initial Saturation with Sabkha Brine and Volume Change Measurements**

**Fig. 8a Stress-Strain Data      Fig. 8b Volume Change Measurement**

**Fig. 8c Mohr-Coulomb Failure Envelope**

*STRENGTH CHARACTERISTICS OF SABKHA*

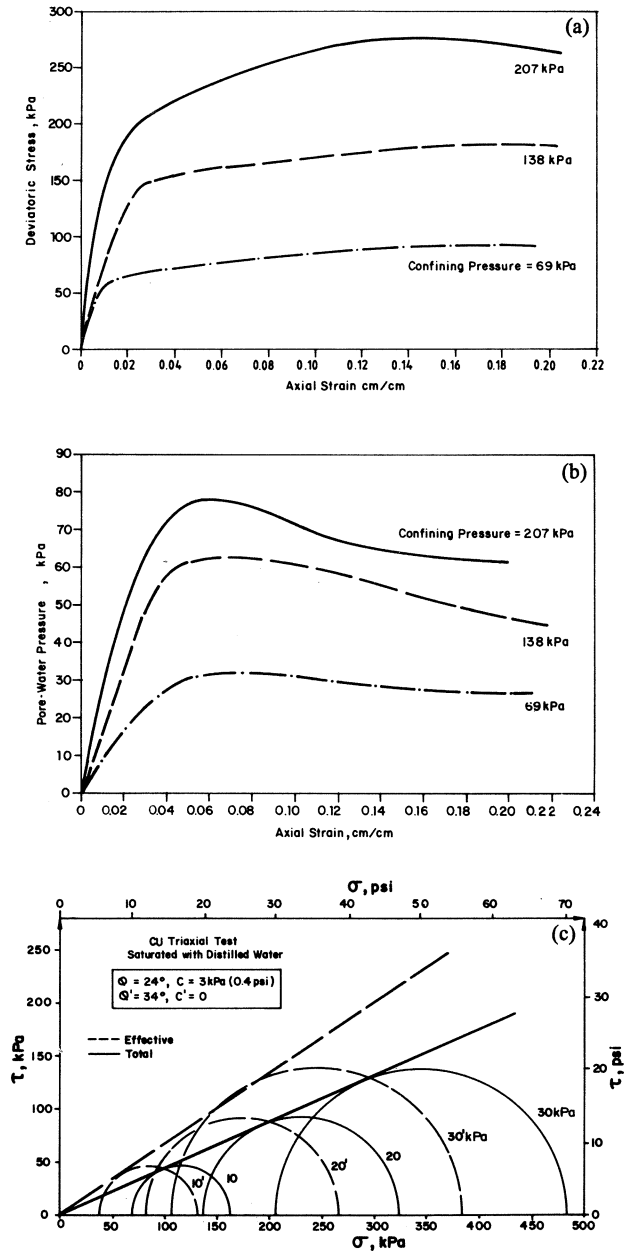


**Fig. 9 CU Triaxial Test Results with Initial Saturation with Distilled Water and Volume Change Measurements**

**Fig. 9a Stress-Strain Data      Fig. 9b Pore-Water Pressure Measurement  
Fig. 9c Mohr-Coulomb Failure Envelope**

specimens which were initially saturated with distilled water. In this Figure, part (a) presents the stress-strain data, part (b) shows the pore-water pressure-strain data and part (c) shows the effective and total Mohr-Coulomb failure envelopes. Similarly, results for the specimens which were initially saturated with sabkha brine are presented in Figs. 10 (a, b and c). Figures 11 (a and b) show the stress paths for the CD triaxial tests for the specimens which were initially saturated with distilled water and sabkha brine, respectively, in terms of the p-q space, where p and q are defined as follows:

$$q = \sigma_1 - \sigma_3 \quad (1)$$

$$p = \frac{\sigma_1 + 2\sigma_3}{3} \quad (2)$$

For both tests, the paths moved above the projection of the critical state line to the Hvorslev surface before moving back along the same path towards the critical state line. Figures 12 (a and b) show the total stress path and the effective stress path for the CU triaxial tests, where q' and p' are defined as follows:

$$q' = q \quad (3)$$

$$p' = p - u \quad (4)$$

where u is the pore water pressure. The effective stress paths for both tests intersect the critical state line and move along it till failure occurs at the maximum deviatoric stress. The pore water pressures are positive throughout the tests, but tend to decrease when the samples approach the failure conditions. This behavior indicated that the samples are slightly overconsolidated due to the natural cementation. Such characteristics have recently been reported by the authors using oedometer tests (Al-Amoudi et al, 1992a).

Since the ultimate aims of any triaxial test is to virtually determine the effective and total angle of internal friction as well as the effective and total cohesion ( $\phi'$ ,  $\phi$ ,  $c'$  and  $c$ , respectively), results of all triaxial tests conducted in this investigation are therefore summarized and presented in terms of these parameters, as shown in Table 2. Also included in this table are the results of the direct shear tests for relative comparison.

## DISCUSSION OF RESULTS

Table 1 summarizes the field and laboratory CBR results. These CBR values are rated as very poor (from 0 to 3) and as poor to fair (from 3 to 7) (Bowles, 1978). The low CBR values of the naturally-existing sabkha soil reflect the loose condition and the high natural moisture content of these soils (Al-Amoudi 1992). The very poor performance of sabkha in the soaked CBR tests is a manifestation of the susceptibility of sabkha to collapse once water dissolves the cementing agents in the sabkha matrix (Al-Amoudi & Abduljawwad, 1994). This is evidenced from the mineralogical composition of sabkha (Fig. 3), whereby halite (NaCl), constituting 15% by weight of surficial sabkha soil, renders sabkha collapsible characteristics upon exposure to water due to its high solubility.

**STRENGTH CHARACTERISTICS OF SABKHA**

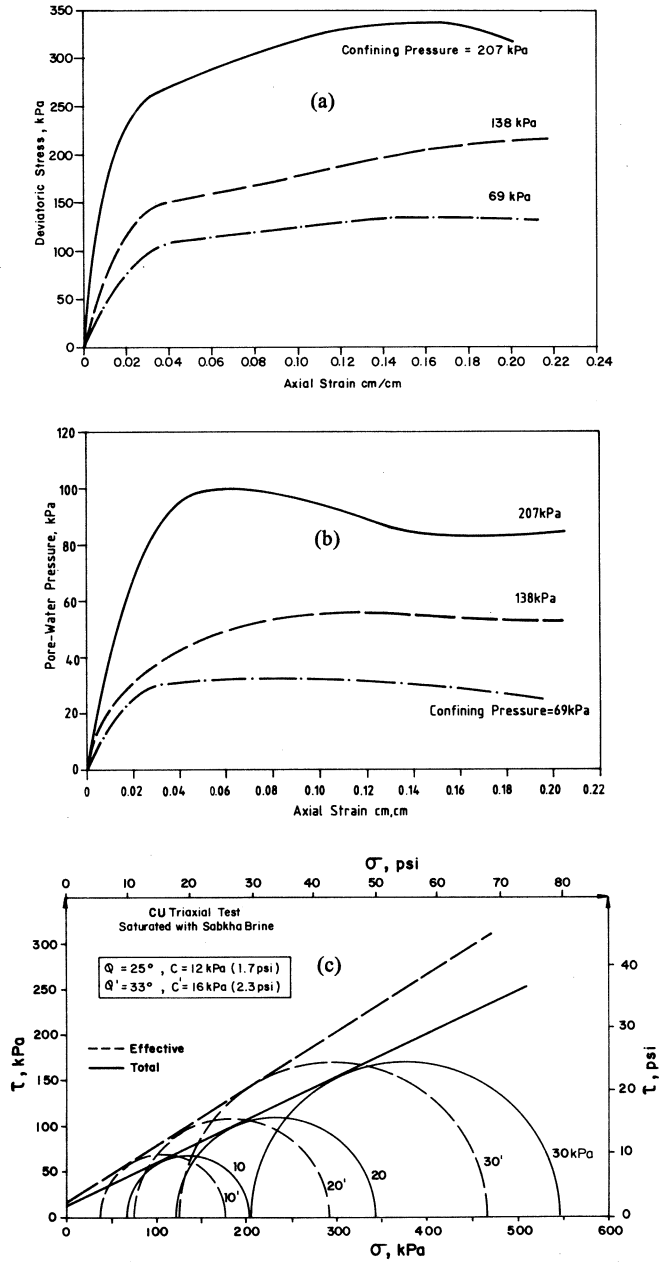


**Fig. 10 CU Triaxial Test Results with Initial Saturation with Sabkha Brine and Volume Change Measurements**

**Fig. 10a Stress-Strain Data**

**Fig. 10b Pore-Water Pressure Measurement**

**Fig. 10c Mohr-Coulomb Failure Envelope**

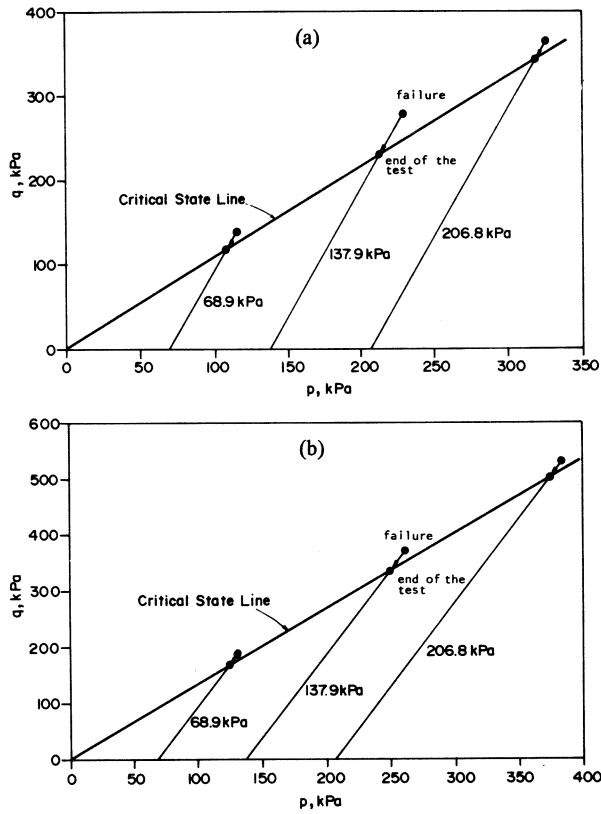


**Fig. 11 Stress Path Results for the CD Triaxial Tests**  
**Fig. 11a Specimens Saturated with Distilled Water**  
**Fig. 11b Specimens Saturated with Sabkha Brine**

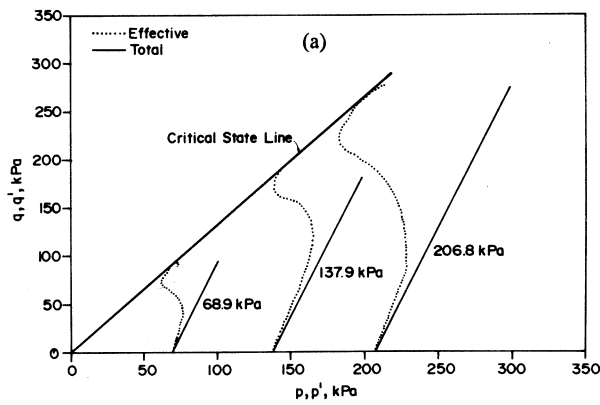


**Fig. 12 Stress Path Results for the CU Triaxial Tests**  
**Fig. 12a Specimens Saturated with Distilled Water**

## STRENGTH CHARACTERISTICS OF SABKHA

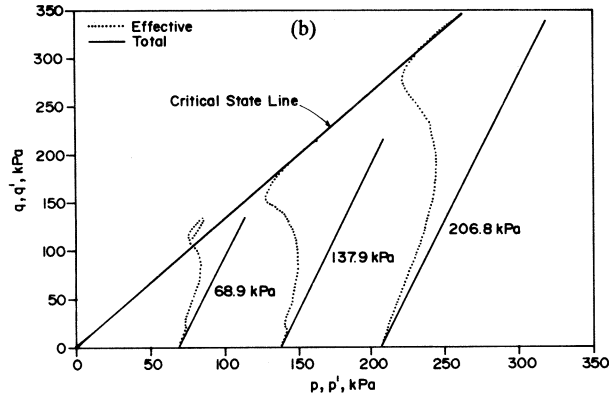


**Fig. 12b Specimens Saturated with Sabkha Brine**

Results of the unconfined compression tests also indicate that surficial sabkhas possess very low strength of only 18.6 kPa (2.7 psi). This has recently been confirmed by the authors based on standard penetration test (SPT) (Al-Amoudi et al, 1991) and also by both field and laboratory California-bearing ratio (CBR) tests.

For the case of triaxial and direct shear tests, the data presented in Table 2 reveal the following observations:

- (i) All triaxial tests, with the exception of CD ones in which the specimens were initially saturated with distilled water, had the same  $\sigma'$  value (approximately  $34^\circ$ ), while  $c'$  values varied from 0 to 16 kPa. Moreover, the value of  $\phi$  was also the same for all CU tests whether saturated with distilled water or sabkha brine ( $24^\circ$  and  $25^\circ$ ). This value is very close to that obtained from the CD tests in which the specimens were initially saturated with distilled water ( $27^\circ$ ). Again, the value of  $c$  varied insignificantly from 3 to 12 kPa.
- (ii) Comparison of the three CD tests indicates that only the one in which the specimens were saturated with distilled water and for which volume change measurements were taken showed a reduced  $\phi'$  compared with the other two CD tests in which the specimens were tested at their natural moisture content or those which were initially saturated with sabkha brine ( $27^\circ$  compared with  $34.5^\circ$  and  $34^\circ$ ). The variation in  $c'$  was again similar to observation (i).
- (iii) The reason behind reduction in  $\phi'$  value due to saturation with distilled water and volume change measurement was primarily attributed to salt dissolution in spite of the relatively small volume change that took place (i.e., the volume change varied from 3.5% to 5.0% depending on the confining pressure, as shown in Fig. 7(b)). The small amount of distilled water expelled out during the deviatoric loading was apparently sufficient to dissolve and leach out some salts which altered the initial cemented fabric of the sabkha and, consequently, led to  $5^\circ$  reduction in  $\phi'$ . Similar findings have recently been reported by Ismail, et al. (1986) based on soaked and



**Table 2 Summary of Shear Strength Parameters for Various Triaxial and Direct Shear Tests.**

Triaxial Test*	Saturation with	Parameter Measured	Shear Strength Parameter*			
			$\phi$ , deg.	$c'$ , kPa	$\phi$ , deg.	$c$ , kPa
CD	No Saturation	No Volume Change Measurement	34.5	14	--	--
CD	Distilled Water	Volume Change	27	10	--	--
CD	Sabkha Brine	Volume Change	34	0	--	--
CU	Distilled Water	Pore-Water Pressure	34	0	24	3
CU	Sabkha Brine	Pore-Water Pressure	33	16	25	12
Direct Shear Test			36	50	--	--

\*CD = consolidated-drained  
 CU = consolidated-undrained  
 $\phi'$  = effective angle of internal friction  
 $c'$  = effective cohesion  
 $\phi$  = total angle of internal friction

unsoaked direct shear tests. They observed that the angle of internal friction of calcareous desert sands was reduced from 40° to 35.5° due to saturation. This hypothesis is further supported by both results of either the CD test in which no saturation took place or the CU tests in which the specimens were initially saturated with distilled water. For the latter, prevention of distilled water expulsion during deviatoric stress application did not cause any reduction in  $\phi'$ , which implies that saturation alone does not bring about a significant collapse in the fabric of sabkha. The present authors have recently pointed out (Al-Amoudi & Abduljawad, 1994), based on consolidation tests on similar undisturbed sabkha specimens using conventional and modified oedometers, that saturation or wetting will induce a marginal collapse, however, when distilled water is allowed to percolate through the sabkha and hence dissolves the salt cementing agents, a significant collapse occurs.

- (iv) The inducement of collapse due to salt dissolution can be somewhat observed by comparing Fig. 7(b) with Fig. 8(b), where saturation with distilled water increased the volume change by about 2.5 times compared to saturation with sabkha brine. This relatively large increase in volume change due to saturation with distilled water

## *STRENGTH CHARACTERISTICS OF SABKHA*

(which indicates an increased reduction in void ratio) is a manifestation of the collapse of sabkha structure.

- (v) The variation of both  $c'$  and  $c$  values in the case of triaxial test results is rather surprising in spite of the fact that  $\phi'$  and  $\phi$  showed a high degree of consistency. This might be attributed to the initially-heterogeneous fabric of these undisturbed surficial sabkha samples. These samples were generally highly cemented and desiccated, as observed by many researchers (El-Naggar 1988; Fookes et al, 1985; Ellis, 1973; Al-Amoudi et al, 1991; Akili & Torrance, 1981; Al-Amoudi et al, 1992a; Al-Amoudi, 1992), and these characteristics were more reflected by variation in the cohesion than in the angle of internal friction (Aiban 1985). Ismail, et al. (1986) have observed the same phenomenon upon testing cemented calcareous sand under unsoaked and soaked direct shear test conditions. They reported that the angle of internal friction ( $\phi$ ) varies from  $40.4^\circ$  to  $41.7^\circ$  and from  $35.5^\circ$  to  $35.8^\circ$  for unsoaked and soaked tests, respectively. On the contrary,  $c$  varies from 0 to 24 kPa for the unsoaked tests while the soaked ones produced zero cohesion. It is worth mentioning that the soil in the above investigation (Ismail, et al. 1986) was brought from four different localities in Kuwait. To sum up, the maximum difference in cohesion was only 16 kPa (2.3 psi), which is practically very small.
- (vi) Comparison of the CD tests in which neither saturation nor volume change measurements were recorded, with the CD tests in which the specimens were initially saturated with sabkha brine or with both CU tests indicates that the volume change measurement did not have any significant effect on the angle of internal friction. This is indicative of the invariant fabric of the tested specimens, as no salt dissolution took place. In the absence of salt dissolution, initial saturation with sabkha brine in the CD tests or with both liquids in the CU tests will have no significant effect on the angle of internal friction. The marginal increase in  $c'$  value in the CD non-saturated specimens was attributed to the less moisture content of these specimens compared to the other specimens which were initially saturated. High moisture contents have been observed by authors to cause spongy characteristics in compaction tests (Al-Amoudi, et al. 1992a). It is therefore rational to conclude that the high moisture content did not have a significant impact on the friction angle, and the relatively higher cohesion in the non-saturated specimens was primarily attributed to the lower moisture content in these specimens.
- (vii) Comparison of the shear strength parameters developed by the use of direct shear tests and the non-saturated CD triaxial tests (i.e. both had the same initial conditions) reveals the relatively higher effective angle of friction and cohesion as determined by the direct shear test than those determined by the triaxial test (i.e.  $\phi' = 36^\circ$  and  $c' = 50$  kPa compared with  $\phi' = 34.5^\circ$  and  $c' = 14$  kPa). This was primarily attributed to the confining phenomenon provided by the shear box. Das (1983) reported that the angle of internal friction is slightly lower in the triaxial test (from  $0^\circ$  to  $3^\circ$ ) compared to the direct shear test due to the confining effect. This agrees very well with the present results.

- (viii) The last observation is the development of cohesion in spite of the cohesionless nature of this sabkha. Such cohesion was observed in Fig. 4 for the unconfined compression tests as well as in the triaxial tests. This “apparent” cohesion was the result of cementation and desiccation that were developed by the presence of salt in sabkha. With the continuous daily and seasonal variations in temperature and humidity regimes, such surficial soils develop a high overconsolidation ratios of 15 to 23 (Al-Amoudi et al, 1992a; Al-Amoudi & Abduljawwad, 1994). Such characteristics have also been observed for other sabkhas (Hossain & Ali, 1988). This type of cohesion is temporary and it is easily disrupted or destroyed if the soil is subjected to continuous exposure to water, as observed in the soaked CBR tests.

Interpretation of the test results conducted in the present investigation as well as their applications from foundation design point of view may lead to deceptive conclusions. While the unconfined compressive strength and the CBR values for the Ras Al-Ghar surficial sabkha have been observed to be very low in its natural condition, the shear strength parameters developed by the direct shear test as well as the various triaxial tests ( $\phi' = 33^\circ$  and  $c' = 15$  kPa, on the average) convey the impression that this same soil is rather strong enough to provide an allowable bearing pressure of more than 1,000 kPa (6,900 psf) according to Terzaghi's bearing capacity theory for a typical square foundation (Bowles 1982). This is contrary to the very low strength provided by the unconfined compression and the CBR test results. It seems that both the triaxial and direct shear test results do not provide a good assessment of the shear strength parameters for surficial soils because of the lack of proper confinement. It can therefore be concluded, based on the present results, that both triaxial and direct shear tests do not represent a proper means for assessing surficial soils unless the confining and normal pressures in these tests are comparable to those prevailing in actual field conditions.

## CONCLUSIONS

Based on the field and laboratory CBR, unconfined compression, direct shear and the various types of consolidated-drained (CD) and consolidated-undrained (CU) triaxial tests conducted on surficial, undisturbed sabkha soil retrieved from eastern Saudi Arabia, the following main concluding remarks can be stated:

1. Surficial sabkha soils possess very low strength.
2. Sabkhas are highly susceptible to collapse upon percolation with water.
3. The shear strength parameters ( $\phi'$  and  $c'$ ) obtained by the use of direct shear tests were somewhat more than those obtained by the triaxial tests under the same soil conditions.
4. All CD and CU triaxial tests produced the same effective angle of internal friction ( $\phi'$ ) whether the specimens were initially saturated with distilled water or sabkha brine. Only those specimens which were initially saturated with distilled water and for which volumetric change was allowed to take place exhibited a  $5^\circ$  reduction in  $\phi'$ .

## *STRENGTH CHARACTERISTICS OF SABKHA*

5. The effective cohesion ( $c'$ ) seems to be affected by the initial degree of saturation. Almost all saturated specimens tested under both CD and CU triaxial conditions developed a reduced  $c'$  compared to the non-saturated specimens.
6. The shear strength parameters ( $\sigma'$  and  $c'$ ) developed by the direct shear and both the CD and CU triaxial tests revealed a high bearing capacity for these soils; a situation contrasting the loose and low strength characteristics of surficial sabkha soils. This was attributed to the much higher confining pressures in these tests compared to those prevailing in the field. The unconfined compressive strength and CBR values seem, therefore, to correlate well with the field tests thereby providing a better assessment for foundation design.

### **ACKNOWLEDGEMENTS**

The assistance provided by Mr. Hasan Zakariya Saleh is greatly appreciated. The moral support of the Department of Civil Engineering is acknowledged. Mr. Solano Cruz typed this manuscript. The senior author would like to thank the Rector of KFUPM, Dr. Bakr Abdulla Bin Bakr, and the Dean of Engineering, Dr. Habib I. Abualhamayel, for their encouragement.

### **REFERENCES**

- ABU-TALEB, M.G. and EGELI, I. (1981). "Some Geotechnical Problems in Eastern Province of Saudi Arabia". Proceedings, Symposium on Geotechnical Problems in Saudi Arabia, Riyadh, 799-811.
- AIBAN, S.A. (1985). Static Strength Properties of Lightly Cemented Sands. *M.S. Thesis*, Department of Civil Eng., King Fahd University of Petroleum and Minerals, Dhahran.
- AKILI, W. and TORRANCE, J.E. (1981). "The Development and Geotechnical Problems of Sabkha with Preliminary Experiments on the Static Penetration Resistance of Cement Sands". *Quarterly Journal of Engineering Geology*, 14, 59-73.
- AL-AMOUDI, O.S.B. (1992). "Studies on Soil-Foundation Interaction in the Sabkha Environment of Eastern Province of Eastern Saudi Arabia". Ph.D. Dissertation, Vol. 1, Department of Civil Eng., King Fahd University of Petroleum & Minerals, Dhahran.
- AL-AMOUDI, O.S.B. and ABDULJAUWAD, S.N. (1994). "Modification to Suggested ASTM Standard Methods when Testing Arid, Saline Soils". *ASTM, Geotechnical Testing Journal*, 17 (2), 243-253.
- AL-AMOUDI, O.S.B., ABDULJAUWAD, S.N., EL-NAGGAR, Z.R. and RASHEEDUZ-ZAFAR (1992a). Response of Sabkha to Laboratory Tests: A Case Study. *Engineering Geology*, 33, 111-125.
- AL-AMOUDI, O.S.B., ABDULJAUWAD, S.N., EL-NAGGAR, Z.R. and SAFAR, M.M. (1991). "Geotechnical Considerations on Field and Laboratory Testing of Sabkha". Proceedings, Symposium on Recent Advances in Geotechnical Engineering III, Singapore, 1-6.

- AL-AMOUDI, O.S.B., EL-NAGGAR, Z.R. and ASI, I.M. (1992b). "The Sabkha Soil in the Kingdom of Saudi Arabia and Its Engineering Problems". *Al-Muhandis (Saudi Arabia)*, 6(2), 56-62 (in Arabic).
- American Geological Institute (1974). "Dictionary of Geological Terms". Anchor Books, New York.
- BOWLES, J.E. (1978). "Engineering Properties of Soils and Their Measurement", 2nd ed. McGraw-Hill Book Company, New York.
- BOWLES, J.E. (1988). "Foundation Analysis and Design", 4th ed. McGraw-Hill Book Company, New York.
- BUTLER, G.P. (1969). "Modern Evaporite Deposition and Geochemistry of Coexisting Brines, the Sabkha. Trucial Coast, Arabian Gulf". *Journal of Sedimentary Petrology*, 39(1), 70-89.
- DAS, B.M. (1983). "Advanced Soil Mechanics". Hemisphere Publishing Corporation, New York.
- ELLIS, G.I. (1973). "Arabian Salt-Bearing Soil (Sabkha) as an Engineering Material". *TRRL Report LR 523*, Crowthorne, Berkshire.
- EL-NAGGAR, Z.R. (1988). "Foundation Problems in Sabkha Deposits". In Short Course on Foundation Engineering for Practicing Engineer, coordinator, S.N. Abduljawad, KFUPM, April, SD1-SD54.
- FOOKES, P.G. and COLLIS, L. (1975). "Problems in the Middle East". *Concrete*, 9(7), 12-17.
- FOOKES, P.G., FRENCH, W.J. and RICE, S.M.M. (1985). "The Influence of Ground and Groundwater Geochemistry on Construction in the Middle East". *Quarterly Journal of Engineering Geology*, 18, 101-128.
- HOSSAIN, D. and ALI, K.M. (1988). "Shear Strength and Consolidation Characteristics of Obhor Sabkha, Saudi Arabia". *Quarterly Journal of Engineering Geology*, 21, 347-359.
- ISMAIL, N.F., AL-KHALIDI, O. and MOLLAH, M.A. (1986). "Saturation Effects on Calcareous Desert Sands". *Transportation Research Record No. 1089*, 39-48.
- KINSMAN, D.J.J. (1969). "Modes of Formation, Sedimentary Association, and Diagenetic Features of Shallow-Water and Supratidal Evaporites". *The American Association of Petroleum Geologists Bulletin*, 53(4), 830-840.
- RENFRO, A.R. (1974). "Genesis of Evaporite-Associated Stratiform Metalliferous Deposits - A Sabkha Process". *Economic Geology*, 69(1), 33-45.
- SHEHATA, W.M., AL-SAAFAN, A.K., HARARI, Z.Y. and BADER, T.A. (1990). "Potential Sabkha Hazards in Saudi Arabia", *Proceedings, 6th International IAEG Congress*, ed. D.G. Price, Amsterdam, 2003-2010.

# EFFECT OF BITUMEN CONTENT AND CURING CONDITION ON STRENGTH CHARACTERISTICS OF ASPHALT STABILIZED SOILS

A.A. Basma<sup>1</sup>, A.S. Al-Homoud<sup>2</sup>, T.S. Khedaywi<sup>3</sup> and A.M. Al-Ajlouni<sup>4</sup>

## SYNOPSIS

The main objective of this study was to determine the potential of bitumen as a soil stabilizing agent. For this purpose, four different soils from Northern Jordan were selected. Soil-bitumen mixtures were prepared at 3%, 5%, 7% and 10% bitumen by dry weight of soil. Both the natural and bitumen treated soils were subjected to similar laboratory tests to observe the effectiveness of bitumen on the physical and engineering properties of the selected soils. The test results showed that bitumen is effective in stabilizing the tested soils. Upon mixing bitumen with soils, it acts as a binding agent between soil particles. Experimental results indicated that curing conditions have a marked influence on strength, modulus of elasticity and strain at failure.

## INTRODUCTION

Low shear strength and internal erosion of some soils present problems for civil engineers. Problematic soils may cause damage to many structures. To avoid such damage, it is very useful to stabilize the natural soil using some agents. Soil stabilization is the collective term for any physical, chemical or biological method, or any combination of such methods employed to improve certain properties of natural soils to make them serve an intended purpose. Bitumen is one possible stabilizing material. It is used with soil as a waterproofing and binding agent that maintains low moisture content. Wintercorn & Fang (1975) stated that "bituminous soil stabilization is the name given to those methods of construction in which bituminous materials are incorporated into a soil or a soil aggregate to provide base course and occasionally wearing course which can carry the applied traffic loads under all normal conditions of moisture".

Most cohesive soils have satisfactory bearing capacity for construction uses at low moisture content. These soils, however, tend to lose stability at high moisture content. When bitumen is mixed with soils, the mixture does not absorb water so readily as untreated soil even when relatively small quantities are used (2 to 4 percent). This condition prevents an

---

<sup>1</sup> Assoc. Prof. of Civil Engrg, Jordan Univ. of Sci. and Tech., Irbid 22110 - Jordan. (Current affiliation: Sultan Qaboos University, Al-Khod, Muscat 123-Oman).

<sup>2</sup> Asst. Prof. of Civil Engrg, Jordan Univ. of Sci. and Tech., Irbid 22110 - Jordan.

<sup>3</sup> Prof. of Civil Engrg, Jordan Univ. of Sci. and Tech., Irbid 22110 - Jordan.

<sup>4</sup> Research Asst., Civil Engrg Dept., Jordan Univ. of Sci. and Tech., Irbid 22110 - Jordan.

appreciable amount of moisture change within the soil mass and maintains the inherent cohesive strength of the soil. To better understand this an experimental program to evaluate both the addition of bitumen as stabilizing agent and curing conditions for the strength of soils was undertaken.

### **EXPERIMENTAL PROGRAM**

The basic objectives of this research were to assess the unconfined compressive strength characteristics of soils treated with bitumen and to study the effect of curing conditions.

The experimental program involved four soils obtained from Northern Jordan, five levels of treatment: 0% (after molding with no bitumen), 3%, 5%, 7% and 10% of bitumen by dry weight of soil, and three curing conditions namely "seven days with cover", "seven days with air drying" and "seven days followed by immersion".

### **MATERIALS USED**

#### **Soils**

A laboratory testing program was carried out on four different soils from locations in Northern Jordan. Table 1 presents the physical and engineering properties of the experimental soils. Of the selected soils, two were collapsible while the other two were expansive in nature. The collapsible soils were extracted from sites in Mafraq (soil A) and within the campus of Jordan University of Science and Technology, JUST (soil B). The expansive soils were obtained from sites in Irbid (soil C) and another from Ramtha (soil D). Fig. 1 shows a location plan of the sites within Jordan from which these soils were extracted.

#### **Bitumen**

Liquid bitumen materials were used to treat the soils. Such materials are suitable for soil stabilization due to their low softening temperature and low melting viscosity (Wintercorn & Fang, 1975; Asphalt Institute, 1977). The bitumen used in this study is cutback asphalt (MC-70). The general properties of this type of asphalt are presented in Table 2.

Soil-bitumen mixtures (excluding solvents) were prepared with 0% (untreated), 3%, 5%, 7% and 10% bitumen based on the dry weight of the soil.

### **LABORATORY PROCEDURE**

#### **Pulverization**

The soils were initially dried at 60° C for 5 days, then pulverized using a plastic hammer and separated on the No. 4 sieve (4.75 mm mesh opening) for the compaction tests and the No. 10 sieve (2 mm mesh opening) for the unconfined compression tests. It is important to

*EFFECT OF BITUMEN CONTENT*

**Table 1 Properties of Selected Soils**

Property	Units	Soil			
		A	B	C	D
Location	-	Mafraq	JUST	Irbid	Ramtha
Depth of sampling	m	0.5	0.5	0.5	0.5
Consistency limits					
Liquid Limit	%	39.5	33.7	72.0	53.0
Plasticity Index	%	16.8	13.2	37.0	22.4
Grain size distribution					
Sand (2 - 0.075 mm)	%	12.3	47.8	4.0	32.0
Silt (0.075 - 0.002 mm)	%	54.7	32.2	30.0	30.0
Clay (< 0.002 mm)	%	33.0	20.0	66.0	38.0
Compaction					
Maximum dry unit weight	kN/m <sup>3</sup>	16.8	17.9	13.9	15.7
Optimum water content	%	17.8	15.2	29.0	19.9
Specific gravity of solids	-	2.74	2.72	2.71	2.56
Unified soil classification*	-	ML	CL	CH	MH

\* After Wagner, 1957

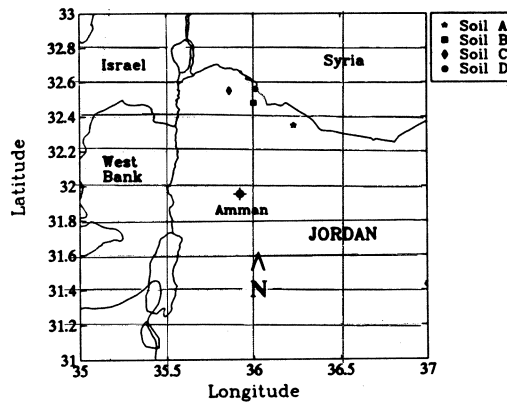


**Fig. 1 Location Map of Selected Sites.**

point out that these sieves were used in accordance with ASTM specifications (ASTM, 1990)



**Table 2 Properties of Bitumen Used (Medium Curing Cutback Asphalt, MC-70)**

Property	Units	Result
Viscosity		
Kinematic viscosity at 140° F	cSt	125
Saybolt furol viscosity at 122°F	sec.	85
Flash point	°C	100
Fire point	°C	105
Distillation test		
Distillate by volume of		
total distillate to 225° C	%	20 maximum
260° C	%	20 - 60
316° C	%	65 - 90
Residue from distillation to 360 ° C	%	55 minimum
Percent volume by different test on residue from distillation		
Penetration at 25° C, 100 gr., 5 sec.	0.1mm	120 - 250
Ductility at 25° C	cm	100 minimum
Solubility in trichloroethylene	%	99 minimum
Water	%	0.2 maximum
Specific gravity	-	0.960

### Sample Preparation

To prepare the test specimens with a specific bitumen percentage, the bitumen was added to the dry soil and initially mixed using a spoon. This is followed by mixing the sample in a mechanical mixer for at least two minutes until a uniform mixture was attained. To study the influence of bitumen on the strength and deformation characteristics, specimens from the natural (untreated soil) and the bitumen treated soils were prepared at the optimum fluid content and maximum dry unit weight. It should be noted that the word "fluid content" is used to indicate the total content of fluid substances in the soil which include the water and the liquid bitumen.

### Curing

Before testing for strength in the unconfined compression test, sample were initially cured under different conditions according to the following schemes:

- I) Immediately after molding without water loss. This will be referred to hereafter as "after molding".

## *EFFECT OF BITUMEN CONTENT*

- II) After leaving the specimen for seven days wrapped in a plastic sheet with small holes at the corners to reach a condition of small water loss and large volatile loss. This will be called “7 days with cover”.
- III) After leaving the specimen for seven days to air dry and reach a constant mass. This will be designated as “7 days with air drying”.
- IV) After seven days air drying then leaving the specimen to soak in a condition of partial immersion by immersing it to half its height in a water dish for three hours. This will be denoted by “7 days then immersion”.

### Testing

To prepare the unconfined compressive test specimens at the appropriate optimum fluid contents and maximum dry unit weights, it was necessary first to conduct compaction tests for both the untreated and treated soils. For this purpose the Standard Proctor test, ASTM D 688 (ASTM, 1990) was utilized. Immediately after the aforementioned curing schemes, specimens were tested in unconfined compression according to ASTM D 1663. Samples were loaded at a constant rate of 1.5 mm/min at room temperature. The loads and corresponding deformation were recorded and used to plot the stress-strain diagrams.

## **RESULTS AND DISCUSSION**

### **Compaction Test**

The optimum water content and maximum dry unit weight were evaluated from the compaction tests for each bitumen percentage added to the soil. In calculating the dry unit weight of the treated soils, the weights of both water and bitumen were subtracted for the compacted samples. The water content corresponding to the peak on the compaction curve defines the optimum water content. It should be reiterated that for the treated samples, the percentage bitumen present was added to the optimum water content to produce an optimum fluid content corresponding to the maximum dry unit weight. The results from the compaction curves (not shown here) are presented in Fig. 2 for the four soils. This figure clearly shows that increasing the percentage of bitumen in the soils decreases the maximum dry unit weight and increases the optimum fluid content. The decrease in the maximum dry unit weight could be attributed to the fact that bitumen films in treated samples surrounding the soil particles have high viscosity resulting in an increased resistance by the mixture to compaction.

### **Unconfined Compression Test**

In studying the effect of bitumen content on strength of bitumen treated soils, it is important to consider the effect of various curing conditions which result in different volatile loss and gain or loss of water content. This needs to cover all possible cases and conditions expected in the soils from each site.

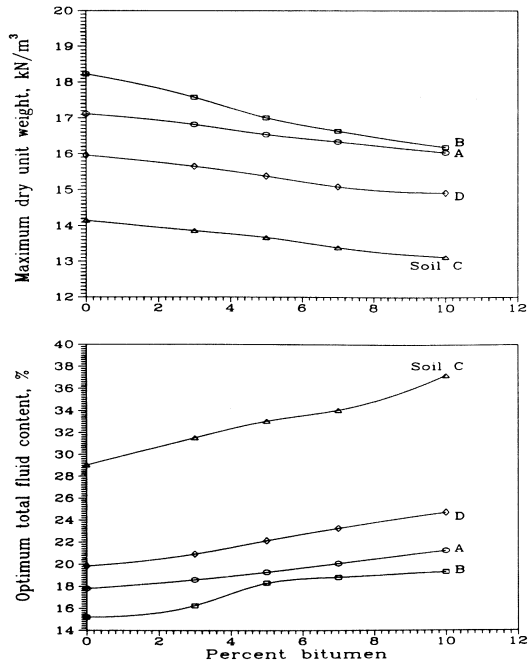


Fig. 2 Variation of Maximum Dry Unit Weight and Optimum Fluid Content with Percent Bitumen.

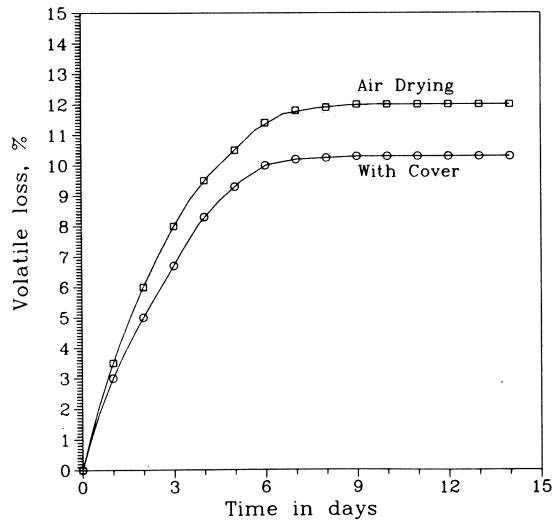


Fig. 3 Variation of Volatile Loss with Time for Air Drying and Curing with Cover (Soil B).

## EFFECT OF BITUMEN CONTENT

To estimate the amount of volatile loss from the total percent bitumen added to each specimen at different curing conditions, soil B was considered. Specimens for each percentage bitumen were prepared at maximum unit weight in the unconfined compression test mold without water but rather with a total fluid content being equal to the percent bitumen. Thus, only the required amount of bitumen, corresponding to desired percentage, was mixed with the dry soil. For each percentage bitumen two specimens were prepared. The first was for the condition of air-drying while the second was for curing with cover. The weight of the specimens was measured daily for 14 days. The loss in weight due to the loss in volatiles was used to calculate the percent of volatile loss. It should be noted that the observed percent volatile loss was approximately the same for all bitumen percentages used. The volatile loss with time is presented in Fig. 3. The results in this figure suggest that for both air-drying and curing with cover the percent volatile loss is negligible after about seven days. Moreover, it is noted the difference in volatile loss between these two conditions after seven days is less than 1.5%.

In a similar fashion, and in order to estimate the gain and loss of moisture content as a function of bitumen content, Figs. 4 and 5 were prepared. From Fig. 4 it could be concluded that increasing bitumen content causes a great decrease in water loss for the air-drying condition and a minor decrease for the curing with cover while having virtually no effect on volatile loss for both curing conditions. Fig. 5 indicates that as bitumen content increases, the percent loss of fluid by air-drying decreases slightly while causing a major reduction in the percent water gain by immersion following air drying. From these figures it is concluded that for air drying there is a decrease in the rate of water absorption which is one of the primary purpose for using bitumen in soil. Furthermore, this observation indicates that most of the inherent stability of the bitumen stabilized soil mass is mobilized

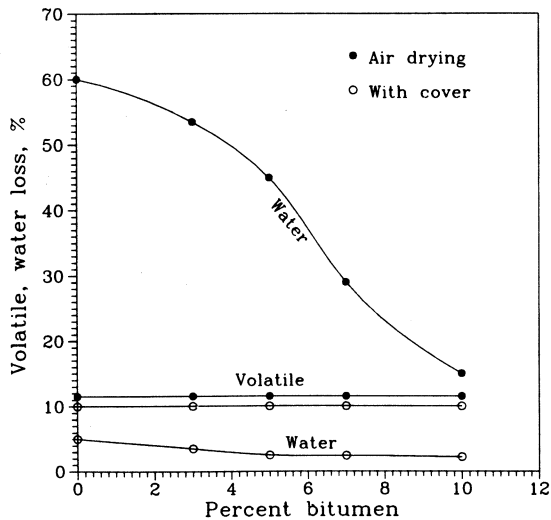
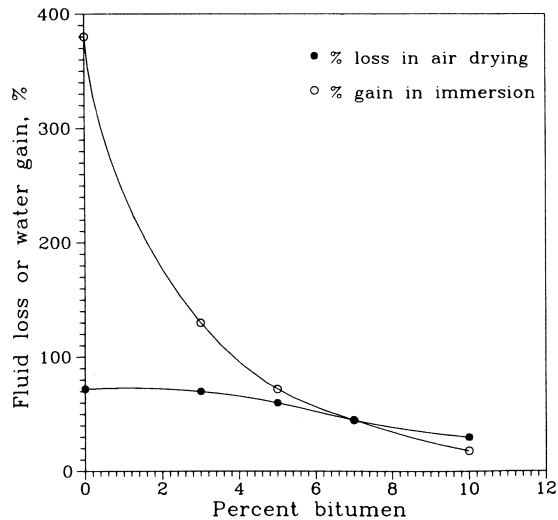


Fig. 4 Variation of Volatile and Water Loss with Bitumen Content (Soil B).



**Fig. 5 Variation of Fluid Loss or Water Gain with Bitumen Content (Soil B).**

and is retained even after subsequent saturation.

Unconfined compression tests on compacted soil-bitumen specimens were used to evaluate the strength over a range of curing conditions. The results of these tests are plotted and shown in Fig. 6. Upon studying the curves in this figure, the following general observation for the four bitumen treated soils could be stated:

- a) For both “after molding” and “7 days with cover” the strength of the treated specimens increases at 3% bitumen content. As the bitumen content increases beyond 3%, the strength decreases. This suggests that the binding effect of bitumen serves initially to increase strength, however, beyond a certain point (3% in this case), the decrease in unit weight due to the resistance of the mixture to compaction offsets the increase in strength.
- b) For the “7 days with air drying” the strength decreases progressively with increasing bitumen content. This may be explained by the fact that in air drying most of the water evaporates while the remaining water retreats into the narrow voids in the soil. The air-water interface in these capillary size voids places the water under tension resulting in a negative excess pore water pressure. Thus, the actual effective stress increases and becomes greater than the total external stress applied by the unconfined compression test. As the percent bitumen increases, the amount of water in the specimen decreases. This tends to dilute the ion concentration causing the decrease of water under tension. Subsequently, the double layer repulsion decreases leading to a loss in strength.
- c) As was noted earlier (Fig. 3) the percent loss in volatile for 7 days air drying with cover increases with time to reach a constant value of about 10.4%. As the percent volatile loss increases, the strength increases. This may explain why the strengths of specimens

## EFFECT OF BITUMEN CONTENT

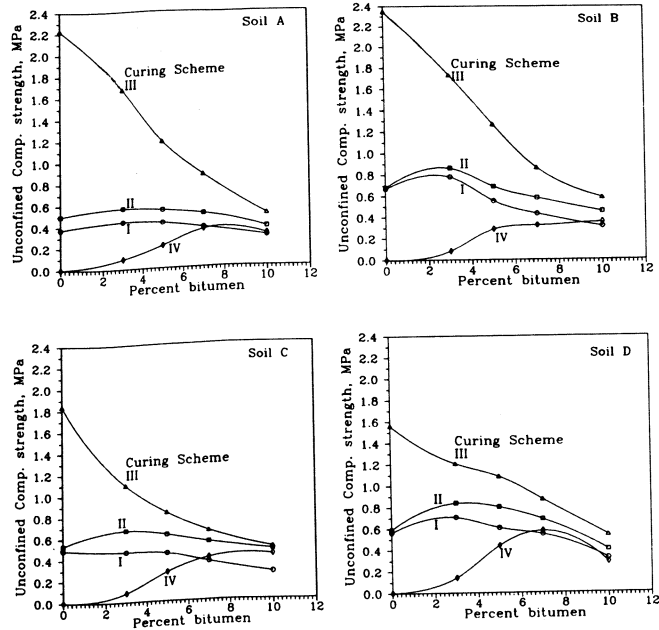


**Fig. 6 Variation of Unconfined Compressive Strength with Bitumen Content for Tested Soils.**

cured for 7 days air drying with cover are greater than those for specimens tested immediately after molding.

- d) The strength of specimens cured for 7 days air drying then partially immersed in water for three hours increases with bitumen content. This may be attributed to the water gain during immersion which decreases as the percent bitumen increases thus causing an apparent increase in strength.
- e) For all curing techniques utilized, it was noted that the strength values converge with bitumen content over 8 to 10%. This phenomenon may be associated with the fact that bitumen, at high percentages, replace most of the free water already existing in the soil, consequently, causing a marginal effect on either water loss or gain regardless of the curing method applied resulting in an almost constant value for strength.
- f) The variational trends observed for the unconfined compression strength seem to apply to both collapsable (A and B) and expansive (C and D) soils. However, the collapsable soils tend to experience a greater reduction in strength than expansive soils with increasing bitumen content when cured for 7 days with air drying (scheme III). The estimated average reduction in strength values were about 76% and 64% for collapsable and expansive soils, respectively .

In addition to the unconfined compressive strength, the variation of the secant moduli of elasticity and strains at failure as obtained from the stress-strain diagrams (not shown

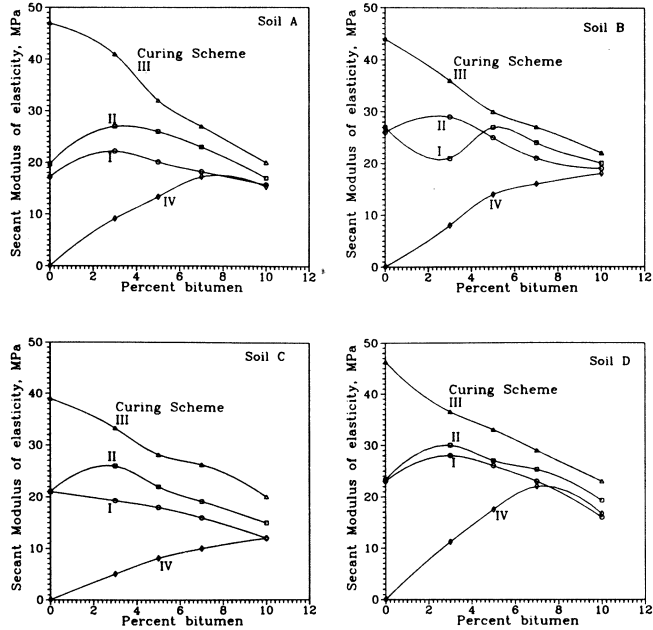


**Fig. 7 Variation of Modulus of Elasticity with Bitumen Content for Tested Soils.**

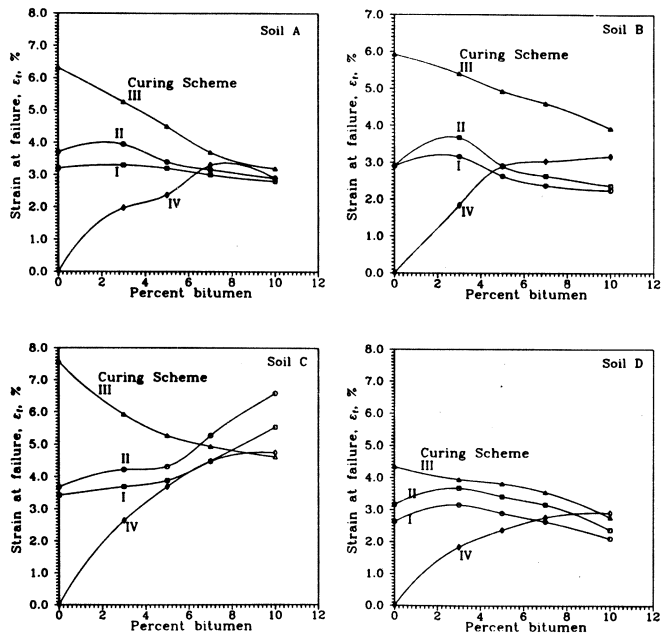


**Fig. 8 Variation of Strain at Failure with Bitumen Content for Tested Soils.**

## *EFFECT OF BITUMEN CONTENT*

here) with bitumen content was investigated. These are shown in Figures 7 and 8. It should be noted that the secant modulus of elasticity was taken as the slope of the straight line connecting the origin to the point of 1/3 peak stress. Generally speaking, the trends presented in these figures is similar to those in Fig. 6. For specimens "after molding" and "7 days with cover" there is an increase in both the modulus of elasticity (except for soil B) and strain at failure (except for soil C) at 3% bitumen. Further increase in bitumen content beyond this point causes a reduction in these properties. On the other hand, for "7 days with air drying" and "7 days then immersion" the values of these properties respectively decrease and increase with increasing bitumen content.

### **CONCLUSIONS**

Based on the results of this study and the conditions evaluated, the following conclusions are reached.

- 1) Increasing the bitumen content of a soil reduces the maximum compaction dry unit weight while increasing the optimum fluid content.
- 2) Curing conditions of bitumen treated soils have a marked influence on the strength characteristics
- 3) Generally speaking, the unconfined compressive strength for the after molding and the seven days curing with cover increases with bitumen content up to 3%. Any further increase in bitumen may result in lower strength values. However, the strength characteristics for the four tested soils decrease with increasing bitumen content for seven day curing with air drying. The opposite was noted for seven days curing then immersion.
- 4) Regardless of the curing technique employed, it was observed that the strength values converge for bitumen content over 8 to 10%.
- 5) Collapsible soils tend to experience greater reduction in strength than expansive soils with increasing bitumen content when cured for 7 days with air drying.
- 6) Similar trends as in (3) were noted for the modulus of elasticity and strain at failure. This latter observation suggests that increasing the percent bitumen beyond 3% may result in a more deformable and less brittle soil.

### **REFERENCES**

- AMERICAN SOCIETY OF TESTING and MATERIALS, ASTM (1990). "Annual Book of ASTM Standards". Vol. 4.08, ASTM, Philadelphia, PA.
- ASPHALT INSTITUTE (1977). "A Brief Introduction to Asphalt and Some of its Uses". Manual series No. 5, College Park, Md.
- WAGNER, A. A. (1957). "The use of the unified soil classification system by the Bureau



of Reclamation”. Proceedings of the 4th International Conference on Soil Mechanics and Foundation Engineering, London, p. 125.

WINTERCORN H. F. and FANG, H. Y. (1975). “Foundation Engineering Handbook”. Van Nostrand Reinhold, New York.

#### **ACKNOWLEDGMENT**

The authors would like to extend their sincere appreciation to the Deanship of Scientific Research at Jordan University of Science and Technology for supporting this research. The work presented herein is part of the fourth author's Thesis submitted in partial fulfillment for the degree of Master of Science in Civil Engineering.

## DISCUSSION

DISCUSSION by S.B. Tan<sup>1</sup> and T.K. Lim<sup>2</sup>

**“Hyperbolic Method for Evaluation of Settlement of Ground Pretreated by Drains and Surcharge” by S.A. Tan, Geotechnical Engineering, Vol 25 No.1, June 1994.**

The author is to be commended for devising a quick, practical and useful method of locating the 50% and 90% consolidation points on the  $t/\delta$  versus  $t$  plot and their corresponding times. The method appears helpful in monitoring the progress of consolidation in field applications using drains and surcharge, and in deciding the appropriate time for surcharge removal.

The hyperbolic method has always been a very practical and useful method of analysing field data relating to the settlement phenomenon. Chin (1970) used it for estimating the ultimate loads of piles. Tan (1971) used the method (then called an empirical method) to predict ultimate settlements for laboratory consolidation tests, footing and raft foundations, friction piles foundation and embankments. Tan (1977a) also used it to predict ultimate settlements of structures on uncompacted rubbish and that of rockfill embankments on soft clay (Tan 1977b). The method has also been applied in Singapore to various soil improvement works involving preloading, including the sand drains project for the soil improvement works at Changi Airport, Singapore (Tan & Phang, 1979; Poh, 1981; Tan, Yang & Yap, 1982; Vijiaratnam et al, 1982; Tan et al, 1985). In the case of a clay undergoing both primary and secondary consolidations, Chin (1975) distinguished two distinct straight lines in the  $\delta/t$  versus  $t$  plot. He suggested that the inverse of the first slope be used to estimate the magnitude of primary settlement and the inverse of the second slope be used for the magnitude of the secondary settlement.

The writers wish to comment on the use of the  $\delta_{50}$  and  $\delta_{90}$  values to predict ultimate settlements. In the comparison tables of hyperbolic settlement estimates with observed ultimate settlements, the author has presented four different ways of estimating ultimate settlements. However, the methods of estimating ultimate settlements based on  $2\delta_{50}$  (2 times the settlement at 50% consolidation) and  $1.11\delta_{90}$  (1.11 times the settlement at 90% consolidation) may be basically variations of the same method as the inverse slope method for the first linear portion. This is because their slopes originating from the origin are derived from the same slope whose inverse is used for estimating ultimate settlement (see Equations 4 and 5 in the paper). Hence, theoretically, all the three methods mentioned above should yield the same estimated values. The small differences in the estimated values from the three methods shown in the tables of comparison may be just inevitable inaccuracies arising from the graphical constructions.

---

<sup>1</sup> Director-General and <sup>2</sup> Senior Engineer, Public Works Department, Ministry of National Development, Maxwell Road, #19-00, #20-00, Tower Block MND Complex, Singapore 0106.

**REFERENCES**

- VIJARATNAM A., TANS.B., NG P. F.W. and CHOA V. C.E. (1982), "Reclamation and Soil Improvement Works for Changi Airport", Proc. Int. Symposium on Airport Planning and Development, Singapore, pp. 88 - 105.
- CHIN F.K. ( 1970), "Estimation of the Ultimate Load of Piles from Tests not Carried to Failure", Proc. 2nd S.E. Asian Conf. on Soil Engineering, Singapore, pp. 81- 90.
- CHIN F.K. (1975). "The Seepage Theory of Primary and Secondary Consolidation", Proc. 4th S.E.Asian Conf. on Soil Engineering, Kuala Lumpur, pp. 3-54 to 3-61.
- POH K.B. (1981). "Merits and Demerits of Displacement and Non-Displacement Methods Used in the Installation of Sand Drains in Singapore Marine Clay", JKR Seminar on Aircraft Pavement Design, Construction and Maintenance, Kuala Lumpur, 3-31 to 3-35.
- TAN S.B. (1971). "An Empirical Method for Estimating Secondary and Total Settlement", Proc. 4th Asian Regional Conf. on Soil Mech. and Found. Engg., Bangkok, Vol2, pp. 147-151.
- TAN S.B. (1977a). "Settlement of Structures on Uncompacted Rubbish". Proc. 9th Int. Conf. on Soil Mech. and Found. Engg., Tokyo, Vol. 1, pp.395 - 397.
- TAN S.B. (1977b). "Instrumentation for the Widening of the Singapore / Johore Causeway", Proc. 5th S.E.Asian Conf. on Soil Engg., Bangkok, pp. 261 -273.
- TAN S.B. and PHANG C.P. (1979). "Performance of Sand Drains ( at Taxiway 1, Changi Airport)". Proc. 6th Asian Regional Conf. on Soil Mech. and Found. Engg., Singapore, Vol 1, pp. 183-186.
- TAN S.B., YANG K.S. and YAP N.C. (1982). "Effectiveness of Non-Displacement Sand-Drains at Changi Airport". Proc. 7th S.E.Asian Geot. Conf., Hong Kong, pp. 659 - 673.

## NOTES FOR THE GUIDANCE OF AUTHORS

General: Manuscripts of original papers, technical notes and discussions should be submitted to the Editor, Geotechnical Engineering, Planning Division, Civil Engineering Department, 101 Princess Margaret Road, Homantin, Kowloon, Hong Kong. Papers will be accepted for review on the understanding that they have **not been submitted or published elsewhere** and that they become the copyright of the South East Asian Geotechnical Society.

**Papers** on major geotechnical topics of wide interest to the South East Asian region are welcomed, where as those of a specialist interest that are more suitable for other specialist journals are less likely to be accepted. Normally, **papers should not exceed 16 pages, including references, figures and tables**: there are about 450 words on a printed page. Short topical papers of 8 pages or less will be reviewed more quickly.

**The format which must be followed** for the preparation of manuscripts is in general that adopted in this issue of the Journal. **Manuscripts which do not conform to this format will be returned to the author(s) without review.**

**Three complete copies of the manuscript, in English**, should be submitted to the Editor (two copies for technical notes and discussions) together with the original drawings and photographs. In addition, a copy of the text should be submitted on 5 1/4" or 3 1/2" floppy disc formatted using DOS 3.0 (or later version) and the file should be in ASCII or Wordperfect 5.0 (or later version) format. Typescripts must be accurate and in their final format as outlined below. Owing to the high cost of corrections at proof stage, the Editor reserves the right to charge authors the full cost of corrections resulting from changes made at the proof stage.

**Layout:** Typescripts must be **double spaced**, including references, on one side only of **A4 paper**, with a **25 mm margin on each side**. All pages should bear the authors name and be numbered serially. Papers should be succinct and arranged as follows:

1. **Title:** brief and specific in **bold and uppercase, centred** at the top of the first page
2. The **author(s) full name(s) should appear centred below the title in bold**. The author(s) position and affiliation should be indicated as a footnote at the bottom of the first page. A **synopsis (with main heading) of not more than 200 words** should appear immediately below the authors name(s). The synopsis must be intelligible **without** reference to the paper and should highlight the essential new information and interpretations in the paper; it should not be a mere recital of the subjects covered. A synopsis is not required for technical notes.
3. **Figures** should be drawn boldly in black ink on one side of good quality tracing paper or smooth white board, with a **line weight and lettering suitable for reduction to fit the journal page width**. A separate caption list should be included. All maps should include a metric scale and north point. **Photographs** should be sharp and of **good contrast** (black and white preferred). The authors name should be given on each sheet and the **"top"** indicated.
4. **Formulae** should be expressed as simply as possible, and lengthy proofs avoided. **SI units** should be used throughout.
5. **Symbols** should be defined when they first appear.
6. **References** should appear in the text as the author(s) name(s) followed by the year of publication in brackets. A **list of references** should be given at the end of the text in alphabetical order of author(s) name(s) with the author(s) name(s) in capitals and bold. Some examples of the format to be used in the reference list are given below:

PREMCHITT, J. & SHAW, R. (1991). Marine geotechnical engineering for development projects in Hong Kong. *Proceedings of the International Workshop on Technology for Hong Kong's Infrastructure Development*, Hong Kong, pp 721-738.

PUN, W.K. (1990). Seismicity of Hong Kong. M.Sc. Thesis of the University of London (unpublished)

PUN, W.K. & AMBRASEYS, N.N. (1992). Earthquake data review and seismic hazard analysis for the Hong Kong region. *Earthquake Engineering and Structural Dynamics*, vol. 21, pp 433-443.

HOEK, E. & BROWN, E.T. (1982). *Underground Excavations in Rock (2nd Edition)*. The Institution of Mining & Metallurgy, London, 527 p.

# GEOTECHNICAL ENGINEERING

## CONTENTS

### Photographic Feature:

Shield Driven Tunneling Method by M. SUGIMOTO.....	1
---	---

### Main Papers:

Improvement of Plasticity and Swelling Potential of Calcareous Expansive Clays by S.N. ABDULJAUWAD.....	3
Effect of Tail Void Closure on Ground Movement During Shield Tunnelling in Sandy Soil by C.Y. OU and J.C. CHERNG.....	17
Soil Particle Migration through Slots in Drains, Part I - Unidirectional Flows by B. TAHAR and T.H. HANNA.....	33
Soil Particle Migration through Slots in Drains, Part II - Reversing Flows by B. TAHAR and T.H. HANNA.....	51
Strength Characteristics of Sabkha Soils by O.S.B. AL-AMOUDI and S.N. ABDULJAUWAD.....	73
Effect of Bitumen Content and Curing Condition on Strength Characteristics of Asphalt Stabilized Soils by A.A. BASMA, A.S. AL-HOMOUD, T.S. KHEDAYWI and A.M. AL-AJLOUNI.....	93
Discussion by S.B. TAN and T.K. LIM.....	105
Paper Entitled "Hyperbolic Method for Evaluation of Settlement of Ground Pretreated by Drains and Surcharge" by S.A. Tan, Geotechnical Engineering, Vol. 25, No. 1, June 1994	

---

**Abstracted and/or Indexed in *Geotechnical Abstracts***